Univerzita Tomáše Bati ve Zlíně
Fakulta technologická

Doctoral Thesis

Composite materials with photo-responsive capability

Kompozitní materiály s fotocitlivou odezvou

Author:	**Ing. Josef Osička**
Degree program:	P2808 Chemie a technologie materiálů
Degree course:	2808V006 Technology of Macromolecular Compounds
Supervisor:	Ing. Miroslav Mrlík, Ph.D.
Consultant:	doc. Dr. Ing. Vladimír Pavlínek, Ph.D.
Reviewers:	Prof. Ing. Berenika Hausnerová, Ph.D.
	Ing. Igor Lacík, DrSc.
	Doc. Ing. Petr Filip, CSc.

Zlín, September 2020

Published by Tomas Bata University in Zlín in the Edition **Doctoral Thesis**. The publication was issued in year 2020

Keywords: SI-ATRP; graphene oxide; photo-actuation; light-stimuli materials; dielectrics, dynamic mechanical analysis; intelligent materials

Klíčová slova: SI-ATRP; grafen oxid; fotoaktuace; světlostimulující materiály; dielektrika; dynamická mechanická analýza; inteligentní materiály;

Full text of the scientific publication is available in the Library of TBU in Zlín

ISBN 978-80-…….

ABSTRACT

Photo-responsive materials belong among novel, fast-developing intelligent materials of modern era. They seem to be promising smart systems in many current and future technologies i.e. in medicine, mechanical and construction engineering, energy harvesting, sensors etc. Very encouraging group of these materials is represented by photo-actuating (PA), shape-memory systems. Their main feature known as photo-actuation is capability to rapidly and reversibly change their shape after external light exposure.

However, there are several limitations reducing their real-life utilization. Generally known PA systems, mainly solid materials, suffer from not very significant dimension change that is usually in order of 0.001% of original shape. Hence, the main aim of this work is focused on composite systems, in which the combined PA effect of matrix and filler is frequently synergic, but those systems also possess many drawbacks that need to be solved, i.e. low compatibility of filler to the matrix related poor dispersibility in such system, resulting to the low thermal conductivity and finally poor mechanical properties as well as PA capabilities. The mentioned drawbacks can be reduced by modifying the filler with compact polymer layer possessing such surface properties those can significantly enhance particle/matrix compatibility and thus contribute to considerably improve overall properties.

ABSTRAKT

Fotocitlivé materiály patří mezi nové, rychle se rozvíjející inteligentní materiály moderní doby. Ukazují se být slibnými inteligentními systémy, které lze využít v mnoha současných a budoucích technologiích v oblastech jako jsou medicína, strojírenství, stavebnictví, získávání energie, senzorech a dalších. Velmi nadějnou skupinou těchto materiálů jsou foto-aktuující systémy s tvarovou pamětí. Jejich hlavní funkcí známou pod pojmem foto-aktuace, je schopnost rychle a reverzibilně měnit svůj tvar po vystavení se vnějšímu světelnému stimulu.

Jejich reálné využití v praxi se potýká s několika omezeními. Obecně známe foto-aktuující systémy, zejména pak pevné materiály, nevykazují významnou změnu jejich rozměru, ta se obvykle pohybuje řádově 0.001% původní velikosti. Proto je hlavní cíl této práce zaměřen na kompozitní systémy, kde kombinace matrice i plniva, které mají schopnost foto-aktuace, má synergický efekt. Nicméně, tyto systémy mají řadu nevýhod, které je třeba vyřešit. Nízká kompatibilita plniva s matricí způsobuje nedostatečnou disperzi částic v takovémto systému, což vede k nízké tepelné vodivosti a finálně ke špatným mechanickým vlastnostem, stejně tak k nedostatečných foto-aktuačním schopnostem. Zmíněné nevýhody mohou být eliminovány modifikací plniva kompaktní polymerní vrstvou, která má takové povrchové vlastnosti, které mohou významně zvýšit kompatibilitu plniva s matricí, a tak přispět k podstatnému zlepšení celkových vlastností.

ACKNOWLEDGEMENTS

Here I would like to express my enormous gratefulness to those without whom this work could not have arisen.

First, I would like to express my great gratitude to my supervisor Dr. Miroslav Mrlík for his guidance who provided me with the opportunity to join his research group and has such patience, endurance and comprehension with myself during my whole Ph.D. study.

I would like to thank his amazing wife Dr. Markéta Ilčíková for her incredibly great help and valuable advice, which had remarkable impact on my research.

I am highly grateful to assoc. prof. Michal Sedlačík for his assistance and support during the period of time my supervisor was working abroad.

My special thanks to Dr. Jaroslav Mosnáček for his help and support regarding the atom transfer radical polymerization.

My appreciation also goes to assoc. prof. Vladimír Pavlínek, who allowed me to study the Ph.D. degree and supporting me during whole this period.

I would like to acknowledge the co-authors of my publications and my colleagues without it would not be possible to complete this dissertation.

Finally, my superior thanks to my mother, fiancée and my family for their endless understanding and support.

CONTENTS

1 THEORETICAL BACKGROUND

1.1 Introduction

The intelligent materials have its place in increasingly evolving areas of material science and engineering. The external stimulus-responsive materials are of attention for many scientific researchers, due to their capability of reversibly change their dimension upon the application of an outside stimulus i.e. electric [1] and magnetic [2] field, temperature [3], pH [4], light (UV, VIS), etc. [5]

Actuators provide the driving force and motion for a variety of natural and manmade requirements. Naturally, occurring actuators include the muscles of animals and plants, and manufactured actuators include hydraulics [6], pneumatics [7] and solenoids [8]. Other fabricated actuators, such as piezoelectric [9], shape memory alloy [10] and magnetostrictive [11] devices, are based on shape-changing materials; these are used increasingly in novel applications. Actuators offer a wide variety of performance and operate in many different ways.[12]

Light-induced actuators are attractive to scientists since they propose an effective means to couple light energy into the actuator configurations, and bring advantages of basic systems with wireless functionality, remote control, green energy, and high-level integration [13, 14]. The effect of the Photo-induced Optical Anisotropy (POA) is a phenomenon that was observed in many molecular systems such as solutions [15], polycrystalline films [16], polymer films [17] and Langmuir-Blodgett (LB) films [18, 19]. The photomechanical actuators (also known as photo-actuators) are a class of smart materials that can alter their dimensions or undergo mechanical motion when exposed to photons (light emission) [20]. Absorption of the energy from photons leads to a contract or a generation of a certain mechanical motion of polymeric chains, which is called photo-actuation. [21-23]

Graham Bell firstly used a concept of so-called photo-actuation in 1881. He used the opto-acustic effect to make sound in a gas with chopped beam of sun light that has been used to study the absorption of light by materials throughout the next 100 years. [24] An optically operated fluidic actuator was presented in 1980 [25]. In 1983, the optical heating of closed gas filled volume was used to change a flexible diaphragm in a flapper nozzle device [26]. In 1990, the first direct optical to mechanical actuation was achieved by optically modifying the viscosity of a fluid[27]. The rapid development in materials research in the early 1990's led to the expansion of range of photomechanical actuators based on direct and indirect optical to mechanical energy conversion [26].

This thesis aims to develop such photo-actuator in form of composite, which combines photo-actuation properties of matrix and filler to produce such shape-change material that will rapidly exceed dimension change of individual components.

1.2 Mechanisms of photo-actuation

Materials that can reversibly change their physical properties upon application of external stimuli are used as actuators for robotics, optical switches, optical displays, prosthetic devices, micro pumps, computer accessories, automotive sensors, and interplanetary space missions. The best-known materials used today for actuation are piezo-electrics, ferro-electrics, shape-memory alloys, electro-restrictive materials and conducting polymers. However, the maximum allowable operation temperature, the need for high voltages, and the limitations on the work density per cycle restrict applications of these materials [26]. The phenomenon of photo-induced strain has been previously observed in lead zirconate titanate (PLZT) ceramics [28], polymers [5], nematic elastomers [29], polarizable liquids [30] and chalcogenide glasses [31].

1.2.1 Polymers

The most common principle of photo-actuation of chemically cross-linked elastomers and/or TPEs is based on the presence of soft segments responsible for shape changes under illumination, and hard segments responsible for returning the material to its stage before illumination. Thus, the pre-strained material containing some light absorbers absorbs the energy from the light and converts it to heat that is conducted through the material [32]. The heat causes that the pre-strained polymer chains in the soft segments shrink, i.e., contract to form coil, and that results in shape changes of the material [33], as can be seen in Figure 1.

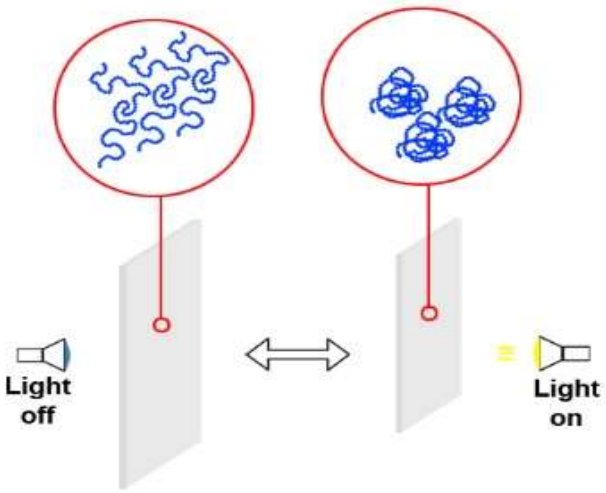

Figure 1. Photo-actuation of polymers [34].

1.2.2 Nematics elastomers

Photo-anisotropic materials are widely investigated for optical storage and processing applications. The most promising of them seem to be azo-dye-polymer systems because of the large value of the photo-induced birefringence in them

[35]. Photo-actuation in azobenzene polymers are caused due to the optical switching of the polymeric material from cis (contraction) to trans (expansion) isomeric states of the polymeric material. Actuation occurs in the UV region between 260–300 nm wavelengths. [36, 37] Liquid-crystalline polymers (LCPs) are one of the representative actuating materials. When liquid-crystalline monomers are polymerized in the nematic phase, they form liquid-crystalline polymer networks with aligned molecular structures. Incorporating azobenzene into an LCP system yields an azobenzene-functionalized liquid-crystalline densely cross-linked polymer (azo-LCP) system, which can convert UV or blue-light irradiation into mechanical deformations [38].

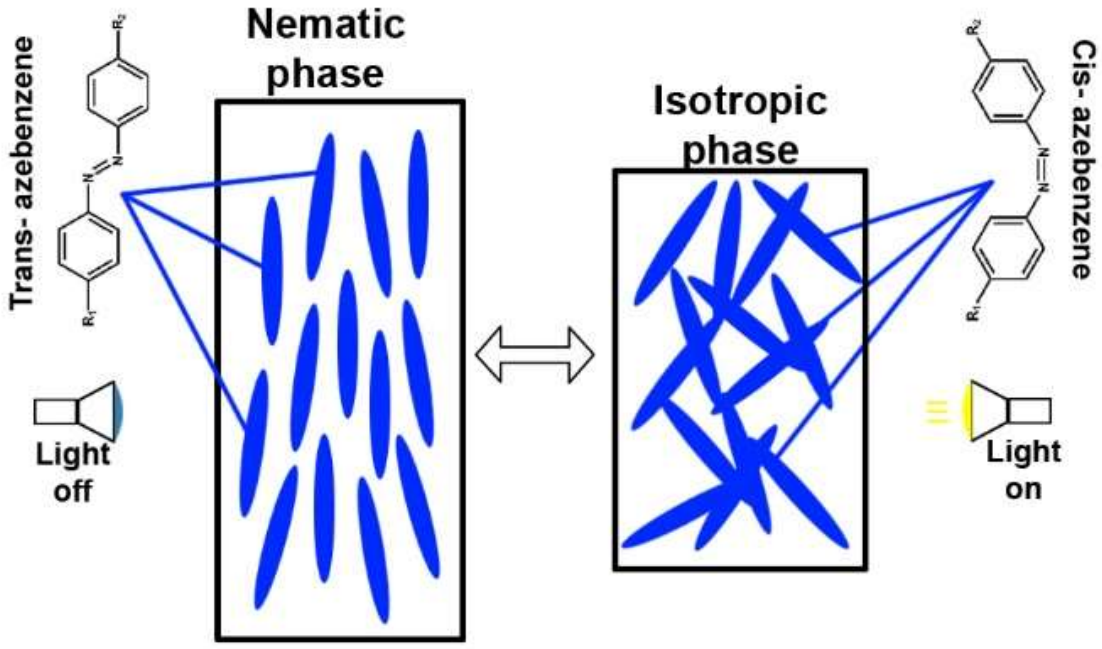

Figure 2. Photo-actuation of nematic elastomers [39].

1.2.3 Ceramics

Photo-actuation in PLZT ceramics is triggered by the superposition of photovoltaic effects, and the converse piezoelectric effect. It arises only in resources which are non-centro symmetric (typically piezo and ferro-electric). The large photo-voltage that is produced, reasons to the expansion or contraction of the frame in the way of unprompted polarization of the material and is reliant on impurity doping and crystal asymmetry. Such effects have practical application in creation micro-mechanisms, photo-relays and wireless actuators. The change in dimension reached by the PLZT materials does not exceed ~0,1% and is comparable to piezoceramics [23].

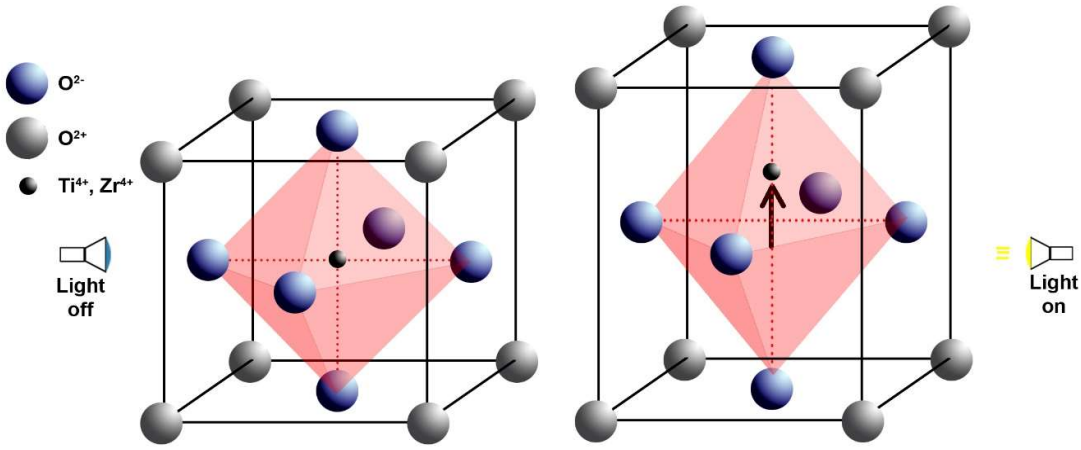

Figure 3. Photo-actuation of ceramics [40].

1.2.4 Chalcogenide glasses

More recently, chalcogenide glasses have been observed to directly convert light into mechanical energy. The investigations showed that upon irradiation with polarized light, thin film of chalcogenide glasses exhibit reversible nano-contraction parallel to the direction of the electric vector of the polarized light and nano-dilation along the axis orthogonal to the electric vector of the light. This new actuator technology shows promise of using polarized light for actuation that is scalable using massively parallel manufacturing techniques. However, the kinetics for contraction and relaxation are in the range of 1 min to 2 min making this actuation slow and the strains achieved are small (<0.001%). The range of actuation is also within nanometers, which have to be extended to micro and millimeters for more practical applications in MEMS and macro-scale actuation technologies. [26, 41-51]

1.2.5 Composites

Previously mentioned materials have different ability to change their shape after using light stimuli on them. The enhancement of their performance requires to increase their rubbery modulus and to minimize strain-recovery after deformation while maintaining processability, durability, deformability and to perform many cycles by means of repeatability [52]. In addition, there is an increased activity in integrating those materials with nanotechnology to prepare new materials for the realistic applications. Composites filled with neat particles and/or modified particles develop the photo-actuation phenomenon and may provide additional impact on the mechanical properties of the final composite system, which considerably influence the final photo-actuation performance.

1.3 Composition of Photo-actuating systems

Generally, the actuating materials can be pure polymers or polymer composites, but they need to have the energy absorber that serves as a trigger to actuation.

That is why usual photo-actuator is consisting of two main phases. Usually filler, which is kind of energy absorber that is dispersed in elastomeric matrix. Various elastomers were investigated for their photo-actuation behavior, including liquid crystalline elastomers [53], poly(dimethylsiloxane) (PDMS) [54], different thermoplastic elastomers based on polyurethane [55], poly(ethylene-co-vinyl acetate) (EVA) [56], polystyrene-block-polyisoprene-block-polystyrene (SIS) [57], and acrylic-based block copolymers, as well as hydrophilic copolymers such as NAFION [58] or hydrogels based on copolymers of acrylic acid and N-isopropyl acrylamide [33].

1.3.1 Matrix

1.3.1.1 Chemically cross-linked elastomers

Chemically cross-linked elastomers have the characteristics of rubber in terms of their flexibility and elasticity. The long, randomly coiled, loosely cross-linked materials can be stretched easily and they return to their original shapes when the force or stress is removed [59]. Most commonly used materials are liquid crystals and PDMS, because they provide good actuation behavior [60]. Because of the structure of LCs, by integration of the light-triggered materials to the LCs, the alignment can be controlled over large parts, and hence the materials can be effectively applied in photonic applications such as photo-actuation [33].

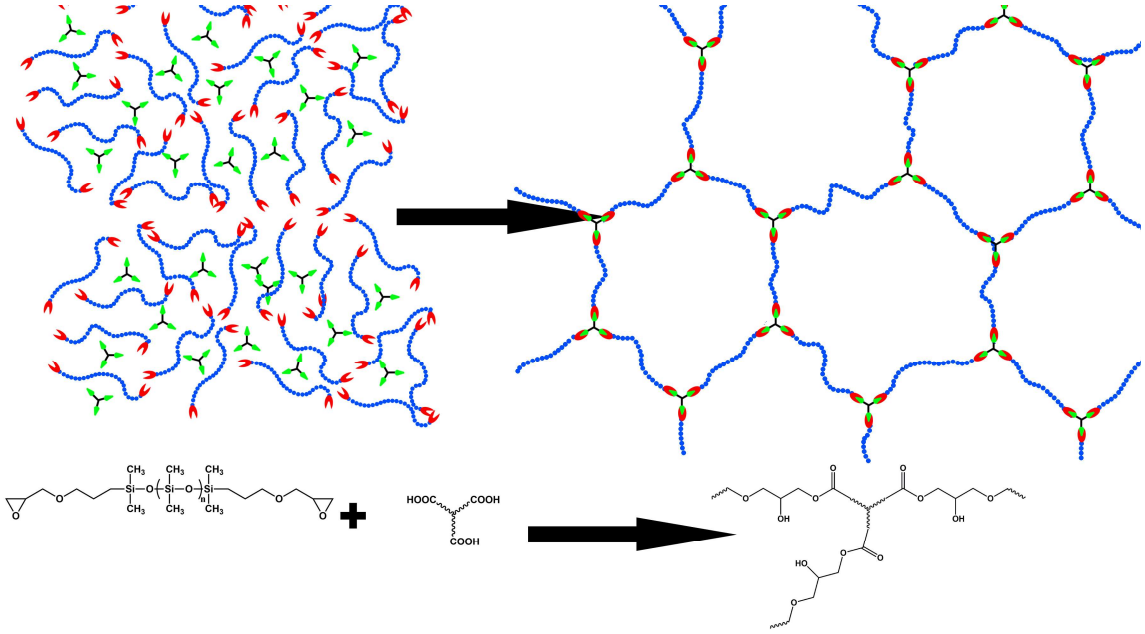

Figure 4. Chemical cross-linking of poly(dimethyl siloxane) [61].

1.3.1.2 Physically cross-linked elastomers

Physically cross-linked structure have several benefits in contrast with chemically cross-linked elastomers. The repeatable processing by large-scale techniques and potentiality of tuning mechanical properties are their main advantages. They are also cheap in comparison to LCs and PDMS. They are very

promising in terms of large-scale industrial use. Psychical cross-linking can be acquired by absorption of chains onto the surface of finely dispersed fillers, formation of small crystallites, coalescene of ionic centers and coalescene of glassy blocks [62]. Such obtained materials are part of group of polymers, called thermoplastic elastomers (TPE). Most TPE are phase separated systems. One phase is usually hard and solid at laboratory temperature and other is an elastomer [63]. TPEs can be divided into seven currently known groups: Styrenic block copolymers [64], crystalline multiblock copolymers [65], miscellaneous block copolymers, combinations of hard polymer/elastomer [62], hard polymer/elastomer graft copolymers, ionomers [66] and polymers with core-shell morphologies [67].

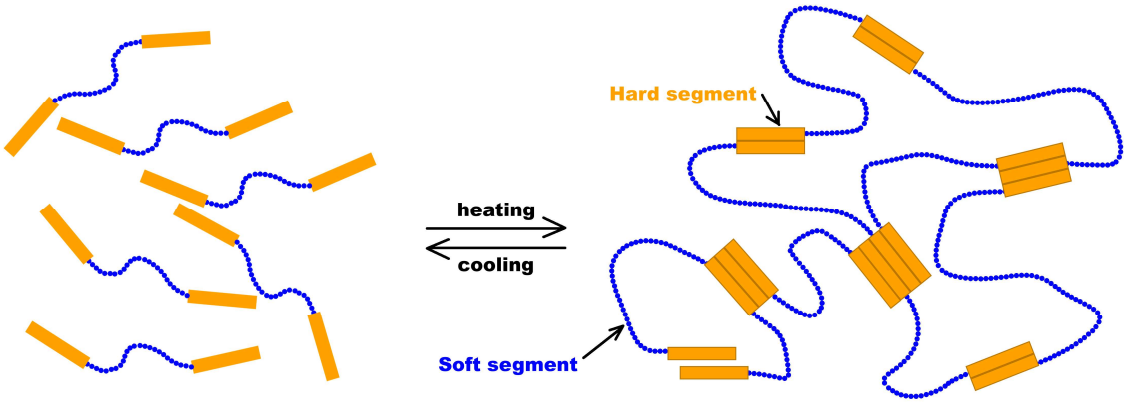

Figure 5. Physical cross-linking of thermoplastic elastomer [68].

1.3.2 Fillers

1.3.2.1 Organic fillers

As an organic filler, the azobenzene moieties in the main chains polymer films are used. Visible light facilitated the photo-isomerization of azobenzene moieties with directly modified cores or added substituents in LCPs [69]. Triplet-triplet annihilation-based up conversion luminescence materials were used to convert red light at 635 nm into short wavelength light, indirectly stimulating the prepared cross-linked LCPs containing azotolane [70].

1.3.2.2 Carbon-based fillers

Carbon nanotubes (CNT) based composites provide remarkable mechanical properties with very high elastic modulus and electrical conductivity [71]. CNTs can serve as photo-actuators due to the electrostatic interaction between the CNT bundles caused by light-induced thermoelectric (or photovoltaic) effects [72]. However, such photo-actuators are limited by the small mechanical deformations [73]. Carbon nanofibers have the potential to be used in nano-electronic devices, such as in artificial muscles, as well as in electrochemical energy storage matrices. Carbon-based nanoparticles like GO show the enhanced thermal conductivity and storage modulus, while the glass transition temperature is slightly decreased [74].

In practical applications, the conductive PA systems may be used as strain sensors based on the relation between electrical conductivity and strain.

1.4 Crucial parameters of photo-actuating systems

From information mentioned above, the crucial parameters are depending on used matrix and filler. Size, shape and dispersion are limits of filler, which affect final PA performance. In case of the size, fillers can be nano or micro sized. Advantages of nanoparticles are their high aspect ratio, large surface area; superior mechanical and thermal properties [75] on the other hand micro particles dimension shape-change is higher, due to the generally better and more homogenous dispergation in polymer matrix in comparison to nanoscale filler those form aggregates in there is not performed surface modification. In this consequence, the thermal energy redistribution in the sample is a crucial factor for the final photo-actuation and is better for the systems with homogenous filler distribution than for system with local inhomogenities formed by aggregates. In the case of matrix, the most crucial parameter is flexibility. The more flexible system is, the higher the PA performance can be achieved.

1.5 General characterization of materials

1.5.1 Dynamic mechanical behavior

The most precise tool for the photo-actuation investigation is dynamic mechanical analysis (DMA) in iso-strain tensile mode. Dynamic mechanical properties are ones of the most crucial factors influencing the applicability of materials as photo-actuation systems. Reversible contraction/elongation of the sample by light stimulation is a rather dynamic process and, therefore, investigation upon dynamic conditions is very important. Obtained data allow the calculation of the complex modulus in Equation (1) (knowing storage and loss moduli), damping or tan delta, δ, as well as viscosity data. The dynamic mechanical properties of a polymer are described in terms of a complex dynamic modulus [71]:

$$E = E' + iE'' \qquad (1)$$

where E′ is the storage modulus and is a measure of the recoverable strain energy; when deformation is small, it is approximately equal to the Young's modulus. E″ means the loss modulus and is related to the energy dissipation. DMA allows the rapid scanning of the viscoelastic moduli of composites as a function of temperature or frequency [71]. In addition, DMA is very sensitive to the motion of polymer chains and, therefore, they are powerful tools for measuring the glass transitions in polymer matrix. Moreover, the proper incorporation of the filler to polymer matrix can be estimated using Arrhenius equation (2) a can be quantified using calculation of pseudo-activation energy E_a.

$$lnf = lnf_0 - \frac{E_a}{RT_g} \qquad (2)$$

Where f is the tested frequency, f_0 is the constant characteristic of material, T_g is the glass transition temperature and R is the universal gas constant.

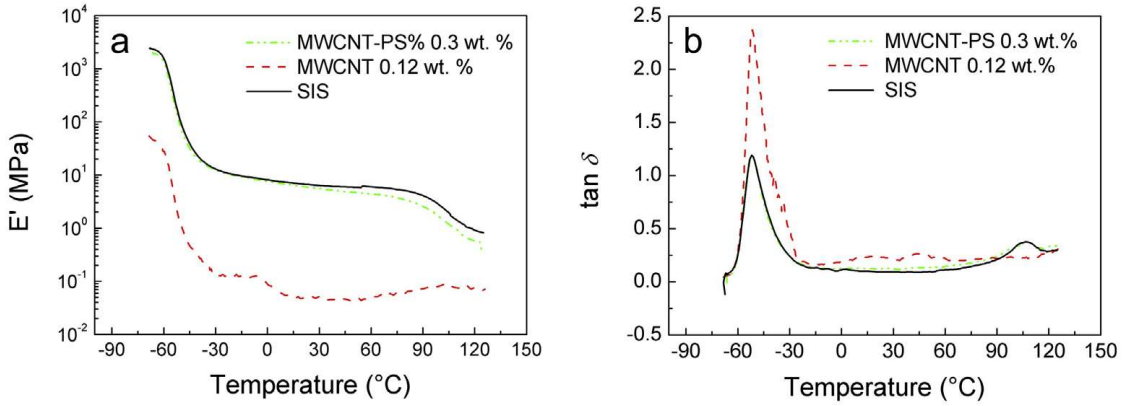

Figure 6. Temperature dependence of a) elastic modulus and b) tan δ of composite [57].

1.5.2 Dielectric properties

Dielectric properties are very often used as tools for investigation of polymer chain dynamics.

Investigation of dielectric properties is very important due to the fact that with the help of measurement in a broad temperature range and frequency-dependent permittivity it is possible to calculate E_a of the glass transition and T_g, which provides information about the polymer chain flexibility in the presence of particles. The flexibility of the polymer matrix is given by two factors, the mobility of the main chain characterized by an α relaxation, corresponding to T_g, and the side chains mobility characterized by α' relaxation, indicating how the entanglements of the side chains got stiff. Therefore, both relaxations are investigated using the Arhenius equation (3) [76].

$$\tau = \tau_0^{\frac{E_a}{kT}} \tag{3}$$

where τ is relaxation time, τ_0 is pre-exponential factor, E_a is activation energy, k is Boltzmann constant, T is temperature [77].

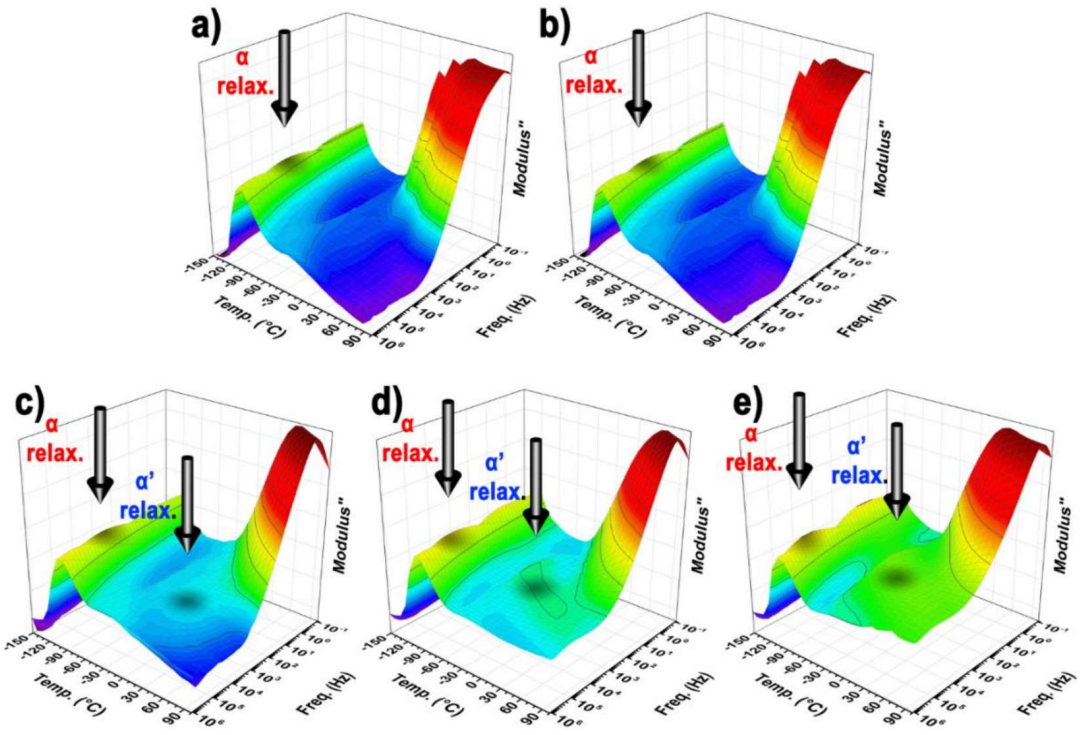

Figure 7. 3D plots of the dielectric properties of the neatPDMS matrix (a), and PDMS matrix filled with GO [76].

In order to appropriately study the polymer chains dynamics, the loss permittivity desired to be recalculated to the loss modulus. This recalculation is achieved according to equation (4, 5, 6).

$$M^* = \frac{1}{\varepsilon^*} \tag{4}$$

$$M' = \frac{\varepsilon'}{\varepsilon'^2 + \varepsilon''^2} \tag{5}$$

$$M'' = \frac{\varepsilon''}{\varepsilon'^2 + \varepsilon''^2} \tag{6}$$

where ε* is the complex permittivity, ε' and ε'' are relative permittivity and loss permittivity, respectively. M*, M' and M'' are complex, storage, and loss dielectric moduli, respectively.

Then the activation energies are calculated to show flexibility of the matrix, the lower activation energy system possess, the lower energy is needed for its actuation.

1.5.3 Viscoelastic properties

Due to their exceptional conformation, the PA systems show complicated flow characteristics, which are essential to be determined in order to evaluate their suitability in practical application. To evaluate suitable compatibility of the matrix and filler the rotational rheology mainly in case of TPEs is used [78]. From the position of the crossover point is able to determine whether the filler was properly

mixed into matrix and the particles are well-dispersed through the composite [79]. The viscoelastic properties of the matrix and nanocomposite are investigated in oscillatory shear mode. The values of G′ and G″ shows the interactions between the matrix polymer chains and the filler as is shown in Figure 8.

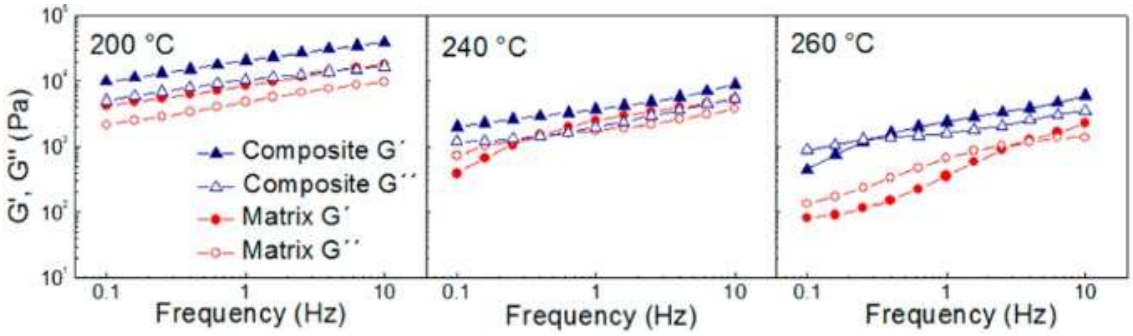

Figure 8. Frequency dependence of storage (G') and loss modulus (G") [79].

1.5.4 Thermal conductivity

Some sorts of electrically conductive fillers may be combined with polymer matrixes to design conductive composites. In order to evaluate thermal activity performance, many investigators have used several methods to determine the thermal conductivity [71]. Generally, the mechanical energy output of shape-memory actuators is determined by the relationship between recoverable stress and strain (shape deformation) [80]. Thus, mechanical properties (Young's modulus) and the capability for heat transfer absorbed by light are important for light-induced stress recovery. The reinforcement and enhanced thermal conductivity of nanocomposites are shown in Figure 9. Through the well-dispersed filler in the composite, one can observe synergic effect in shape-change enhanced by thermal conductivity.

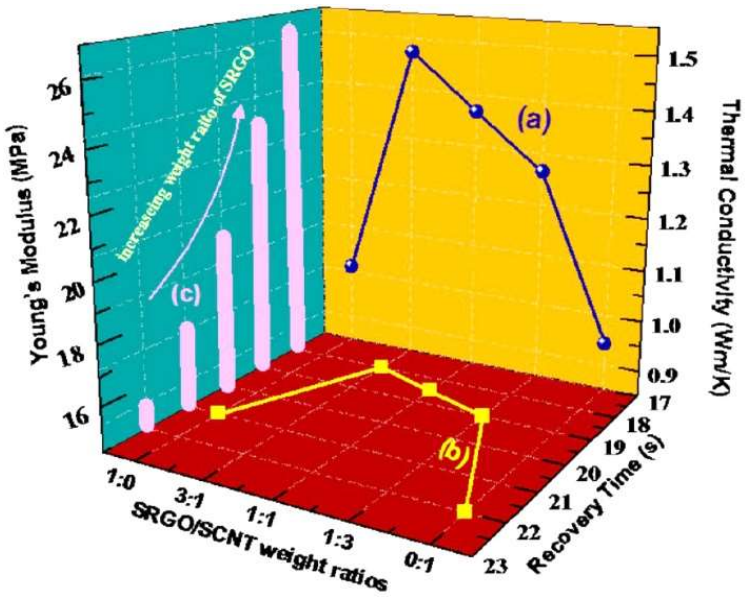

Figure 9. Thermal conductivity (a), the recovery time (b), and Young's modulus of composites (c). [80].

1.6 Methods for determination of photo-actuation behavior

Due to unusual composition of photo-actuating systems a numerous different approaches where settled to investigate photo-actuating ability. The properties of these systems are typically evaluated in absence or presence of the stimulus, usually light in off or on-state.

1.6.1 Dynamometer

One of the setup used to measure PA behavior is the use of dynamometer [56, 81] as is shown in Figure 10. Sample in the strip-shape is fixed into two clamps horizontally, on the both sides of the strip. On the bottom clamp, the weight of several values is attached. Therefore, the preliminary strain is applied. The strip is exposed to the light (ordinarily LED light or laser beam) and then the change in the horizontal dimension is measured. However, the method is fast and the setup is easy to build, materials with different mechanical properties, reported different pre-strain with the same pre-load applied. Thus, the adjusting to certain pre-strain is rather impossible using various weights [33].

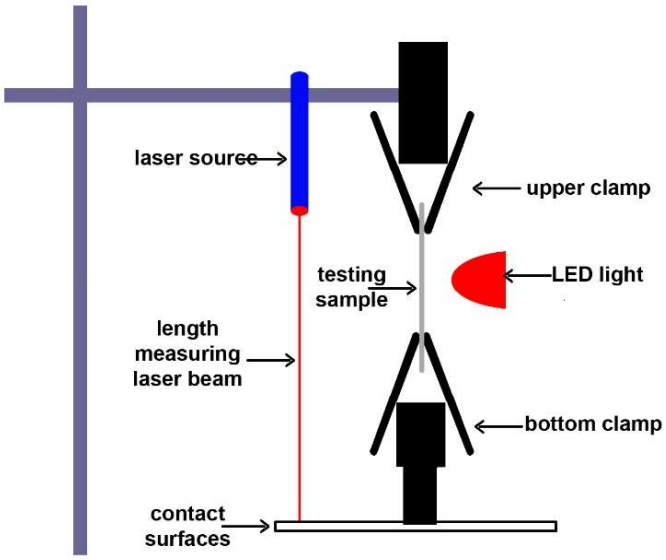

Figure 10. Dynamometer setup used for determination of photo-actuation behavior [33].

1.6.2 Thermomechanical analysis

More accurate method using same principle is, measuring sample with thermomechanical analyzer. Compared to the previous setup, this device is very accurate and a certain value of pre-strain can be finely tuned. The TMA device is able to collect the data each 0.1 s depending on the settings and is able to record the change in the length automatically with very high precision usually in 0.1 μm scale [33, 78, 79, 82].

1.6.3 Dynamic mechanical analysis

The one of the best solution to measure photo-actuation is dynamic mechanical analysis in iso-strain tensile mode (Figure 11). The sample is stretched between two clamps and pre-strain is set. The sample stress is stabilized and then the light is applied. Due to the precise sensor, which calculates the position of the clams, the device record very accurately the load stress caused by actuation of light-stimulated sample. However, DMA is very accurate, some samples cannot be investigate by this method, because, they are not possible to possess such load stress that can be record by the device [56].

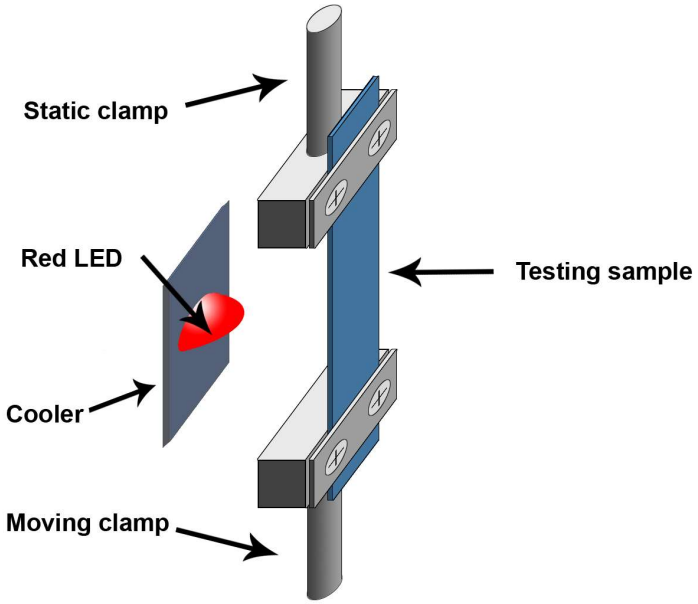

Figure 11. DMA setup for photo-actuation investigation [56].

1.6.4 Atomic force microscopy

Several photo-actuation performance measurements were done by Atomic force microscopy (AFM). This device detects material shape-change through the AFM tip that is placed on the top of the material, as can be seen in the Figure 12. After exposition of sample to the light, the AFM record the tip movement. Although, this technique is suitable to investigate the PA kinetics, there is no option how to calculate the actuation stress and the measurement of the displacement is limited due to the limitation of the AFM tip movement.

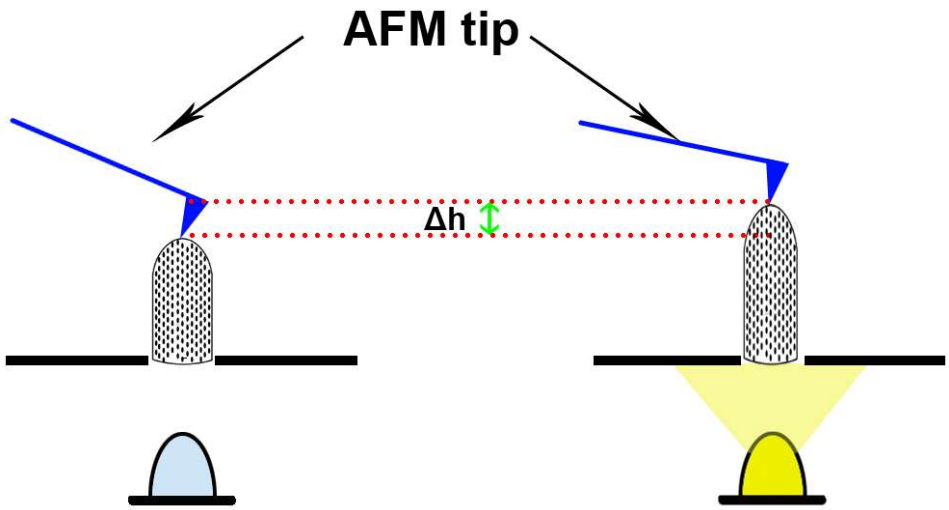

Figure 12. AFM device for determination of the photo-actuation performance [57].

1.7 Drawbacks of the current systems

Despite the enhanced properties, the composites suffer from several drawbacks, which hinder their potential. One of the issue is the poor compatibility of the filler in the matrix. The key role in performance of PA system plays the interface between the particles and the matrix. The elastomeric matrix is usually hydrophobic and particles are hydrophilic or of very different nature with considerably foreign surface properties, from the surface energy point of view. Due to this issue, particles usually form aggregates and their distribution in the system is very poor, and thus lead to the decreased thermal conductivity and unsuitable mechanical properties of the final composite structure.

Another problem is the tenuous deformation of the composite, resulting from weak interaction between filler and matrix, which leads to reducing of the mechanical properties and finally the PA capability and repeatability of the phenomenon.

1.8 State of the art

In order to reduce drawbacks of the PA systems, several techniques and procedures have been investigated. As specified in the beginning, this work was dedicated to photo-actuating systems along with the performance enhancements of the structures through particle's modifications. Indisputably, a big amount of PA research has been done in field that deals with just photo-switchable polymeric films or composites consists of elastomeric matrix and filler which is usually pure carbon-based nanoparticles or nanotubes [73].

Many investigations deal with different photo-actuated materials resulting to different reversible shape-change performances. General investigations are summarized in Table 1.

Table 1. Typical components, benchmark performance, and features of these schemes [73].

Typical components	Benchmark performance	Strengths and weaknesses
- CNT/polymer composites - Gradient rGO/GO structure - Graphene/polymer composites - Graphite/polymer - Amorphous carbon/polymer composite	- High-loading capacity: up to 140 times its own weight - Fast response time and displacement rate: up to 0.3 s at 14 cm/s - Large deformation: up to 479° for bending, 30–400% for contraction, 36° s^{-1} for rotation - Cycling durability: 60000 cycles at ≈2 Hz	- High energy conversion efficiency - Wide light source wavelength range - Fast response - Multiple deformation modes - Reversible deformation - Certain ambient conditions (temperature, humidity, air pressure, etc.) required - Large CTE mismatch required

In one of the studies [83], authors fabricated visible-light-responsive actuators with diverse and tunable deformations by embedding aligned CNTs in paraffin wax on a polyimide substrate. The aligned CNTs play role as cellulose fibrils, and the paraffin wax look like the soft cells/tissues of a plant. Depending on alignment

of the CNTs the prepared strips performed different actuation. The samples expanded perpendicularly in orientation of aligned CNTs. the edges of the CNT/paraffin wax composite film extended outward by 28 μm along the transverse direction.

Another work, [84], deals with modified of graphene-based filler. Surface of graphene was modified by polydopamine and grafted by poly(N-isopropylacrylamide (PNIPAM). The polymer brushes PNIPAM possess flower-form structures, which change their shape after light stimulation. The authors prepared monolayers of this material and encapsulated them into live cells.

In a different investigation [85] light-driven bilayer composite comprising an IR-sensitive reduced graphene oxide in PDMS polymeric composite as an active layer and an IR-inert PDMS as a passive layer, was developed. These bilayer sheets with excellent responsive bending properties and high mechanical properties were used as active hinges for remote construction of complex 3D configurations (such as bidirectionally folded columns, boxes, pyramids, and cars) that demonstrated the three capabilities of these bilayer composites. Their large deformation and excellent stability, their ability to produce complex structures, and their remote-autonomous assembly upon IR irradiation.

In this work [86] authors constructed the rolled CNT/polymer bilayer composite actuators. This actuator with tubular shape exhibits electrically and sunlight-induced actuation with fast response, large deformation, and multiform biomimetic motions through simple configuration design. After light exposure, sample shows mechanical actuation, from flat shape to roller shape, the angle change was 280° in 0.83 s.

Further study [87] demonstrated a novel method of mixing graphene oxide with polycarbonate membrane to form a bilayer assembly through vacuum filtration technique. When IR light stimulated the GO face of GO/PC bilayer, the bilayer foil started deflecting from its equilibrium position rapidly with a response time of less than 1 s. The deformation then grew with time and reached its maximum value i.e. 12 mm within 3 s.

1.9 Synthesis of core-brush nanoparticles

However, GO particles are could serve as very good filler in composites due to their relatively easy preparation process, large surface area, possibility to enhance overall performance of various matrices, they are quite inert, which conclude to poor dispersibility, weak filler/matrix interaction which leads to the local inhomogenities and finally to bad heat distribution through the system. To solve this problem, particles have to be modified. One of the solution is the grafting of polymer brushes onto the surface of the particles. Polymer brushes create a layer on the surface of particles, which prevents their aggregation, enhance their compatibility to the matrix etc. The most common approaches for covalent attachment of macromolecular chains on to GO surface can be classified as “grafting-to”, “grafting-from” and “grafting through” [88].

1.9.1 Grafting-to approach

In this technique, the polymer is firstly synthetized and then covalently link to the surface of the particle, which possess with a reactive group. This approach shows the benefit of being relatively simple, although the number of functional groups per surface area (grafting density) that can be obtained is both kinetically and thermodynamically limited [89]. Once, the surface is covered by polymer brushes, the polymer concentration at interfaces becomes larger than in solution. This leads to slowing down the immobilization reaction at the surface and decreasing of attachment rate. Another problem is that this approach creates impurities of non-grafted chains [90].

1.9.2 Grafting-from approach

On the other hand, grafting-from strategy is based on the growth of polymer brushes from the surface by using initiator, which is attached to the particle [91]. This method is also known as surface-initiated polymerization and is typically used for synthesis of inorganic-organic core-brush morphologies [88]. It has been assumed as an effective technique to control the interfacial behavior [92]. First, the initiator is immobilized at the surface and then the polymer chain start to growth from this initiator species. Contrary previous method high grafting density can be obtained [93].

1.9.2.1 Free radical polymerization

This method of polymerization is the most commonly used for synthesis of commercially available polymers. This is caused by many attractive characteristics that this method possesses. It is applicable to the wide range of monomers and copolymers with any functional group, compared to other polymerization methods it has higher tolerance to the water and other impurities, a wide range of temperatures, available media can be used as suitable reaction conditions, and it is cheaper compared to other technologies [94]. Although many advantages mentioned above, free radical polymerization is an uncontrolled process, which has no capability of controlling polymer architecture, i.e. molecular weight and molecular weight distribution of the grafts. The reaction begins with the generation of free radical spots on the main backbone that react with the vinyl or acrylic monomer to propagate a new polymer chain covalently bonded to the backbone. Finally, grafted chains terminate through termination or chain transfer reactions [92].

1.9.2.2 Nitroxide-Mediated Polymerization (NMP)

This polymerization method belongs to the group of the stable free radical polymerization procedures. It is built on the usage of a stable nitroxide radical. It appears to be very simple technique because it needs only addition of a proper alkoxyamine to the polymerization medium. The propagating species reacts with a stable radical to form dormant species. The resulting dormant species can then reversibly cleave to transform the free radicals [92]. The chain is starting to grow

until the monomer is consumed. This method is usually used for styrene and acrylate monomers [95].

1.9.2.3 Atom transfer radical polymerization (ATRP)

ATRP is great technique for grafting polymer brushes, which allows precisely control the chemistry of size, functionalities and construction of the polymers as well as to achieve the identical growth of all the chains [96]. The mechanism of ATRP is depict by Figure 13.

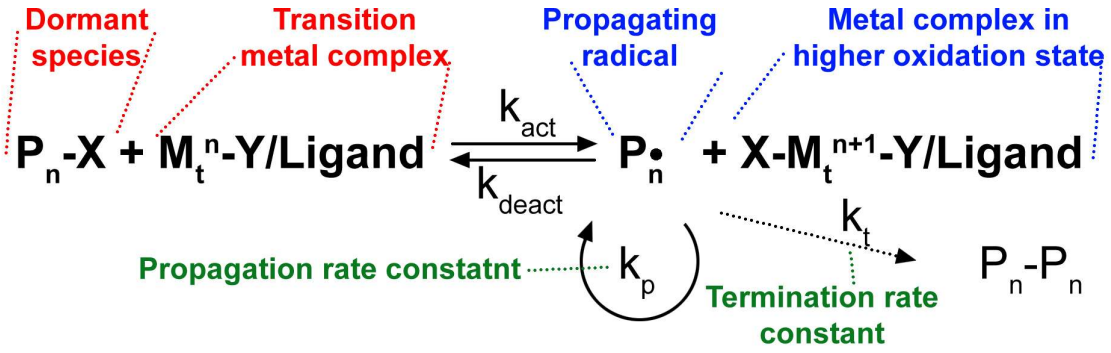

Figure 13. Scheme of the ATRP reaction [97].

ATRP is based on an inner sphere electron transfer procedure, which contains a reversible halogen transfer from a dormant species to a transition metal complex [97]. This leads to formation of propagating radicals and the metal complex in higher oxidation state. Polymer chains grow by the connecting monomers to the created radicals. They respond reversibly with the oxidized metal complexes, a dormant species and the transition metal complex in the lower oxidation state. Radicals also terminate with the rate constant of termination [98]. ATRP can be used on the nearly all of vinyl and acrylic monomers over wide temperature range. ATRP controls the sustained radical effect; therefore, the concentration of catalyst should be high to maintain a high polymerization rate [99]. In these high concentrations , most of metal catalysts are expensive and toxic, thus to remove them from the polymer needs expensive and time-consuming techniques [92].

1.9.3 Grafting-through

This strategy is also known as the macromonomer method and it could be reputed as in-between method of previously described techniques. The polymerizable groups are anchored onto the surface of nanoparticles. The reaction solution contains initiator, monomers and modified nanoparticles, which play role as crosslinking agent. Thus, both monomers copolymerize and the inorganic phase is incorporated inside polymer chains [100]. This process is not much explored from scientific point of view and the mechanisms that control the polymerization progression are not entirely understood [101].

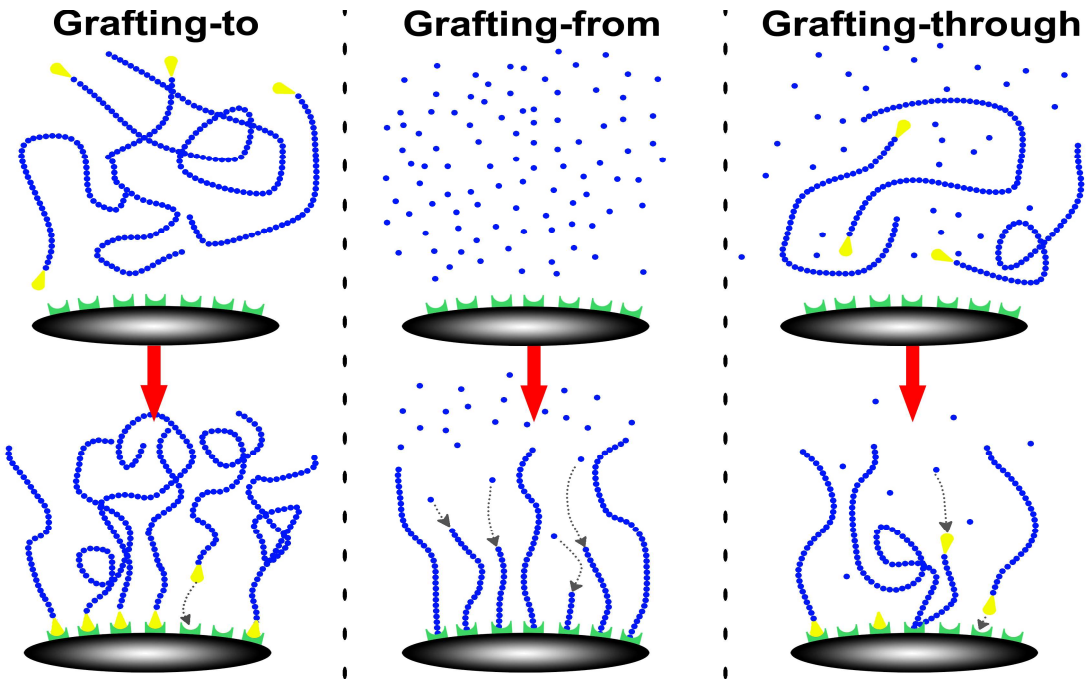

Figure 14. Schematic presentation of grafting-to, grafting-from and grafting-through techniques. Blue dots representing monomer, blue chain represents polymer, yellow shape is functional group, green shape is surface-attached initiator [92].

2 MOTIVATION AND AIMS OF THE DOCTORAL STUDY

2.1 Motivation

The PA systems belong among intelligent materials that can reversibly change their physical properties after the application of external light. These materials play a significant role in many industries ranging from civil to biomechanical engineering.

2.2 Aims of the doctoral study

The main aim of this thesis was to analyze and compare the performance properties of the PA systems containing differently ATRP-grafted graphene oxide particles. The key tasks were defined as follows:

a) Complex study of physical and chemical aspects affecting the performance of the PA systems,
b) Synthesis and preparation of novel particles with tailored properties via SI-ATRP, which could be successfully used as active fillers in PA systems in order to improve their PA performance,
c) Analysis of the modified particles and their influence on mechanical properties, compatibility with polymer matrix and thermal conductivity of the systems.
d) Analysis of the effect of the particles modification on the PA performance and physical properties. Evaluation of the system's efficiency by comparing their properties with unmodified GO particles.

3 SUMMARY OF RESULTS

This thesis deals with the synthesis of particles and their modification via surface-initiated ATRP and their possible use in the PA systems in order to reduce the outlined drawbacks. Due the fact that most of the papers are connected via SI-ATRP technique, synthesis and general characterization of the particles are firstly specified. Additional, the most significant results of the individual papers are stated.

3.1 Preparation of graphene oxide particles

In order to find good conductive material, it was decided to prepare our own graphene oxide particles, with capability of easy and accurate way of changing their conductivity. There are several methods to prepare GO particles from graphite [102-104].

GO was prepared according to modified Hummer's method [105]. GO was fabricated from graphite powder. The raw graphite was stirred with concentrated sulfuric acid. Subsequently, sodium nitrate and potassium permanganate were gradually added. The mixture was additionally stirred then the deionized water was added. Finally, concentrated hydrogen peroxide was added, and the solution turned its color into brilliant brown, which indicated complete oxidization of graphite. The product was separated in a high–speed centrifuge. The cleaning routine was based on dispersion of the GO in hydrochloric acid, and the re–separation in a centrifugal field. The particles were lyophilized in order to remove the residual water after the purification process.

.

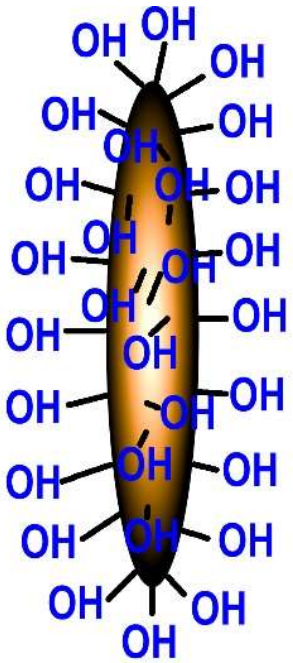

Figure 15. Functional groups of Hummer's method [1].

3.2 Modification of GO particles through SI-ATRP

The problem with GO particles is with their bad affinity to matrixes and attribute to coagulate and sediment. To enhance particles attraction to matrix and reduce their sedimentation and coagulation process, GO particles were grafted with polymer via SI-ATRP [106]. The GO particles were modified via amidation reaction with α-Bromoisobutyryl bromide (BiBB). The particles were then washed and dried. Finally, the initiator-modified GO sheets were grafted with poly(methyl methacrylate) (PMMA), poly(butyl methacrylate) (PBMA), poly(glycidyl methacrylate) (PGMA) or poly(trimethylsilyloxyethyl methacrylate) (PHEMATMS) under precise argon atmosphere. Through different ratio between monomer, initiator, ligand (N,N,N′,N″,N″-Pentamethyldiethylenetriamine) (PMDTA) and catalyst (CuBr) by length of reaction mixing and changing them reaction temperature, the length of resulting polymer chains is easy to control.

The GO particles modified by PMMA and PMMA were utilize to prepare photo-actuators in order to investigate polymer compatibility to the chemically (PDMS) and physically Poly(propylene-co-ethylene) cross-linked matrix (Paper I, IV). Particles grafted with PGMA in different molar ratio of reactants were prepared to investigate compatibility to the matrix (PDMS) and graphene oxide reduction (Paper II). The PHEMATMS is hydrophobic, hence we expected the silyl-based polymer would improve the interaction of GO particles with PDMS served as matrix (Paper III).

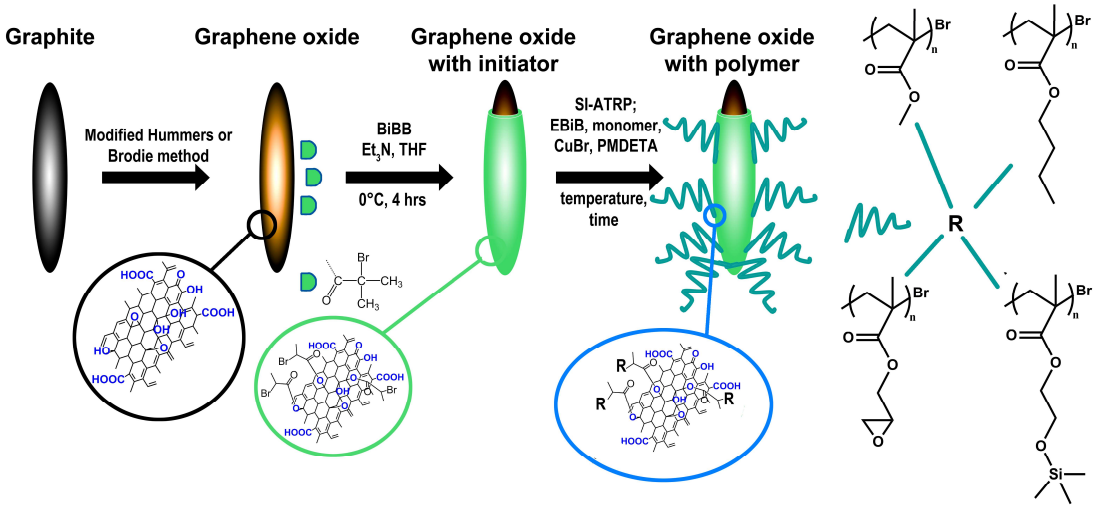

Figure 16. Immobilization of BIBB initiator on functionalized GO particles with their subsequent grafting with polymer via SI-ATRP [105].

For each reaction, the molar ratio between the monomer and the initiator was defined in order to obtain the desired polymer chain length, which was theoretically designated before the experiment. The determination of the molecular weight was able due to the presence of a free initiator ethyl α-bromoisobutyrate (EBiB) in reaction. The molecular weight was investigated by

gel permeation chromatography (GPC) and monomer conversion was calculated using nuclear magnetic resonance (NMR). The results were evaluated according to literature [107] and are summarized in Table 2.

Table 2. Molecular characteristics of prepared GO particles

Sample name	Monomer	Initiator	Ligand	Catalyst	M_n (g·mol^{-1})	DP_n (-)	PDI (-)	Conversion (%)
GO-PMMA	100	1	4	1	5600	56	1.18	89
GO-PBMA	100	1	4	1	5200	37	1.21	91
GO-PGMA 1	100	1	2	1	5900	42	1.28	43
GO-PGMA 2	100	1	4	1	6100	43	1.26	46
GO-PHEMATMS	100	1	4	1	12600	62	1.19	67
GO-PMMA-V	100	1	4	1	6800	68	1.18	89
GO-PBMA-V	100	1	4	1	5800	41	1.21	89

3.3 Characterization of prepared grafted and non-grafted GO particles

Results, which describe grafted and non-grafted GO particles characteristics obtained from each paper (P), are summarized in Table 3. Raman spectroscopy served to show variation in I_D/I_G ratio which indicates the reduction of GO which also leads to higher electrical conductivity (Cond.). This enhance the heat distribution through the composite system. Contact angle measurement (CA) was performed to prove GO particles affinity to the matrix. Small droplet of siloxane was added to the GO pellet and in all cases, modified GO particles posses with lower CA, which means that they are more compatible to the matrix, thus the better dispersion could be reached.

Table 3. Results from measurements done on GO particles

Paper	Material	I_D/I_G (-)	CA (°)	Cond. (S·cm^{-1})	Other measurements done
P I	Neat GO	0,90	49.9	2.1×10^{-7}	^{1}H NMR, TEM, TGA-FTIR, GPC, AFM
	GO-PMMA	1.05	38.7	6.3×10^{-8}	
	GO-PBMA	1.08	28.7	2.1×10^{-7}	
P II	GO-PGMA1	1.08	40.1	5×10^{-7}	^{1}H NMR, TEM, TGA-FTIR, GPC
	GO-PGMA2	1.26	40.1	2.3×10^{-3}	
PIII	GO-PHEMATMS	1.09	26.3	6×10^{-7}	^{1}H NMR, TEM, TGA-FTIR, GPC
P IV	GO-PMMA	1.05	-	6.3×10^{-8}	^{1}H NMR, GPC, TGA-FTIR, TEM, XPS
	GO-PBMA	1.08	-	2.1×10^{-7}	

3.4 Characterization of composites

The composites properties are depicted in Table 4. For each composite, the dielectric spectroscopy was measured. The flexibility of the polymer matrix is given by two factors, mobility of the main chain characterized by α relaxation, corresponding to T_g, and side chains mobility characterized by α' relaxation, indicating how the entanglements of side chains are stiff. Therefore, both relaxation were investigated using Arhenius equation. The activation energy (E_a) of α relaxation is significantly shifted to the lower values after grafting the particles, indicating the improved flexibility of the polymer matrix. Thermal conductivity (TC) shows the slightly increase which is resulting to the better heat distribution through the composite.

Table 4. Composite performance with grafted and non-grafted GO particles in 0.1 vol. % concentration

Paper	Material	E_a ($kJ \cdot mol^{-1}$)	TC ($W \cdot mK^{-1}$)	Δl (μm)	ε (%)	Other measurements
P I	neat PDMS	45.70	0,071	7,1	0,071	DMA, Diel. spectroscopy
	GO/PDMS	36.57	0.144	9.1	0.091	
	GO-PMMA/PDMS	35.99	0.153	9.4	0.094	
	GO-PBMA/PDMS	25.39	0.151	11.8	0.118	
P II	GO-PGMA 1/PDMS	31.32	0.152	12.50	0.125	DMA, Diel. spectroscopy
	GO-PGMA 2/PDMS	23.80	0.161	20.20	0.202	
P III	GO-PHEMA/PDMS	22.01	-	34	0.34	DMA, Diel. spectroscopy
P IV	neat Vistamaxx	-	0.89	12	0.12	Rheology
	GO/Vistamaxx	-	0.156	20	0.2	
	GO-PMMA/Vistamaxx	-	0.196	30	0.3	
	GO-PBMA/Vistamaxx	-	0.202	68	0.68	

The photo-actuation performance was studied for various composite structures, and the influence of the filler modification and the filler loading on the final properties was explained. Substantial part of the work deals with photo-actuation of composites in which filler is modified GO by different polymer brushes, and matrix is cross-linked PDMS (Paper I, II, III). Paper IV discuss the PA performance of PMMA and PBMA modified GO particles in thermoplastic elastomer matrix, specifically, poly(ethylene-co-propylene) (Vistamaxx). The dimension change in absolute value are explained by Δl. To compare PA performance with other scientific researches the relative value of prolongation was counted (ε)

$$\varepsilon = \frac{\Delta l}{l_0} \times 100 \quad (7)$$

where Δl is the dimension change in absolute value and l0 is the initial length of the sample.

The Figure 17 shows difference in PA deformation for four different samples. Neat PDMS matrix maximum value of actuation was ΔL, was 7.1 μm. With addition of 0.1% of GO particles, this value increased to 9.1 μm, which was caused by improved heat transfer. The matrix with modified GO particles performed even higher ΔL value, 9.4 μm and 11.8 μm for GO-PMMA and GO-PBMA respectively. The reason for this behavior is due to proper incorporation of the particles into PDMS matrix, which causes better shape recovery and improved heat transitions within the samples.

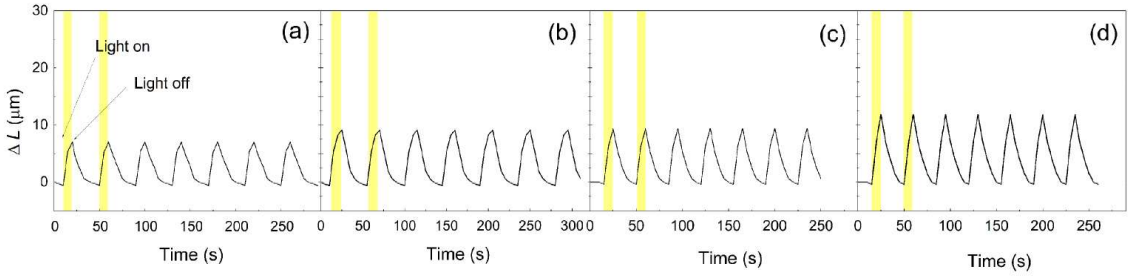

Figure 17. Photo-actuation performance of the pure PDMS (a) and the PDMS composites containing 0.1 vol % of neat GO (b), GO–PMMA (c) and GO–PBMA (d) [108].

By using TPE matrix the PA performance is even better compared to PDMS matrix. Composites containing the same filler but vistamaxx matrix show significant enhancement in shape change in dimension as it can be seen in Figure 18.

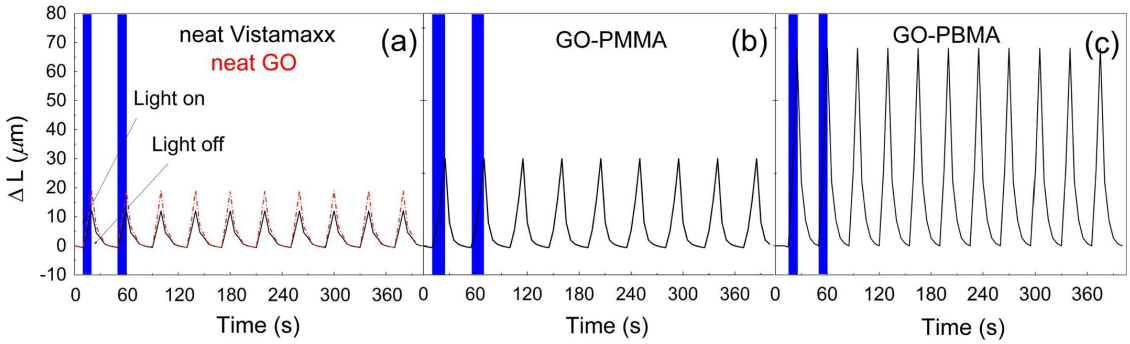

Figure 18. Photo-actuation performance of neat vistamaxx and composite containing 0.1 vol.% of neat GO (a), GO-PMMA (b) and GO-PBMA (c) [20].

After increasing of GO particles concentration in the system to the 1 vol.% the maximum actuation value was roughly five times higher as it is showed in Figure 19. The main reason for this significant enhancement was already proposed by earlier researches and is likely the improved flexibility of the polymer composite, which was confirmed by the lower activation energy, higher damping and

enhanced thermal conductivity, improving the heat delivery within the composite samples [108].

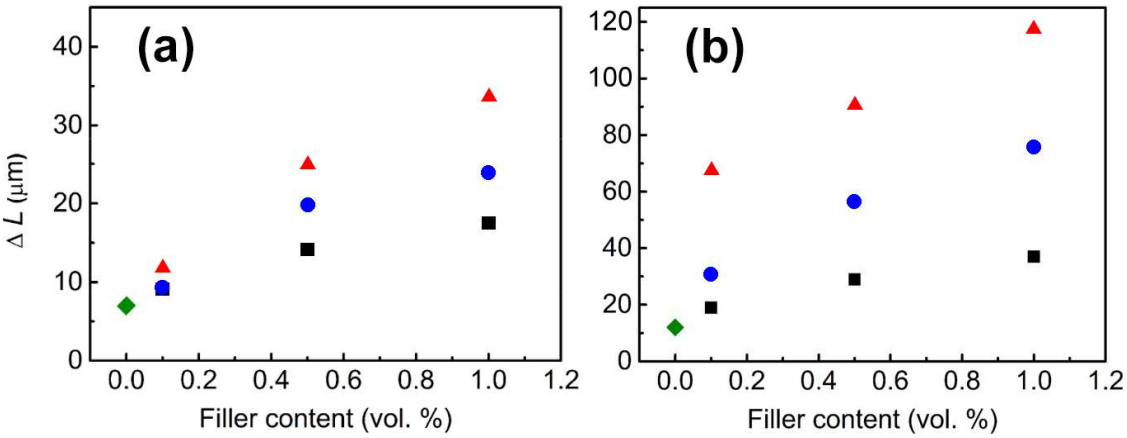

Figure 19. Dependence of the filler content on the change in the length for the pure matrix (green diamond), GO-PMMA (black squares), GO-PBMA (red triangles) for composite with PDMS (a) and Vistamaxx (b) matrix [20, 108].

4 CONTRIBUTIONS TO THE SCIENCE

The main outputs and crucial points of this doctoral study those are beneficial to the both, scientific audience as well as industry, are highlighted below:

- SI-ATRP modification of GO particles with various monomeric systems.
- Confirmation that the simultaneous reduction of GO and modification with polymer brushes is possible for variety of monomers.
- Developed PA device based on thermo-mechanical analyzer which was applied as national utility model no. 31633, named " Zařízení pro sledování změny rozměrů vlivem světelné stimulace".
- Improved compatibility between the polymer matrix and GO particles due to the SI-ATRP modification and knowledge how the similarity of the grafting moiety contribute to this compatibility.
- Improved and homogenous dispersibility of the GO-grafted filler in polymer matrix which contribute to enhanced thermal conductivity.
- Direct comparison of PA performance between the chemically cross-linked systems and TPEs.
- Showed that various filler content and various light intensities can alter the final PA capability.
- Confirmation, that SI-ATRP approach used of GO modification can be effectively applied for filler modification and subsequently mixed into the elastomeric matrix, those capabilities are in the range suitable to be applied as a pre-stretched films in the tactile display systems.

CONCLUSIONS

Some of the common drawbacks of conventional PA systems were successfully eliminated using novel approach based on the fabrication of the precisely grafted GO particles via SI-ATRP. The modification of particles were done in controlled regime; hence, the possible of prepared materials exceeded the properties of the systems without modification.

In conclusion, this thesis summarizes utilization of GO particles modified by different polymer chains and also using different matrix that significantly improved the PA ability of whole systems. Due to this modifications, the GO particles possessed better compatibility to matrices, such as chemically cross-liked PDMS or thermoplastic elastomers based on polyolefins and led to enhanced dispersion through the matrix, therefore the heat distribution could be easily transferred into the entire composite. The PA ability was verified by system based on thermo-mechanical analysis, which confirmed the significantly enhanced photo-actuation capability (in some cases even more than ten times higher) compared to neat matrix material and in contrast to other publications as well as systems containing unmodified particles.

REFERENCES

[1] MENG, H.; HU, J. L. A Brief Review of Stimulus-active Polymers Responsive to Thermal, Light, Magnetic, Electric, and Water/Solvent Stimuli. *J. Intell. Mater. Syst. Struct.* **2010**, vol. 21, no. 9, pp. 859-85.

[2] AHN, S. K.; KASI, R. M.; KIM, S. C.; SHARMA, N.; ZHOU, Y. X. Stimuli-responsive polymer gels. *Soft Matter*. **2008**, vol. 4, no. 6, pp. 1151-57.

[3] XIE, T. Recent advances in polymer shape memory. *Polymer*. **2011**, vol. 52, no. 22, pp. 4985-5000.

[4] KIEVIET, B. D.; SCHON, P. M.; VANCSO, G. J. Stimulus-responsive polymers and other functional polymer surfaces as components in glass microfluidic channels. *LChip*. **2014**, vol. 14, no. 21, pp. 4159-70.

[5] AHIR, S. V.; TERENTJEV, E. M. Photomechanical actuation in polymer-nanotube composites. *Nat. Mater.* **2005**, vol. 4, no. 6, pp. 491-95.

[6] TIWARI, R.; MELLER, M. A.; WAJCS, K. B.; MOSES, C.; REVELES, I.; GARCIA, E. Hydraulic artificial muscles. *J. Intell. Mater. Syst. Struct.* **2012**, vol. 23, no. 3, pp. 301-12.

[7] YU, N.; HOLLNAGEL, C.; BLICKENSTORFER, A.; KOLLIAS, S. S.; RIENER, R. Comparison of MRI-compatible mechatronic systems with hydrodynamic and pneumatic actuation. *IEEE/ASME Trans. Mechatron*. **2008**, vol. 13, no. 3, pp. 268-77.

[8] RAHMAN, M. F.; CHEUNG, N. C.; LIM, K. W. Position estimation in solenoid actuators. *ITIA*. **1996**, vol. 32, no. 3, pp. 552-59.

[9] CRAWLEY, E. F.; DELUIS, J. Use of piezoelectric actuators as elements of intelligent structures. *AIAA J.* **1987**, vol. 25, no. 10, pp. 1373-85.

[10] JANI, J. M.; LEARY, M.; SUBIC, A.; GIBSON, M. A. A review of shape memory alloy research, applications and opportunities. *Mater. Des.* **2014**, vol. 56, no., pp. 1078-113.

[11] GONG, D. C.; XIANG, Z. Q.; PAN, X. H.; TANG, Z. F.; IEEE. Strategy and experiment of Giant Magnetorestrictive Actuator's orientation control based on preisach model. Wcica 2006: Sixth World Congress on Intelligent Control and Automation, Vols 1-12, Conference Proceedings; 2006; New York: Ieee.

[12] HUBER, J. E.; FLECK, N. A.; ASHBY, M. F. The selection of mechanical actuators based on performance indices. *Proc. R. Soc. London, Ser. A*. **1997**, vol. 453, no. 1965, pp. 2185-205.

[13] JIANG, H. R.; LI, C. S.; HUANG, X. Z. Actuators based on liquid crystalline elastomer materials. *Nanoscale*. **2013**, vol. 5, no. 12, pp. 5225-40.

[14] YU, H. F. Photoresponsive liquid crystalline block copolymers: From photonics to nanotechnology. *Prog. Polym. Sci.* **2014**, vol. 39, no. 4, pp. 781-815.

[15] JUNG, B. D.; STUMPE, J.; HONG, J. D. Influence of multilayer nanostructures on photoisomerization and photoorientation of azobenzene. *Thin Solid Films*. **2003**, vol. 441, no. 1-2, pp. 261-70.

[16] MAEDA, M.; YAMASAKI, S. Effect of silica addition on crystallinity and photo-induced hydrophilicity of titania-silica mixed films prepared by sol-gel process. *Thin Solid Films*. **2005**, vol. 483, no. 1-2, pp. 102-06.

[17] LEFIN, P.; FIORINI, C.; NUNZI, J. M. Anisotropy of the photo-induced translation diffusion of azobenzene dyes in polymer matrices. *Pure Appl. Opt.* **1998**, vol. 7, no. 1, pp. 71-82.

[18] PALTO, S. P.; DURAND, G. Friction model of photoinduced reorientation of optical-axis in photoi-oriented langmuir-blodgett-films. *J. Phys. II*. **1995**, vol. 5, no. 7, pp. 963-78.

[19] KOZENKOV, V. M.; YUDIN, S. G.; KATYSHEV, E. G.; PALTO, S. P.; LAZAREVA, V. T.; BARACHEVSKII, V. A. Photoinduced optical anisotropy in multilayered langmuir films. *PZhTF*. **1986**, vol. 12, no. 20, pp. 1267-72.

[20] OSICKA, J.; MRLIK, M.; ILCIKOVA, M.; KRUPA, I.; SOBOLCIAK, P.; PLACHY, T.; MOSNACEK, J. Controllably coated graphene oxide particles with enhanced compatibility with poly(ethylene-co-propylene) thermoplastic elastomer for excellent photo-mechanical actuation capability. *React. Funct. Polym.* **2020**, vol. 148, no., pp. 8.

[21] HU, Y.; LI, Z.; LAN, T.; CHEN, W. Photoactuators for Direct Optical-to-Mechanical Energy Conversion: From Nanocomponent Assembly to Macroscopic Deformation. *Adv. Mater.* **2016**, vol. 28, no. 47, pp. 10548-56.

[22] HU, Y.; WU, G.; LAN, T.; ZHAO, J. J.; LIU, Y.; CHEN, W. A Graphene-Based Bimorph Structure for Design of High Performance Photoactuators. *Adv. Mater.* **2015**, vol. 27, no. 47, pp. 7867-73.

[23] POOSANAAS, P.; TONOOKA, K.; ABOTHU, I. R.; KOMARNENI, S.; UCHINO, K. Influence of composition and dopant on photostriction in lanthanum-modified lead zirconate titanate ceramics. *J. Intell. Mater. Syst. Struct.* **1999**, vol. 10, no. 6, pp. 439-45.

[24] BELL, G. A. The production of sound by radiant energy. *Science*. **1881**, vol. 2, no. 49, pp. 242-53.

[25] GURNEY, J. O. Photofluidic interface. *J Dyn Syst Meas Control*. **1984**, vol. 106, no. 1, pp. 90-97.

[26] LU, S.; AHIR, S.; VELASCO, V.; KING, B.; XU, P.; TERENTJEV, E. M.; PANCHAPAKESAN, B. Photo-mechanical actuation of carbon nanotubes: mechanismsand applications in micro and nano-devices. *J. Microbio. Robot*. **2009**, vol. 5, no. 1-2, pp. 29-41.

[27] HOCKADAY, B. D.; WATERS, J. P. Direct optical-to-mechanical actuation. *Appl. Opt.* **1990**, vol. 29, no. 31, pp. 4629-32.

[28] LIU, K.; WANG, W.; LIU, Q.; SONG, L.; GUO, Y. W.; YE, F. Photostriction properties of PLZT (4/52/48) ceramics sintered by SPS. *Ceram. Int.* **2019**, vol. 45, no. 2, pp. 2097-102.
[29] LI, C. S.; LIU, Y.; LO, C. W.; JIANG, H. R. Reversible white-light actuation of carbon nanotube incorporated liquid crystalline elastomer nanocomposites. *Soft Matter*. **2011**, vol. 7, no. 16, pp. 7511-16.
[30] LV, J. A.; LIU, Y. Y.; WEI, J.; CHEN, E. Q.; QIN, L.; YU, Y. L. Photocontrol of fluid slugs in liquid crystal polymer microactuators. *Nature*. **2016**, vol. 537, no. 7619, pp. 179-+.
[31] LYUBIN, V. M.; TIKHOMIROV, V. K. Novel photoinduced effects in chalcogenide glasses. *J. Non-Cryst. Solids*. **1991**, vol. 135, no. 1, pp. 37-48.
[32] BEHL, M.; LENDLEIN, A. Shape-memory polymers. *Mater. Today*. **2007**, vol. 10, no. 4, pp. 20-28.
[33] ILČÍKOVÁ, M.; MRLÍK, M.; MOSNÁČEK, J. Thermoplastic Elastomers with Photo-actuating Properties. In: Das, C. K., editor. *Thermoplastic Elastomers - Synthesis and Applications*. IntechOpen; **2015**. pp. 115-44.
[34] HASAN, S. M.; NASH, L. D.; MAITLAND, D. J. Porous shape memory polymers: Design and applications. *Journal of Polymer Science Part B-Polymer Physics*. **2016**, vol. 54, no. 14, pp. 1300-18.
[35] YESODHA, S. K.; PILLAI, C. K. S.; TSUTSUMI, N. Stable polymeric materials for nonlinear optics: a review based on azobenzene systems. *Prog. Polym. Sci.* **2004**, vol. 29, no. 1, pp. 45-74.
[36] ILNYTSKYI, J.; SAPHIANNIKOVA, M.; NEHER, D. Photo-induced deformations in azobenzene-containing side-chain polymers: molecular dynamics study. *Condens. Matter Phys.* **2006**, vol. 9, no. 1, pp. 87-94.
[37] GARCIA-AMOROS, J.; SZYMCZYK, A.; VELASCO, D. Nematic-to-isotropic photo-induced phase transition in azobenzene-doped low-molar liquid crystals. *PCCP*. **2009**, vol. 11, no. 21, pp. 4244-50.
[38] LI, C.; YUN, J. H.; KIM, H.; CHO, M. Light Propagation and Photoactuation in Densely Cross-Linked Azobenzene-Functionalized Liquid-Crystalline Polymers: Contribution of Host and Concerted Isomerism. *Macromolecules*. **2016**, vol. 49, no. 16, pp. 6012-20.
[39] WEN, Z. B.; YANG, K. K.; RAQUEZ, J. M. A Review on Liquid Crystal Polymers in Free-Standing Reversible Shape Memory Materials. *Molecules*. **2020**, vol. 25, no. 5, pp. 13.
[40] PRAMANIK, S.; PINGGUAN-MURPHY, B.; ABU OSMAN, N. A. Developments of Immobilized Surface Modified Piezoelectric Crystal Biosensors for Advanced Applications. *International Journal of Electrochemical Science*. **2013**, vol. 8, no. 6, pp. 8863-92.
[41] ATHANASSIOU, A.; KALYVA, M.; LAKIOTAKI, K.; GEORGIOU, S.; FOTAKIS, C. All-optical reversible actuation of photochromic-polymer microsystems. *Adv. Mater.* **2005**, vol. 17, no. 8, pp. 988-+.

[42] UCHINO, K.; POOSANAAS, P.; TONOOKA, K. Photostrictive actuators - New perspective. *Fer*. **2001**, vol. 264, no. 1-4, pp. 1961-66.
[43] SULFRIDGE, M.; SAIF, T.; MILLER, N.; O'HARA, K. Optical actuation of a bistable MEMS. *JMemS*. **2002**, vol. 11, no. 5, pp. 574-83.
[44] CHIOU, P. Y.; MOON, H.; TOSHIYOSHI, H.; KIM, C. J.; WU, M. C. Light actuation of liquid by optoelectrowetting. *SeAcA*. **2003**, vol. 104, no. 3, pp. 222-28.
[45] IKEHARA, T.; TANAKA, M.; SHIMADA, S.; MATSUDA, H. Optically driven actuator using photo-induced phase-transition polymer. *SeAcA*. **2002**, vol. 96, no. 2-3, pp. 239-43.
[46] CVIKLINSKI, J.; TAJBAKHSH, A. R.; TERENTJEV, E. M. UV isomerisation in nematic elastomers as a route to photo-mechanical transducer. *EPJE*. **2002**, vol. 9, no. 5, pp. 427-34.
[47] BELFORTE, G.; EULA, G.; FERRARESI, C.; NAKADA, T. Mechanical microactuators with photostrictive control. *JSME Int J., Ser. C*. **1998**, vol. 41, no. 4, pp. 886-92.
[48] SYMS, R. R. A. Surface tension powered self-assembly of 3-D micro-optomechanical structures. *JMemS*. **1999**, vol. 8, no. 4, pp. 448-55.
[49] JOUSSELME, B.; BLANCHARD, P.; GALLEGO-PLANAS, N.; LEVILLAIN, E.; DELAUNAY, J.; ALLAIN, M.; RICHOMME, P.; RONCALI, J. Photomechanical control of the electronic properties of linear pi-conjugated systems. *Chemistry-a European Journal*. **2003**, vol. 9, no. 21, pp. 5297-306.
[50] KRECMER, P.; MOULIN, A. M.; STEPHENSON, R. J.; RAYMENT, T.; WELLAND, M. E.; ELLIOTT, S. R. Reversible nanocontraction and dilatation in a solid induced by polarized light. *Science*. **1997**, vol. 277, no. 5333, pp. 1799-802.
[51] WARNER, M.; TERENTJEV, E. Thermal and photo-actuation in nematic elastomers. *Macromolecular Symposia*. **2003**, vol. 200, no., pp. 81-92.
[52] KOERNER, H.; PRICE, G.; PEARCE, N. A.; ALEXANDER, M.; VAIA, R. A. Remotely actuated polymer nanocomposites - stress-recovery of carbon-nanotube-filled thermoplastic elastomers. *Nat. Mater.* **2004**, vol. 3, no. 2, pp. 115-20.
[53] BISOYI, H. K.; LI, Q. Light -Driven Liquid Crystalline Materials: From Photo -Induced Phase Transitions and Property Modulations to Applications. *Chem. Rev.* **2016**, vol. 116, no. 24, pp. 15089-166.
[54] OSICKA, J.; MRLIK, M.; ILCIKOVA, M.; HANULIKOVA, B.; URBANEK, P.; SEDLACIK, M.; MOSNACEK, J. Reversible Actuation Ability upon Light Stimulation of the Smart Systems with Controllably Grafted Graphene Oxide with Poly (Glycidyl Methacrylate) and PDMS Elastomer: Effect of Compatibility and Graphene Oxide Reduction on the Photo-Actuation Performance. *Polymers*. **2018**, vol. 10, no. 8, pp. 14.

[55] PUNETHA, V. D.; HA, Y. M.; KIM, Y. O.; JUNG, Y. C.; CHO, J. W. Interaction of photothermal graphene networks with polymer chains and laser-driven photo-actuation behavior of shape memory polyurethane/epoxy/epoxy-functionalized graphene oxide nanocomposites. *Polymer*. **2019**, vol. 181, no., pp.
[56] CZANIKOVA, K.; TORRAS, N.; ESTEVE, J.; KRUPA, I.; KASAK, P.; PAVLOVA, E.; RACKO, D.; CHODAK, I.; OMASTOVA, M. Nanocomposite photoactuators based on an ethylene vinyl acetate copolymer filled with carbon nanotubes. *SeAcB*. **2013**, vol. 186, no., pp. 701-10.
[57] ILCIKOVA, M.; MRLIK, M.; SEDLACEK, T.; CHORVAT, D.; KRUPA, I.; SLOUF, M.; KOYNOV, K.; MOSNACEK, J. Viscoelastic and photo-actuation studies of composites based on polystyrene-grafted carbon nanotubes and styrene-b-isoprene-b-styrene block copolymer. *Polymer*. **2014**, vol. 55, no. 1, pp. 211-18.
[58] LEVITSKY, I. A.; KANELOS, P. T.; WOODBURY, D. S.; EULER, W. B. Photoactuation from a carbon nanotube-nafion bilayer composite. *J. Phys. Chem. B*. **2006**, vol. 110, no. 19, pp. 9421-25.
[59] SASTRI, V.; SASTRI, V. R. Materials Used in Medical Devices. Amsterdam: Elsevier Science Bv; **2014**.
[60] PRIIMAGI, A.; BARRETT, C. J.; SHISHIDO, A. Recent twists in photoactuation and photoalignment control. *J. Mater. Chem. C*. **2014**, vol. 2, no. 35, pp. 7155-62.
[61] ZHANG, H.; CAI, C.; LIU, W. X.; LI, D. D.; ZHANG, J. W.; ZHAO, N.; XU, J. Recyclable Polydimethylsiloxane Network Crosslinked by Dynamic Transesterification Reaction. *Sci. Rep.* **2017**, vol. 7, no., pp.
[62] DROBNY, J. G. 1.1 Elasticity and Elastomers. *Handbook of Thermoplastic Elastomers (2nd Edition)*. Elsevier; **2014**.
[63] HOLDEN, G. Understanding Thermoplastic Elastomers: Hanser; **2000**.
[64] HILLMYER, M. A.; TOLMAN, W. B. Aliphatic Polyester Block Polymers: Renewable, Degradable, and Sustainable. *Acc. Chem. Res.* **2014**, vol. 47, no. 8, pp. 2390-96.
[65] COHN, D.; HOTOVELY-SALOMON, A. Biodegradable multiblock PEO/PLA thermoplastic elastomers: molecular design and properties. *Polymer*. **2005**, vol. 46, no. 7, pp. 2068-75.
[66] KROL, P. Synthesis methods, chemical structures and phase structures of linear polyurethanes. Properties and applications of linear polyurethanes in polyurethane elastomers, copolymers and ionomers. *Prog. Mater Sci.* **2007**, vol. 52, no. 6, pp. 915-1015.
[67] GONZALEZ-LEON, J. A.; RYU, S. W.; HEWLETT, S. A.; IBRAHIM, S. H.; MAYES, A. M. Core-shell polymer nanoparticles for baroplastic processing. *Macromolecules*. **2005**, vol. 38, no. 19, pp. 8036-44.

[68] OYAMA, T. Cross-Linked Polymer Synthesis. In: Kobayashi, S., Müllen, K., editors. *Encyclopedia of Polymeric Nanomaterials*. Berlin, Heidelberg: Springer Berlin Heidelberg; **2015**. pp. 496-505.
[69] KUMAR, K.; KNIE, C.; BLEGER, D.; PELETIER, M. A.; FRIEDRICH, H.; HECHT, S.; BROER, D. J.; DEBIJE, M. G.; SCHENNING, A. A chaotic self-oscillating sunlight-driven polymer actuator. *Nat. Commun.* **2016**, vol. 7, no., pp.
[70] JIANG, Z.; XU, M.; LI, F. Y.; YU, Y. L. Red-Light-Controllable Liquid-Crystal Soft Actuators via Low-Power Excited Upconversion Based on Triplet-Triplet Annihilation. *J. Am. Chem. Soc.* **2013**, vol. 135, no. 44, pp. 16446-53.
[71] LENG, J. S.; LAN, X.; LIU, Y. J.; DU, S. Y. Shape-memory polymers and their composites: Stimulus methods and applications. *Prog. Mater Sci.* **2011**, vol. 56, no. 7, pp. 1077-135.
[72] ZHANG, Y.; IIJIMA, S. Elastic Response of Carbon Nanotube Bundles to Visible Light. *Phys. Rev. Lett.* **1999**, vol. 82, no., pp. 3472.
[73] YANG, M. J.; YUAN, Z. K.; LIU, J.; FANG, Z. S.; FANG, L.; YU, D. S.; LI, Q. Photoresponsive Actuators Built from Carbon-Based Soft Materials. *Advanced Optical Materials*. **2019**, vol. 7, no. 16, pp.
[74] LAN, X.; LENG, J. S.; LIU, Y. J.; DU, S. Y. Investigate of electrical conductivity of shape-memory polymer filled with carbon black. In: Lau, A. K. T., Lu, J., Varadan, V. K., Chang, F. K., Tu, J. P., Lam, P. M., editors. *Multi-Functional Materials and Structures, Pts 1 and 2*. Advanced Materials Research. 47-50**2008**. pp. 714-17.
[75] VO, V. S.; MAHOUCHE-CHERGUI, S.; BABINOT, J.; NGUYEN, V. H.; NAILI, S.; CARBONNIER, B. Photo-induced SI-ATRP for the synthesis of photoclickable intercalated clay nanofillers. *RSC Adv.* **2016**, vol. 6, no. 92, pp. 89322-27.
[76] OSICKA, J.; MRLIK, M.; ILCIKOVA, M.; MUNSTER, L.; BAZANT, P.; SPITALSKY, Z.; MOSNACEK, J. Light-Induced Actuation of Poly(dimethylsiloxane) Filled with Graphene Oxide Grafted with Poly(2-(trimethylsilyloxy)ethyl Methacrylate). *Polymers*. **2018**, vol. 10, no. 10, pp. 12.
[77] MRLIK, M.; MOUCKA, R.; ILCIKOVA, M.; BOBER, P.; KAZANTSEVA, N.; SPITALSKY, Z.; TRCHOVA, M.; STEJSKAL, J. Charge transport and dielectric relaxation processes in aniline-based oligomers. *Synth. Met.* **2014**, vol. 192, no., pp. 37-42.
[78] ILCIKOVA, M.; MRLIK, M.; SEDLACEK, T.; DOROSHENKO, M.; KOYNOV, K.; DANKO, M.; MOSNACEK, J. Tailoring of viscoelastic properties and light-induced actuation performance of triblock copolymer composites through surface modification of carbon nanotubes. *Polymer*. **2015**, vol. 72, no., pp. 368-77.

[79] ILCIKOVA, M.; MRLIK, M.; SEDLACEK, T.; SLOUF, M.; ZHIGUNOV, A.; KOYNOV, K.; MOSNACEK, J. Synthesis of Photoactuating Acrylic Thermoplastic Elastomers Containing Diblock Copolymer-Grafted Carbon Nanotubes. *ACS Macro Lett.* **2014**, vol. 3, no. 10, pp. 999-1003.

[80] FENG, Y. Y.; QIN, M. M.; GUO, H. Q.; YOSHINO, K.; FENG, W. Infrared-Actuated Recovery of Polyurethane Filled by Reduced Graphene Oxide/Carbon Nanotube Hybrids with High Energy Density. *ACS Appl. Mater. Interfaces*. **2013**, vol. 5, no. 21, pp. 10882-88.

[81] LOOMIS, J.; KING, B.; BURKHEAD, T.; XU, P.; BESSLER, N.; TERENTJEV, E.; PANCHAPAKESAN, B. Graphene-nanoplatelet-based photomechanical actuators. *Nanot*. **2012**, vol. 23, no. 4, pp. 10.

[82] MRLIK, M.; OSICKA, J., Instrument for shape-change monitoring upon light stimulation. 34633, *Industrial Property Office,* Czech republic, **2018**.

[83] DENG, J.; LI, J. F.; CHEN, P. N.; FANG, X.; SUN, X. M.; JIANG, Y. S.; WENG, W.; WANG, B. J.; PENG, H. S. Tunable Photothermal Actuators Based on a Pre-programmed Aligned Nanostructure. *J. Am. Chem. Soc.* **2016**, vol. 138, no. 1, pp. 225-30.

[84] XU, W. A.; QIN, Z.; CHEN, C. T.; KWAG, H. R.; MA, Q. L.; SARKAR, A.; BUEHLER, M. J.; GRACIAS, D. H. Ultrathin thermoresponsive self-folding 3D graphene. *Science Advances*. **2017**, vol. 3, no. 10, pp.

[85] TANG, Z. H.; GAO, Z. W.; JIA, S. H.; WANG, F.; WANG, Y. L. Graphene-Based Polymer Bilayers with Superior Light-Driven Properties for Remote Construction of 3D Structures. *Advanced Science*. **2017**, vol. 4, no. 5, pp.

[86] HU, Y.; LIU, J. Q.; CHANG, L. F.; YANG, L. L.; XU, A. F.; QI, K.; LU, P.; WU, G.; CHEN, W.; WU, Y. C. Electrically and Sunlight-Driven Actuator with Versatile Biomimetic Motions Based on Rolled Carbon Nanotube Bilayer Composite. *Adv. Funct. Mater.* **2017**, vol. 27, no. 44, pp.

[87] LEELADHAR; RATURI, P.; SINGH, J. P. Sunlight-driven eco-friendly smart curtain based on infrared responsive graphene oxide-polymer photoactuators. *Sci. Rep.* **2018**, vol. 8, no., pp.

[88] MACCHIONE, M. A.; BIGLIONE, C.; STRUMIA, M. Design, Synthesis and Architectures of Hybrid Nanomaterials for Therapy and Diagnosis Applications. *Polymers*. **2018**, vol. 10, no. 5, pp. 34.

[89] ADVINCULA, R. C.; BRITTAIN, W. J.; CASTER, K. C.; R??HE, J. Polymer Brushes: Synthesis, Characterization, Applications: John Wiley & Sons; **2006**.

[90] KOPF, A.; BASCHNAGEL, J.; WITTMER, J.; BINDER, K. On the adsorption process in polymer brushes: A Monte Carlo study. *Macromolecules*. **1996**, vol. 29, no. 5, pp. 1433-41.

[91] CONZATTI, G.; CAVALIE, S.; COMBES, C.; TORRISANI, J.; CARRERE, N.; TOURRETTE, A. PNIPAM grafted surfaces through

ATRP and RAFT polymerization: Chemistry and bioadhesion. *Colloids and Surfaces B-Biointerfaces*. **2017**, vol. 151, no., pp. 143-55.
[92] LIZUNDIA, E.; MEAURIO, E.; VILAS, J. L. Grafting of Cellulose Nanocrystals. In: Puglia, D., Fortunati, E., Kenny, J. M., editors. *Multifunctional Polymeric Nanocomposites Based on Cellulosic Reinforcements*. Elsevier Science; **2016**.
[93] ALONZI, M.; LANARI, D.; MARROCCHI, A.; PETRUCCI, C.; VACCARO, L. Synthesis of polymeric semiconductors by a surface-initiated approach. *RSC Adv.* **2013**, vol. 3, no. 46, pp. 23909-23.
[94] MOAD, G.; SOLOMON, D. H. Radical Reactions. In: Moad, G., Solomon, D. H., editors. *The Chemistry of Radical Polymerization*. Elsevier Science Ltd,; **2005**. pp. 11-48.
[95] MATYJASZEWSKI, K. Classification and comparison of various controlled/"living" radical polymerizations. *Abstracts of Papers of the American Chemical Society*. **1999**, vol. 218, no., pp. U411-U11.
[96] MATYJASZEWSKI, K. Atom Transfer Radical Polymerization (ATRP): Current Status and Future Perspectives. *Macromolecules*. **2012**, vol. 45, no. 10, pp. 4015-39.
[97] MATYJASZEWSKI, K. Advanced Materials by Atom Transfer Radical Polymerization. *Adv. Mater.* **2018**, vol. 30, no. 23, pp. 22.
[98] SIEGWART, D. J.; OH, J. K.; MATYJASZEWSKI, K. ATRP in the design of functional materials for biomedical applications. *Prog. Polym. Sci.* **2012**, vol. 37, no. 1, pp. 18-37.
[99] FISCHER, H. The persistent radical effect: A principle for selective radical reactions and living radical polymerizations. *Chem. Rev.* **2001**, vol. 101, no. 12, pp. 3581-610.
[100] MINKO, S. Grafting on Solid Surfaces: "Grafting to" and "Grafting from" Methods. In: Stamm, M., editor. *Polymer Surfaces and Interfaces*. Springer, Berlin, Heidelberg; **2008**.
[101] HENZE, M.; MADGE, D.; PRUCKER, O.; RUHE, J. "Grafting Through": Mechanistic Aspects of Radical Polymerization Reactions with Surface-Attached Monomers. *Macromolecules*. **2014**, vol. 47, no. 9, pp. 2929-37.
[102] HOFMANN, U.; FRENZEL, A. Die Reduktion von Graphitoxyd mit Schwefelwasserstoff. *Kolloid Z.* **1934**, vol. 68, no., pp. 149-51.
[103] BRODIE, B. C. On the atomic weight of graphite. *Philos. Trans. R. Soc. London*. **1859**, vol. 149, no., pp. 249-59.
[104] HUMMERS, W. S.; OFFEMAN, R. E. Preparation of graphitic oxide. *J. Am. Chem. Soc.* **1958**, vol. 80, no. 6, pp. 1339-39.
[105] CVEK, M.; MRLIK, M.; ILCIKOVA, M.; MOSNACEK, J.; PAVLINEK, V. Preparation and characterization of graphene oxide sheets controllably grafted with PMMA brushes via Surface-initiated ATRP. 8th International Conference on Nanomaterials - Research & Application; 2017; Slezska: Tanger Ltd.

[106] MOSNACEK, J.; ILCIKOVA, M. Photochemically Mediated Atom Transfer Radical Polymerization of Methyl Methacrylate Using ppm Amounts of Catalyst. *Macromolecules*. **2012**, vol. 45, no. 15, pp. 5859-65.
[107] GONCALVES, G.; MARQUES, P.; BARROS-TIMMONS, A.; BDKIN, I.; SINGH, M. K.; EMAMI, N.; GRACIO, J. Graphene oxide modified with PMMA via ATRP as a reinforcement filler. *J. Mater. Chem.* **2010**, vol. 20, no. 44, pp. 9927-34.
[108] OSICKA, J.; ILCIKOVA, M.; MRLIK, M.; MINARIK, A.; PAVLINEK, V.; MOSNACEK, J. The Impact of Polymer Grafting from a Graphene Oxide Surface on Its Compatibility with a PDMS Matrix and the Light-Induced Actuation of the Composites. *Polymers*. **2017**, vol. 9, no. 7, pp.

LIST OF FIGURES

LIST OF TABLES

LIST OF SYMBOLS AND ABREVIATIONS

^{1}H NMR	Proton nuclear magnetic resonance
AFM	Atomic force microscopy
BiBB	α-Bromoisobutyryl bromide
CA	Contact angle
CNT	Carbon nanotubes
DMA	Dynamic mechanical analysis
DP_n	Degree of polymerization
E'	Storage modulus
E"	Loss modulus
Ea	Activation energy
EBiB	Ethyl α-bromoisobutyrate
EVA	Poly(ethylene-co-vinyl acetate)
FTIR	Fourier-transform infrared spectroscopy
GO	Graphene oxide
GPC	Gel permeation chromatography
IR	Infrared light
k	Boltzmann constant
LB	Langmuir-Blodgett films
LCPs	Liquid-crystalline polymers
LED	Light-emitting diode
M'	Storage dielectric modulus
M"	Loss dielectric modulus
M*	Complex dielectric modulus
M_n	Moleculae weight
PA	Photo-actuation
PBMA	Polybutylmethacrylate
PDI	Polydispersity index
PDMS	Poly(dimethyl siloxane)
PGMA	N,N,N′,N″,N″-Pentamethyldiethylenetriamine
PHEMATMS	Poly(trimethylsilyloxyethyl methacrylate)
PLZT	Lead zirconate titanate
PMDTA	N,N,N′,N″,N″-Pentamethyldiethylenetriamine
PMMA	Polymethylmethacrylate
PNIPAM	poly(N-isopropylacrylamide
POA	Photo-induced Optical Anisotropy
R	Universal gas constant

SI-ATRP	Surface-initiated atom transfer radical polymerization
SIS	Polystyrene-block-polyisoprene-block-polystyrene
T	Temperature
TC	Thermal conductivity
TEM	Transmission electron microscopy
T_g	Glass transition temperature
TGA	Thermogravimetric analysis
TMA	Thermomechanical analysis
TPE	Thermoplastic elastomer
UV	Ultraviolet
VIS	Visible
XPS	X-ray photoelectron spectroscopy
ε	Relative shortening
ε^*	Complex permittivity
ε'	Relative permitivity
ε''	Loss permitivity
τ	Relaxation time
τ_0	Pre-exponential factor

LIST OF FRAMING PAPERS

PAPER I

OSICKA, J.; ILCIKOVA, M.; MRLIK, M.; MINARIK, A.; PAVLINEK, V.; MOSNACEK, J. The Impact of Polymer Grafting from a Graphene Oxide Surface on Its Compatibility with a PDMS Matrix and the Light-Induced Actuation of the Composites. *Polymers*. **2017**, vol. 9, no. 7.

PAPER II

OSICKA, J.; MRLIK, M.; ILCIKOVA, M.; HANULIKOVA, B.; URBANEK, P.; SEDLACIK, M.; MOSNACEK, J. Reversible Actuation Ability upon Light Stimulation of the Smart Systems with Controllably Grafted Graphene Oxide with Poly (Glycidyl Methacrylate) and PDMS Elastomer: Effect of Compatibility and Graphene Oxide Reduction on the Photo-Actuation Performance. *Polymers*. **2018**, vol. 10, no. 8, pp. 14.

PAPER III

OSICKA, J.; MRLIK, M.; ILCIKOVA, M.; MUNSTER, L.; BAZANT, P.; SPITALSKY, Z.; MOSNACEK, J. Light-Induced Actuation of Poly(dimethylsiloxane) Filled with Graphene Oxide Grafted with Poly(2-(trimethylsilyloxy)ethyl Methacrylate). *Polymers*. **2018**, vol. 10, no. 10, pp. 12.

PAPER IV

OSICKA, J.; MRLIK, M.; ILCIKOVA, M.; KRUPA, I.; SOBOLCIAK, P.; PLACHY, T.; MOSNACEK, J. Controllably coated graphene oxide particles with enhanced compatibility with poly(ethylene-co-propylene) thermoplastic elastomer for excellent photo-mechanical actuation capability. *React. Funct. Polym.* **2020**, vol. 148, no., pp. 8.

UTILITY MODEL

Paper I

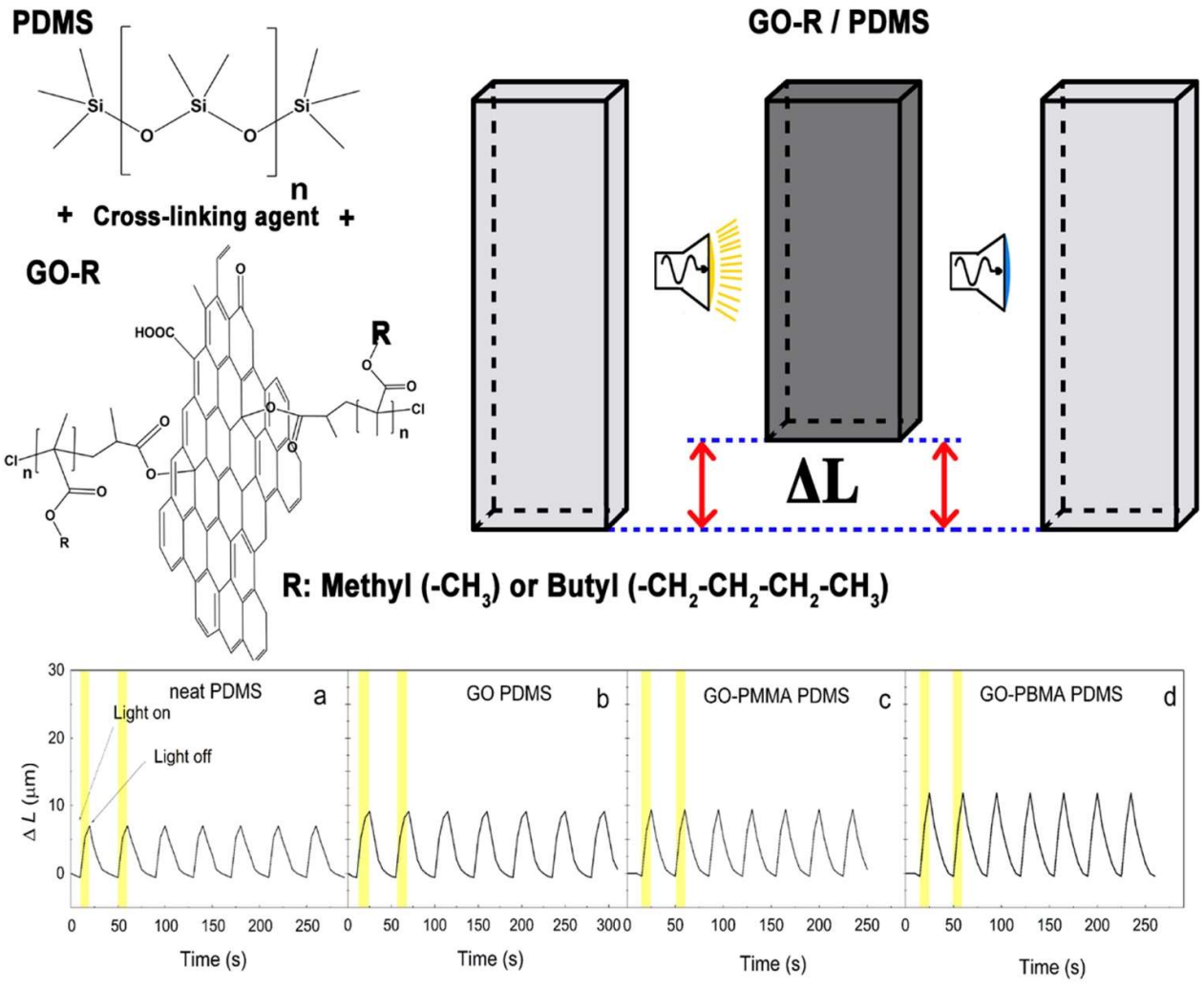
PDMS
Si
O
n
+ Cross-linking agent +
GO-R
HOOC
R
Cl
n
R: Methyl (-CH3) or Butyl (-CH2-CH2-CH2-CH3)
GO-R / PDMS
ΔL
neat PDMS
a
Light on
Light off
GO PDMS
b
GO-PMMA PDMS
c
GO-PBMA PDMS
d
Δ L (μm)
Time (s)

polymers

MDPI

Article

The Impact of Polymer Grafting from a Graphene Oxide Surface on Its Compatibility with a PDMS Matrix and the Light-Induced Actuation of the Composites

Josef Osicka [1], Markéta Ilčíková [2], Miroslav Mrlik [1], Antonín Minařík [1], Vladimir Pavlinek [1] and Jaroslav Mosnáček [2,*]

[1] Centre of Polymer Systems, University Institute, Tomas Bata University in Zlin, Trida T. Bati 5678, 760 01 Zlin, Czech Republic; Josef.osicka@gmail.com (J.O.); mrlik@ft.utb.cz (M.M.); minarik@ft.utb.cz (A.M.); vladimir.pavlinek@5m.cz (V.P.)

[2] Polymer Institute, Slovak Academy of Sciences, Dubravska cesta 9, 845 41 Bratislava 45, Slovakia; upolmail@savba.sk

* Correspondence: upolmosj@savba.sk; Tel.: +421-2-3229-4353

Academic Editors: Chih-Feng Huang, Jinlian Hu and Rui Xiao
Received: 12 May 2017; Accepted: 27 June 2017; Published: 3 July 2017

Abstract: Poly(dimethyl siloxane) (PDMS)-based materials with improved photoactuation properties were prepared by the incorporation of polymer-grafted graphene oxide particles. The modification of the graphene oxide (GO) surface was achieved via a surface initiated atom transfer radical polymerization (SI ATRP) of methyl methacrylate and butyl methacrylate. The modification was confirmed by thermogravimetric analysis, infrared spectroscopy and electron microscopy. The GO surface reduction during the SI ATRP was investigated using Raman spectroscopy and conductivity measurements. Contact angle measurements, dielectric spectroscopy and dynamic mechanical analyses were used to investigate the compatibility of the GO filler with the PDMS matrix and the influence of the GO surface modification on its physical properties and the interactions with the matrix. Finally, the thermal conductivity and photoactuation properties of the PDMS matrix and composites were compared. The incorporation of GO with grafted polymer chains, especially poly(*n*-butyl methacrylate), into the PDMS matrix improved the compatibility of the GO filler with the matrix, increased the energy dissipation due to the improved flexibility of the PDMS chains, enhanced the damping behavior and increased the thermal conductivity. All the changes in the properties positively affected the photoactuation behavior of the PDMS composites containing polymer-grafted GO.

Keywords: smart polymers; grafting method; reversible deactivation radical polymerization

1. Introduction

Photomechanical actuators are materials that convert photons into mechanical motion. In rubbery elastomeric matrices, stress and displacement are generated upon irradiation of a pre-strained sample via an external light source, i.e., the thermoplastic effect. The material absorbs the energy that is transported via thermal convection to the pre-strained polymer chains that contract and generate mechanical motion. The proposed mechanism has been studied in-depth by Cohn et al. [1]. Elastomeric photomechanical actuators are lightweight and remotely controlled. They are utilized as tactile devices [2,3], artificial muscles [4], vascular stents [5], intravascular embolic coils [6], micro-grippers [7], and micro-motors [8]. Liquid crystalline elastomers (LCE) [9,10], thermoplastic elastomers [5,11–15] (TPE) and cross-linked elastomers [6,16] have been reported as matrices for polymer composite-based photomechanical actuators. The negligible role of the host polymer on the actuation mechanism was

revealed [16]. Poly(dimethyl siloxanes) (PDMS) are cross-linked elastomers that provide shape stability over time, biocompatibility and a variety of mechanical properties depending on the cross-linking density. Despite all their advantages compared to thermoplastic elastomers, their main drawback is that they are not re-processable.

The photomechanical actuation response can be enhanced via the utilization of additives or functional fillers, such as carbon nanotubes and graphene oxide [17–19], graphene [15,18], carbon black [18], and molybdenum disulfide [20,21]. The fillers can facilitate the absorption of light energy and its transfer through a material to enhance the actuation response. The actuation response can be affected by the type of filler, the concentration and the arrangement. To maximize its efficacy, the filler should be well-dispersed in the matrix [18,22]. An arrangement in the actuation direction has been reported to promote the actuation as well [9]. Regarding the shape of the fillers, the effectiveness increases with the dimensionality, which facilitates the orientation of the polymer chains; i.e., one dimensional carbon nanotubes were more effective than carbon black, but not as effective as two dimensional graphene platelets [18], and this was ascribed to the better dispersion in PDMS. Surprisingly, graphite oxide flakes did not exhibit a good performance.

Nevertheless, this drawback can be overcome using a suitable surface modification. The oxidized form of graphene, i.e., graphene oxide (GO), is rich in oxygen-containing functional groups that facilitate its further functionalization, and after reduction, it is electrically conductive [23]. Grafting polymer chains onto the surface of inorganic materials is a powerful approach to finely tune the surface chemistry of the particles. This approach enables control of the physicochemical properties, interfaces, and/or biochemical functionalities [24]. In addition, living/controlled polymerizations allow for tailoring of the molecular architecture of polymer brushes, e.g., the polymer chain uniformity (low dispersity), chain composition (homopolymers, block copolymers, gradient, periodic, and statistical), functionality and grafting density (sparse or dense).

Our previous studies revealed that the suitable surface modification of carbon nanotubes (CNTs) can effectively tailor the photoactuation response through the selective location of CNTs in block copolymers exhibiting thermoplastic elastomer properties [14,22,25,26]. Here, GO prepared via the oxidation of expanded graphite was investigated instead of CNTs. The amount and price of the prepared GO are more acceptable for large-scale applications. The hydroxyl and carboxylic groups enabled simple immobilization of the initiators for subsequent atom transfer radical polymerization (ATRP) from the GO surface. The polymer brushes of poly(methyl methacrylate) (PMMA) and poly(*n*-butyl methacrylate) (PBMA), which have comparable molar masses and grafting densities, were grafted from GO. The study focused on the effect of polymer modification on GO surfaces on the photoactuation response of the PDMS composites. The surface modification of GO by methacrylate polymers affected the compatibility with the PDMS matrix and the physical and thermal properties of the PDMS composites. Because of this effect, a polymeric material with high and reversible response to light was obtained.

2. Materials and Methods

2.1. Materials

Graphite (powder, <20 μm, synthetic), sulfuric acid (H_2SO_4, reagent grade, 95–98%), sodium nitrate ($NaNO_3$, ACS reagent, ≥99%), potassium permanganate ($KMnO_4$, 97%) and hydrogen peroxide (H_2O_2, ACS reagent, 29.0–32.0 wt % H_2O_2 basis) were used as the chemical reagents for the proper exfoliation conditions to form the GO sheets. α-Bromoisobutyryl bromide (BiBB, 98%) served as an initiator and was linked onto the GO surface. The initiator bonding was performed in the presence of a proton scavenger, triethyleneamine (TEA, ≥99%). Methyl methacrylate (MMA, 99%), *n*-butyl methacrylate (BMA, 99%), ethyl α-bromoisobutyrate (EBiB, 98%), *N*,*N*,*N*′,*N*″,*N*″-pentamethyldiethylenetriamine (PMDETA, ≥99%), copper bromide (CuBr, ≥99%) and anisole (99%) were used as the monomer, initiator, ligand, catalyst and solvent, respectively. Diethyl ether (ACS reagent, anhydrous, ≥99%) was

used as the drying agent. All the above listed chemicals were purchased from Sigma Aldrich (St. Louis, MO, USA) and all, except the MMA and BMA monomers, were used without further purification. MMA and BMA were purified by passing them through a neutral alumina column to remove the MEHQ inhibitor prior to their use. Tetrahydrofurane (THF, p.a.), acetone (p.a.), dimethylformamide (DMF, p.a.) and hydrochloric acid (HCl, 35%, p.a.) were obtained from Penta Labs (Prague, Czech Republic). Poly(dimethyl siloxane) (PDMS) Sylgard 184 was purchased from Sylgard, MI, USA and was used as received. Deionized water (DW) was used for all the experimental processes and washing routines.

2.2. Graphene Oxide Preparation and Initiator Immobilization

Graphene oxide (GO) was prepared from a graphite powder using a modified Hummers method [27]. The raw graphite (5 g) was vigorously stirred with H_2SO_4 (100 mL), and the mixture was cooled to 5 °C using an ice/water bath. Subsequently, $NaNO_3$ (2.5 g) and $KMnO_4$ (15 g) were gradually added. The mixture was stirred for an additional 6 h, and then, DW (300 mL) was added dropwise, while the temperature was kept below 40 °C. Finally, concentrated H_2O_2 (40 mL) was added, and the solution turned a brilliant brown, which indicated the complete oxidization of graphite. The product was separated in a high-speed centrifuge (Sorvall LYNX 4000, Thermo Scientific, Waltham, MA, USA) operating at 10,000 rpm for 20 min at 25 °C. The cleaning routine was based on the dispersion of GO in 0.1 M HCl and re-separation in a centrifugal field. The procedure was repeated with DW several times until the pH reached a value of 7. Then, the particles were lyophilized to remove any residual water after the purification process. Finally, a brown powder was obtained.

The presence of the reactive groups on the GO surface was used for the reaction with BiBB to immobilize the ATRP initiator on the GO surface and prepare GO-I using the method described elsewhere [28,29].

2.3. Grafting Polymer Chains from the GO Surface

The GO sheets modified with the ATRP initiator (0.75 g) were transferred into a Schlenk flask equipped with a gas inlet/outlet and a septum. The flask was evacuated and replaced with argon several times. BMA (17.5 mL, 110 mmol) or MMA (11.8 mL, 110 mmol), EBiB (0.162 mL, 1.1 mmol), PMDETA (0.92 mL, 4.4 mmol), and anisole (15 mL) were then added to the flask, and the flask was degassed using several freeze–pump–thaw cycles. The CuBr catalyst (0.156 g, 1.1 mmol) was quickly added under an argon flow into the frozen system. Anisole was used as the solvent at an amount of 50 vol %. The polymerization mixture was stirred at 60 °C for 2 h, and then, the polymerization was stopped by exposure to air. The product was filtered, washed with DMF (2 × 200 mL) and acetone (2 × 200 mL), and dried with diethyl ether (2 × 100 mL).

2.4. Composite Preparation

An elastomeric matrix was prepared by mixing PDMS, silicone oil and a curing agent in a volume ratio of 8:2:1. The matrix was filled either with neat GO or GO with grafted PMMA or PBMA chains and was properly homogenized using mechanical stirring for 30 min at room temperature. The concentrations of the fillers were 0.1, 0.5 and 1 vol %. The mixture was poured into a Teflon-lined mold and evacuated at 60 mbar to eliminate the presence of air bubbles. Then, the mold was placed into an oven for 2 h at 60 °C to fully cross-link the PDMS-based composites. It should be stated that same procedure was used for the GO-I particles; however, even after 48 h, the composites were not fully cross-linked probably due to the presence of 2-bromoisobutyryl groups on the GO surface, which could eliminated the function of the cross-linker.

2.5. General Characterizations

Proton nuclear magnetic resonance (^{1}H NMR) spectra were recorded at 25 °C using an instrument (400 MHz VNMRS Varian, Tokyo, Japan) and deuterated chloroform ($CDCl_3$) as the solvent. The

molar mass (M_n) and dispersity ($Đ$) of the polymer chains were investigated by gel permeation chromatography (GPC) using a GPC instrument (PL-GPC220, Agilent, Tokyo, Japan) equipped with GPC columns (Waters 515 pump, two PPS SDV 5 μm columns (diameter of 8 mm, length of 300 mm, 500 Å + 105 Å)) and a Waters 410 differential refractive index detector at 30 °C. The samples for NMR spectroscopy and GPC analyses were prepared by their dilution with $CDCl_3$ and THF, respectively, followed by the purification process, in which they were passed through a neutral alumina column. The neat GO and GO with a grafted polymer layer were observed using a transmission electron microscope (TEM, JEM-2100Plus, Jeol, Tokyo, Japan). The samples for the TEM analysis were prepared by dispersing the particles in acetone using mechanical stirring for 5 and 2 min of sonication and dropping the resultant suspension onto a copper grid. Fourier transform infrared (FTIR) spectra (64 scans, resolution of 4 cm^{-1}) were recorded on a Nicolet 6700 (Nicolet, Madison, WI, USA) within a wavenumber range of 4000–600 cm^{-1}, and the ATR technique with a germanium crystal was employed. The spectra were recorded at room temperature. The Raman spectra (3 scans, resolution of 2 cm^{-1}) were collected on a Nicolet DXR (Nicolet, Madison, WI, USA) using an excitation wavelength of 532 nm. The integration time was 30 s, and the laser power on the surface was set to 1 mW. The powders were compressed to form pellets (diameter of 13 mm, thickness of 1 mm) on a laboratory hydraulic press (Trystom Olomouc, H-62, Olomouc, Czech Republic). The pellets were used for electrical conductivity measurements, and a two–point method at room temperature was applied with the help of an electrometer (Keithley 6517B, Beaverton, OR, USA). The presented results are the average values from 10 independent measurements. The contact angle (CA) measurements were evaluated using the static sessile drop method on the pellets and were performed on a surface energy evaluation system equipped with a CCD camera (Advex Instruments, Brno, Czech Republic). A droplet (5 μL) of PDMS was carefully dropped onto the surface, and the CA value was recorded. The presented CA results are the average values from 10 independent measurements. To confirm that the contact angle results were not affected by the roughness of the GO surface of the investigated pellets, atomic force microscopy (AFM) was used to investigate the surface topography using an atomic force microscope (AFM), model Dimension ICON (Bruker, Billerica, MA, USA). Measurements were performed at a scan speed of 1 Hz with a resolution of 256 × 256 pixels in the tapping mode at room temperature in an air atmosphere. A silicone-nitride probe with a resonant frequency of (150 ± 50) kHz and a stiffness constant of 5 N/m (MPP-12120, Bruker, Billerica, MA, USA) was used. The image analysis and surface roughness (Sa) determination were performed using the program Gwyddion v.2.48 (Gwyddion, Brno, Czech Republic).

The thermal conductivity was measured via a one-side contact method using the TCi model (C-term technologies, Fredericton, NB, Canada). The viscoelastic properties of both the nanocomposite and pure polymer matrix were studied via dynamic mechanical analysis (DMA) in the tensile mode. All the measurements were performed in the linear viscoelastic region. The measurements were performed at 1 Hz in the temperature range from −150 to 150 °C. Dielectric spectroscopy in the temperature range from −150 to 100 °C and in the frequency range from 10^{-1} to 10^7 Hz was used to investigate the polymer chain dynamics.

The glass transition process was evaluated using the activation energies calculated from the Arrhenius equation (Equation (1)) to see the effect of modification on the relaxation processes in the PDMS based composites.

$$f_\beta = f_\infty \exp\left(\frac{E_a}{k_B T}\right) \quad (1)$$

where E_a is the activation energy, f_∞ is the pre-exponential factor, T is the temperature in Kelvin, and k_B is the Boltzmann constant.

2.6. Photoactuation

The photoactuation ability of both the matrix and composite samples was investigated using a thermal mechanical analysis (TMA, Mettler Toledo, Langacher, Switzerland) similar to that previously

published [14]. A red LED diode (Luxeon Rebell, Philips, Amsterdam, The Netherlands) was used for the irradiation. The irradiation was applied for 10 s at 627 nm with a 6 mW light source intensity under a 10% pre-strain of the samples. The maximum value of the actuation is characterized by a change in the sample length during the exposure to light, $\Delta L = (L_0 - L)/L_0$, where L_0 is the length of the non-irradiated sample, and L is the length of the irradiated sample.

3. Results and Discussion

3.1. Synthesis of GO-Polymer-Modified Particles

The modification of the GO particles with PMMA (GO–PMMA) and PBMA (GO–PBMA) polymer chains was performed via surface initiated ATRP, as previously described for other methacrylate-based monomers [29]. The MMA and BMA conversions, which were calculated from the ^{1}H NMR spectra, were 89% and 91%, respectively. Using a sacrificial initiator in addition to the initiator immobilized on the GO surface allowed for the determination of the molecular characteristics of the polymer chains with the consideration that the growth of both the free and GO surface-bonded polymer chains is comparable [30]. The molecular weight (M_n) and polydispersity index ($Đ$) determined for PMMA were 5620 g mol^{-1} and 1.18, respectively, and they were 5210 g·mol^{-1} and 1.21, respectively, for PBMA. The molar masses correlated well with the monomer conversions. The successful grafting process was confirmed by the FTIR investigations with on-line monitoring during the TGA measurements. In Figure 1a, a release of oxygen-containing groups from the neat GO surface can be seen in the temperature range of 150–300 °C. In the same temperature range, the FTIR spectrum in Figure 1b of the released compound was analyzed, and the vibrations from the hydroxyl groups at 3510 cm^{-1}, a small amount from the carbonyl groups at 1723 cm^{-1} and the stretching of the hydroxyl groups at 1423 cm^{-1} were found. The release of the groups from PMMA was observed in the TGA in the range of 220–380 °C, as seen in Figure 1c. The FTIR from the released groups showed an increase in the peaks of the carbonyl groups at approximately 1731 cm^{-1} in comparison to the neat GO, where this peak is almost negligible, and the appearance of peaks in the alkyl vibrations region of 2600–3000 cm^{-1} (Figure 1d), which confirmed the presence of PMMA on the GO surface. Similar results were obtained for the GO modified with the PBMA chains (Figure 1e,f), but the release of the groups from PBMA occurred at higher temperatures. To quantify the amounts of the individual components in the GO, GO–PMMA and GO–PBMA particles, the TGA data were analyzed. It was found that, similar to our previous studies [28,29], the amount of the oxygen-containing groups for the neat GO was app. 30%. On the other hand, for both cases of polymer modification, the amount of polymer on the hybrid particles was app. 9% for PMMA and 11% for PBMA, and the amount of oxygen-containing groups was nearly 21% for PMMA and 19% for PBMA, which indicated partial reduction of GO surface during its modification as observed also previously [28].

3.2. Transmission Electron Microscopy

In Figure 2, the TEM images of all the investigated GO particles are shown. In the case of neat GO, the proper exfoliation of the graphite powder using the Hummers method was achieved, and the neat GO sheet can be clearly seen on the TEM image (Figure 2a). The sheet-like morphology was also observed in the case of the GO modified with the PMMA chains (Figure 2b) when the 2D shape was sustained on the same level. The slightly darker contrast of the GO–PMMA sheet is due to the presence of the polymer layer on the surface of the GO. In the case of the GO–PBMA particles (Figure 2c), the 2D shape was again observed, which indicated they had the same morphology as the neat GO and GO–PMMA. Here, several layers of GO most likely lay on top of each other, and with the sustainable polymer layer of PBMA on the surface of the GO, they provide the higher contrast of the image. The sharp edges of the neat GO become smoother in the case of both the modified GOs due to presence of polymer chains, which again confirmed the successful modification of the GO surface.

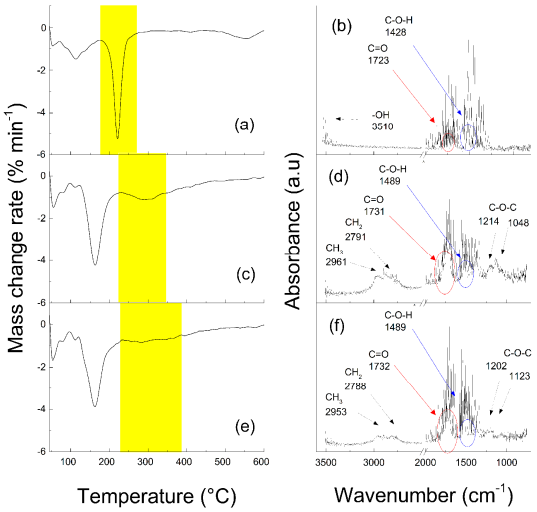

Figure 1. TGA analysis (**a**,**c**,**e**) with on-line monitoring of the Fourier transform infrared (FTIR) spectra (**b**,**d**,**f**) for neat graphene oxide (GO) (**a**,**b**), GO–poly(methyl methacrylate) (PMMA) (**c**,**d**) and GO–poly(*n*-butyl methacrylate) (PBMA) (**e**,**f**) particles.

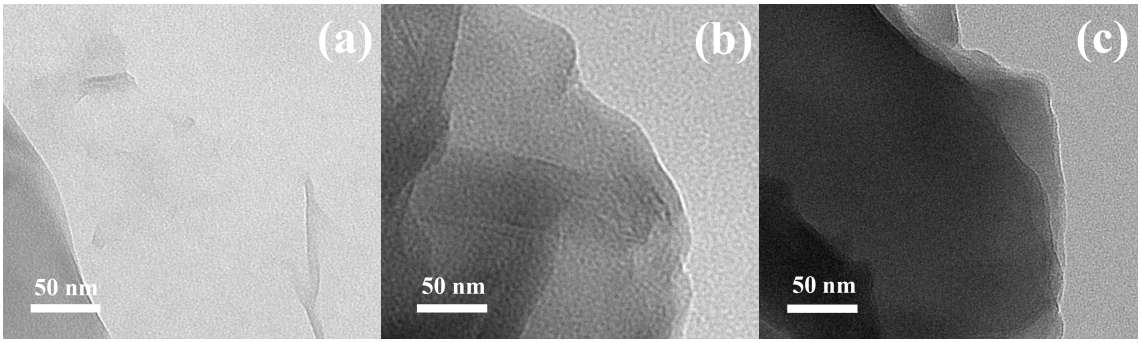

Figure 2. Transmission electron microscope (TEM) images of the neat GO (**a**), GO-PMMA (**b**) and GO–PBMA (**c**).

3.3. Reduction of the GO Particles during the Synthesis

In our previous work, we showed that the reduction of GO can occur during SI ATRP [28]. To confirm the reduction of the GO particles during the SI ATRP process, Raman spectroscopy was used as a useful tool to compare the broad D and G peaks corresponding to the sp^2 and sp^3 hybridized forms of the carbon atoms in the GO sheets. In Figure 3, a comparison among the neat GO sheets, GO–PMMA and GO–PBMA can be seen. A significant reduction in the GO sheets was achieved, and it can be observed from the significant change in the D/G peak intensity ratio (I_D/I_G) obtained after the SI ATRP process. Thus, a change from 0.90 to 1.05 and 1.08 was observed after the SI ATRP of MMA and BMA, respectively. It can also be seen that the 2D structure of GO created during the oxidation was nearly the same after modification with both the PMMA and PBMA brushes. The conductivity measurements confirmed the results obtained from the Raman spectroscopy, which indicated the reduction of GO after modification. The conductivity slightly increased from 1.2×10^{-8} S cm^{-1} for the neat GO to 6.3×10^{-8} S cm^{-1} for the GO–PMMA and 2.1×10^{-7} S cm^{-1} for the GO–PBMA. Therefore, it can be stated that within the SI ATRP process, a partial reduction of the GO with the simultaneous grafting of PBA polymer brushes was achieved.

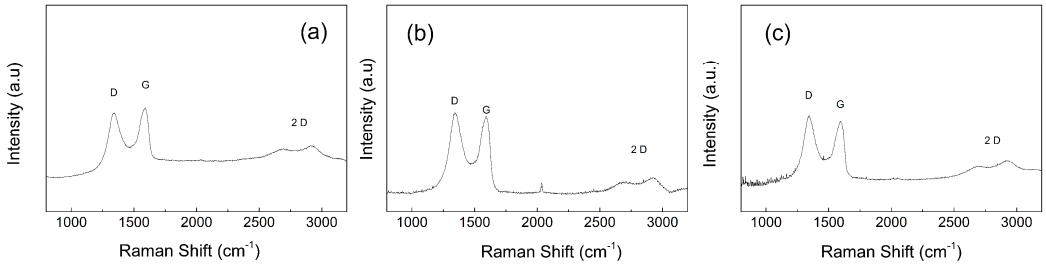

Figure 3. Raman spectra of the neat GO (**a**), GO–PMMA (**b**) and GO–PBMA (**c**).

3.4. Compatibility of the Particles with the PDMS Matrix

The compatibility of the GO particles with the surrounding matrix when they are dispersed is a crucial part of their potential applications as light sensors or actuators [14,25]. Therefore, the compatibility between the neat GO or polymer-functionalized GO and PDMS was investigated via contact angle measurements. As seen in Figure 4a, the contact angle between the neat GO pellet and the PDMS droplet was 49.9° ± 3.2°, which indicated a relatively poor compatibility. The presence of the short polymer chains of PMMA improved the compatibility and decreased the contact angle to 38.7° ± 2.7° (Figure 4b). In addition, the longer aliphatic butyl chain present in PBMA decreased the contact angle to 28.7° ± 2.7° (Figure 4c). This result indicated significantly improved interactions between PDMS and the surface of the GO–PBMA in comparison with the surface of neat GO, which contains only hydroxyl, carbonyl, carboxyl or epoxy groups. To prove that these results were not affected by the surface roughness, an AFM investigation was performed. As seen in Figure 4d–f, the roughnesses were nearly identical for all the investigated samples, and the surface roughness (Sa) was found to be 154, 143 and 162 nm for GO, GO–PMMA and GO–PBMA, respectively. Therefore, it can be concluded that the contact angle was significantly affected by the chemical modification (coating) and that the roughness played a negligible role.

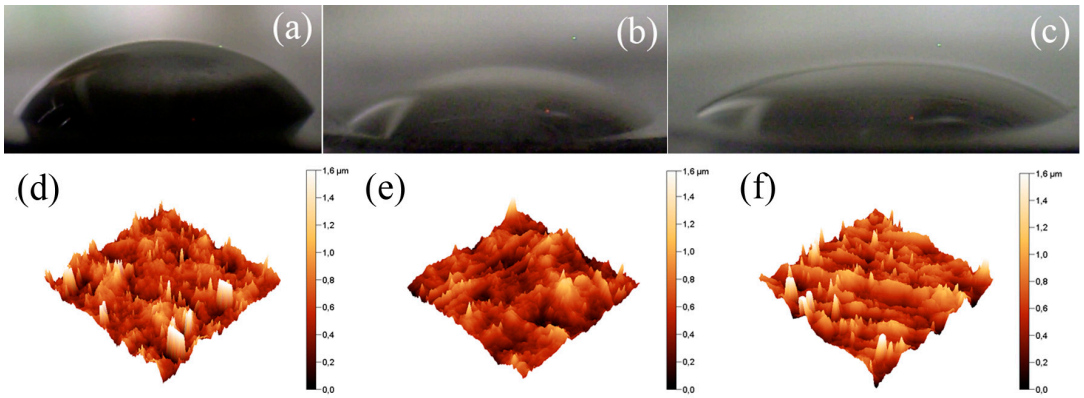

Figure 4. Images from the CCD camera of the 5 µL PDMS droplets on the neat GO (**a**), GO–PMMA (**b**) and GO–PBMA (**c**), and the atomic force microscopy (AFM) investigations of the surface roughness for the (**d**) neat GO; (**e**) GO–PMMA and (**f**) GO–PBMA.

3.5. Dielectric Investigation of the Polymer Chain Dynamics

To investigate the influence of the GO surface modification on the polymer chain dynamics, dielectric spectroscopy measurements were performed. As seen in Figure 5, the presence of the neat GO in the PDMS matrix slightly affected the response of the PDMS polymer chains; however, in the case of GO–PMMA and GO–PBMA, the presence of short polymer grafts significantly shifted the glass transition temperature to lower values. To confirm this change, the activation energies of the glass transition process were calculated, and the effects of the filler nature and its loading were investigated.

Within the range of the studied frequencies, a linear dependence of the T_g on the frequency was observed; therefore, a simple Arrhenius equation was used for the determination of the glass transition activation energies. The values are summarized in Table 1. The activation energy decreased with the increasing amount of filler. This indicated that the filler behaves as a softener in this case and makes the transition easier, and the overall movement of the main PDMS backbone requires less exertion. Moreover, from the results, it can be clearly seen that the longer pendant aliphatic chain in PBMA caused a more significant softening of the polymer backbone, and, thus, the PDMS chains are more movable. This behavior should have a positive impact on the investigated photoactuation performance.

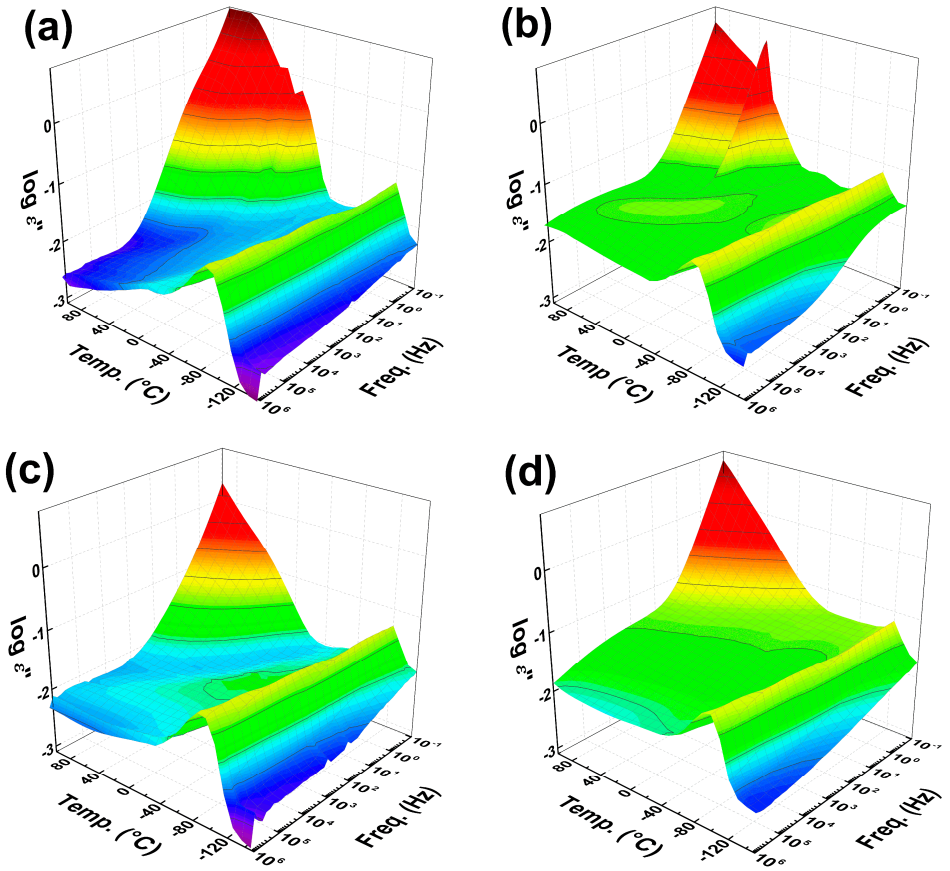

Figure 5. 3D plots of dielectric properties for the neat PDMS matrix (**a**) and GO/PDMS composites with 0.5 vol % of GO (**b**), GO–PMMA (**c**) and GO–PBMA (**d**) particles.

Table 1. Activation energies of the glass transition process for the pure PDMS and PDMS composites with various filler loadings.

Sample Code	Activation Energy (kJ·mol^{-1})
pure PDMS	45.70
0.1 vol % neat GO PDMS	36.57
0.5 vol % neat GO PDMS	34.97
1 vol % neat GO PDMS	20.35
0.1 vol % GO–PMMA PDMS	35.99
0.5 vol % GO–PMMA PDMS	23.58
1 vol % GO–PMMA PDMS	10.16
0.1 vol % GO–PBMA PDMS	25.39
0.5 vol % GO–PBMA PDMS	22.79
1 vol % GO–PBMA PDMS	9.49

3.6. Dynamic Mechanical Analysis

Because photoactuation is a dynamic process, a dynamic mechanical analysis of the prepared composites is crucial to investigate their suitability for intended applications. Through this investigation, the interactions between the particles and the matrix can also be estimated. As seen in Figure 6, below the glass transition temperature, T_g, all the composites exhibited nearly the same mechanical properties (Figure 6a). However, due to the presence of various fillers, the T_g of the composites slightly changed. Moreover, another transition region connected to the melting of the small crystalline phase present in PDMS was observed, which was also observed elsewhere [31]. Only a minor effect of the fillers was seen in the melting temperature region. In the region of utilization, the storage moduli were nearly independent of the temperature up to 40 °C. In this case, the best mechanical performance was observed for the neat GO. The reason for this could be possible covalent bonding between the OH groups and the PDMS polymer chains, which was observed by Bose et al. for OH groups of carbonyl iron and PDMS [32]. After coating of GO with the PMMA or PBMA chains, the partial physical entanglement provided an improved compatibility between PDMS and GO–PMMA or GO–PBMA compared with neat GO. However, at the same time, the short polymer chains at the GO surface can serve as plasticizers and thus the final PDMS material can be more flexible; but the PDMS was still reinforced in comparison to the neat PDMS matrix. The damping properties of the PDMS-containing polymer-grafted GO were slightly enhanced, as indicated by the higher tan delta values (Figure 6b). This is highly desirable from a photoactuation performance point of view because physical entanglements and GO–PBMA can provide the best flexibility in the prepared composite. In fact, this is in good agreement with the activation energies determined from the dielectric spectroscopy and will be confirmed by the photoactuation investigation (see below).

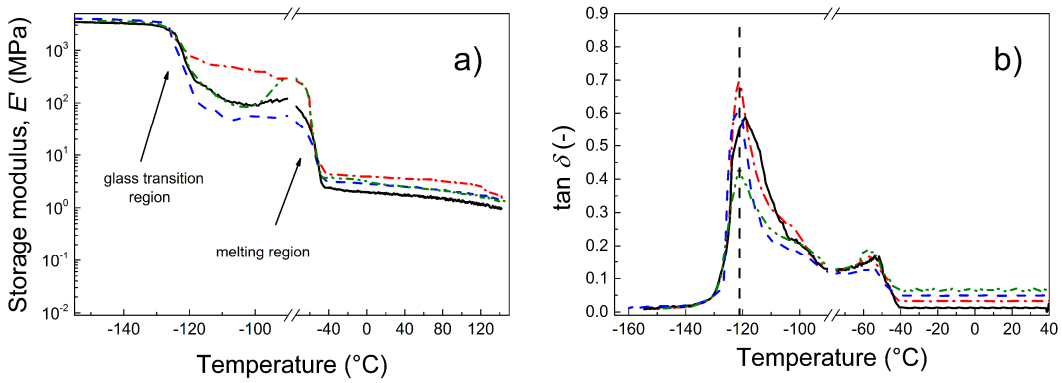

Figure 6. Dependence of the storage modulus (**a**) and tan δ (**b**) for a broad temperature range for neat PDMS (black solid line) and for PDMS composites containing 0.1 vol % of neat GO (red dash dot line), GO–PMMA (blue dashed line) and GO–PBMA (green dash-dot-dot line).

To investigate the effect of the filler loading on the mechanical performance, the composites with the most promising properties, i.e., those containing GO–PBMA particles with various filler loadings (0.1, 0.5 and 1 vol %), were investigated (Figure 7). It can be clearly seen that below the T_g, the materials exhibited nearly the same behavior. Over the T_g, the samples with a higher filler loading (0.5 and 1 vol %) exhibited a significant drop in the storage moduli (Figure 7a) with a subsequent increase to a maximum before melting. The drop can be caused by interactions between the GO-PBMA particles and the polymer matrix, which make the PDMS matrix more flexible, as described above. This behavior can also be connected to the decreased activation energy, which is in good agreement with our previous observations. After the melting of the crystalline phase, the present GO–PBMA particles still act as a reinforcing filler from a storage modulus point of view. The T_g slightly shifted to a lower temperature for all the filler contents (Figure 7b), which indicated the intervention of the GO–PBMA particles in the glass transition process. The right shoulder is most likely connected to

the physical interactions of the polymer chains of GO–PBMA with the PDMS matrix, which were already described in Figure 7a. Moreover, the damping behavior of the composites was enhanced with an increase in the filler content, which indicated the relatively high energy dissipation caused by the more flexible structure present in the GO–PBMA/PDMS composites. It can be concluded that the modification of GO with various polymers can affect the mechanical performance; i.e., the storage moduli can be tailored using various modifications, and the polymer modification of GO particles in PDMS composites significantly contributes to the increasing energy dissipation due to the improved flexibility and provides an enhanced damping behavior.

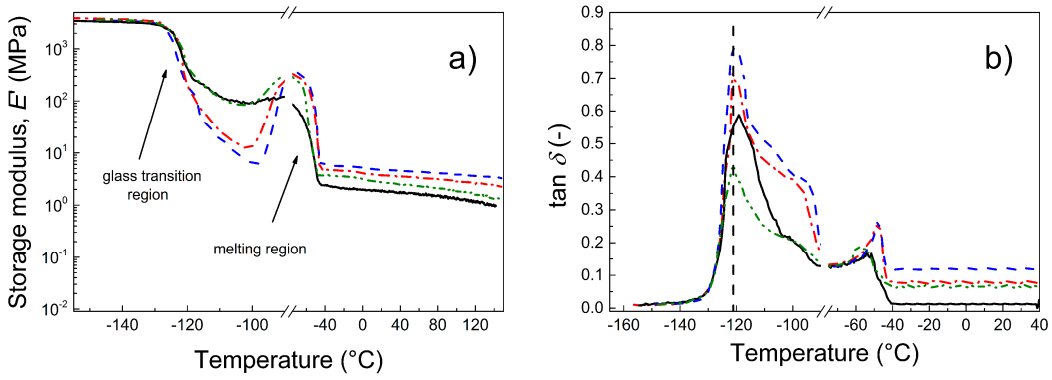

Figure 7. Dependence of the storage modulus (**a**) and tan δ (**b**) for a broad temperature range for neat PDMS (black solid line) and for PDMS composites containing various concentrations of GO–PBMA: 0.1 vol % (green dash-dot-dot line), 0.5 vol % (red dash dot line) and 1 vol % (blue dashed line).

3.7. Thermal Conductivity

According to a previous study [19], the thermal conductivity is another crucial parameter affecting the photoactuation performance. As seen in Table 2, the pure PDMS matrix has a thermal conductivity of 0.071 W mK^{-1}, and it increased with the increasing amount of filler for all the investigated samples. Due to the improved compatibility with the PMMA and PBMA polymer chains attached on the GO surface, these samples exhibited improved thermal conductivities compared to the neat GO. The best thermal conductivity was found for the composites containing the GO–PBMA particles. Thus, these composites can provide a significant contribution to enhanced photoactuation capabilities due to the significantly improved heat distribution within the samples.

Table 2. Thermal conductivity of pure PDMS and PDMS composites with various filler loadings.

Sample Code	Thermal Conductivity (W·mK^{-1})
pure PDMS	0.071
0.1 vol % neat GO/PDMS	0.144
0.5 vol % neat GO/PDMS	0.156
1 vol % neat GO/PDMS	0.161
0.1 vol % GO–PMMA/PDMS	0.153
0.5 vol % GO–PMMA/PDMS	0.174
1 vol % GO–PMMA/PDMS	0.209
0.1 vol % GO–PBMA/PDMS	0.151
0.5 vol % GO–PBMA/PDMS	0.186
1 vol % GO–PBMA/PDMS	0.250

3.8. Photoactuation Performance

The photoactuation performance was investigated for various composite compositions, and the impact of the filler modification and the filler loading on the final properties was elucidated. As seen

in Figure 8, the pure matrix showed some actuation performance. The determined maximum value of actuation, ΔL, was 7.1 µm, and the recovery time was 30 s. The addition of 0.1 vol % of neat GO particles increased the maximum value of the actuation to 9.1 µm, and this was likely due to the improved heat transfer that was observed during the thermal conductivity measurement. However, the recovery time was the same as that for the pure PDMS matrix. In the case of the GO–PMMA-based composite, the maximum actuation increased to 9.4 µm, and the recovery time was shortened to 25 s. A similar behavior was obtained for the sample containing GO–PBMA particles. The actuation performance was 11.8 µm, and the recovery time similar to that of the GO–PMMA composites was achieved. The main reason for this capability is the proper incorporation of the GO–PMMA and GO–PBMA particles into the PDMS matrix, which causes better shape recovery and improved heat transitions within the samples.

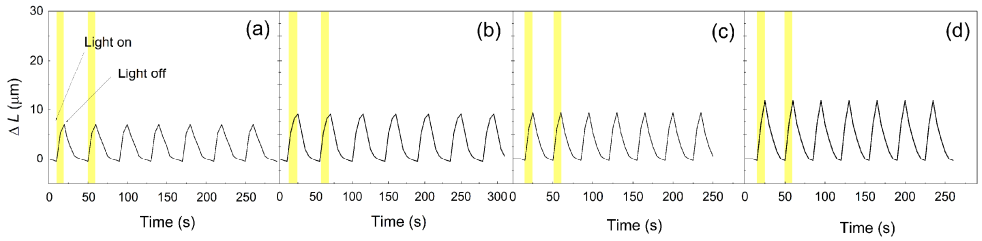

Figure 8. Photoactuation performance of the pure PDMS (**a**) and the PDMS composites containing 0.1 vol % of neat GO (**b**), GO–PMMA (**c**) and GO–PBMA (**d**).

The impact of the filler content on the photoactuation performance of the PDMS materials was investigated, and the results are plotted in Figure 9. In all cases, the ΔL increased with an increasing amount of filler. The best capability was found for the composites containing the GO–PBMA particles, and the maximum actuation value for a composite containing 1 vol % of GO–PBMA was approximately 5 times higher than that for pure PDMS. The main reason for this significant improvement was already proposed by previous investigations and is likely the enhanced flexibility of the polymer composite, which was confirmed by the lower activation energy, higher damping and enhanced thermal conductivity, improving the heat distribution within the composite samples. The polymer grafting from GO approach for the preparation of composites with photoactuation capabilities provides a system with an enhanced performance in comparison to other systems, including 2 wt % of neat CNTs, carbon black, GO or graphene nanoplatelets in the PDMS composites. The systems mentioned last showed a relative change in the length, below 25 µm, when recalculated for our conditions [18].

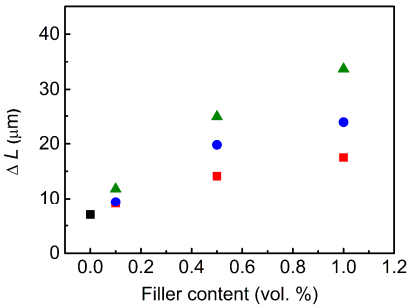

Figure 9. Dependence of the filler content on the change in the length for the pure PDMS matrix (black squares) and PDMS composites containing neat GO (red squares), GO–PMMA (blue circles) and GO–PBMA (green triangles). Error bars are not higher than the size of the symbols.

4. Conclusions

In summary, this study investigated the influence of grafting polymer chains from a GO surface on the properties of the resulting PDMS-based composites. Short PMMA or PBMA polymer chains were grafted from the GO surface via SI-ATRP, and a slight reduction of the GO surface during the grafting was determined using Raman spectroscopy and conductivity measurements. The contact angle measurements confirmed the improved compatibility of the polymer-grafted GO particles with the PDMS matrix, especially when the GO was grafted with the PBMA chains. The polymer chain dynamics were investigated using dielectric spectroscopy, and the Arrhenius equation was applied to calculate the activation energy of the relaxation around the glass transition temperature. It was found that the modifications caused a significant decrease in the activation energy and acted as a plasticizer for the PDMS matrix, which has a positive influence on the photoactuation behavior. This result was confirmed by the dynamic mechanical analysis.

The thermal conductivity was also improved by the presence of the GO particles, and the polymer-grafted GO more significantly enhanced the thermal conductivity due to the better dispersibility of the particles in the PDMS matrix. Finally, the photoactuation performance was elucidated, and it was found that the composites including the GO–PBMA particles had the best capability due to the more flexible polymer chains and better heat distribution within the PDMS matrix.

Acknowledgments: Authors Josef Osicka and Miroslav Mrlik thank the Grant Agency of the Czech Republic (No. 16-20361Y) for financial support. This work was also supported by the Ministry of Education, Youth and Sports of the Czech Republic—program NPU I (LO1504). Markéta Ilčíková and Jaroslav Mosnáček thank for financial support to the grant agencies SRDA and VEGA through projects APVV-15-0545 and VEGA 2/0161/17, respectively, as well as to Slovak Academy of Sciences through project SAS-MOST JRP 2014-9.

Author Contributions: Markéta Ilčíková, Miroslav Mrlik, Vladimir Pavlinek and Jaroslav Mosnáček conceived and designed the experiments; Josef Osicka and Miroslav Mrlik performed the experiments; Markéta Ilčíková, Josef Osicka and Miroslav Mrlik analyzed the data; Antonín Minařík was responsible for designing, performing and discussing the AFM investigations. Markéta Ilčíková, Miroslav Mrlik Vladimir Pavlinek and Jaroslav Mosnáček wrote the paper.

Conflicts of Interest: The authors declare no conflict of interest.

References

1. Cohn, R.; Panchapakesan, B. Spatially nonuniform heating and the nonlinear transient response of elastomeric photomechanical actuators. *Actuators* **2016**, *5*, 16. [CrossRef]
2. Torras, N.; Zinoviev, K.E.; Camargo, C.J.; Campo, E.M.; Campanella, H.; Esteve, J.; Marshall, J.E.; Terentjev, E.M.; Omastova, M.; Krupa, I.; et al. Tactile device based on opto-mechanical actuation of liquid crystal elastomers. *Sens. Actuators A* **2014**, *208*, 104–112. [CrossRef]
3. Camargo, C.J.; Campanella, H.; Marshall, J.E.; Torras, N.; Zinoviev, K.; Terentjev, E.M.; Esteve, J. Batch fabrication of optical actuators using nanotube–elastomer composites towards refreshable braille displays. *J. Micromech. Microeng.* **2012**, *22*, 9. [CrossRef]
4. Marshall, J.E.; Gallagher, S.; Terentjev, E.M.; Smoukov, S.K. Anisotropic colloidal micromuscles from liquid crystal elastomers. *J. Am. Chem. Soc.* **2014**, *136*, 474–479. [CrossRef] [PubMed]
5. Baer, G.M.; Small, W.; Wilson, T.S.; Benett, W.J.; Matthews, D.L.; Hartman, J.; Maitland, D.J. Fabrication and in vitro deployment of a laser-activated shape memory polymer vascular stent. *Biomed. Eng. Online* **2007**, *6*, 43. [CrossRef] [PubMed]
6. Maitland, D.J.; Metzger, M.F.; Schumann, D.; Lee, A.; Wilson, T.S. Photothermal properties of shape memory polymer micro-actuators for treating stroke. *Lasers Surg. Med.* **2002**, *30*, 1–11. [CrossRef] [PubMed]
7. Lu, S.X.; Liu, Y.; Shao, N.; Panchapakesan, B. Nanotube micro-opto-mechanical systems. *Nanotechnology* **2007**, *18*, 065501. [CrossRef]
8. Zhang, X.; Yu, Z.B.; Wang, C.; Zarrouk, D.; Seo, J.W.T.; Cheng, J.C.; Buchan, A.D.; Takei, K.; Zhao, Y.; Ager, J.W.; et al. Photoactuators and motors based on carbon nanotubes with selective chirality distributions. *Nat. Commun.* **2014**, *5*. [CrossRef] [PubMed]

9. Fan, X.M.; King, B.C.; Loomis, J.; Campo, E.M.; Hegseth, J.; Cohn, R.W.; Terentjev, E.; Panchapakesan, B. Nanotube liquid crystal elastomers: Photomechanical response and flexible energy conversion of layered polymer composites. *Nanotechnology* **2014**, *25*, 355501. [CrossRef] [PubMed]
10. Pei, Z.Q.; Yang, Y.; Chen, Q.M.; Terentjev, E.M.; Wei, Y.; Ji, Y. Mouldable liquid-crystalline elastomer actuators with exchangeable covalent bonds. *Nat. Mater.* **2014**, *13*, 36–41. [CrossRef] [PubMed]
11. Czanikova, K.; Torras, N.; Esteve, J.; Krupa, I.; Kasak, P.; Pavlova, E.; Racko, D.; Chodak, I.; Omastova, M. Nanocomposite photoactuators based on an ethylene vinyl acetate copolymer filled with carbon nanotubes. *Sens. Actuator B* **2013**, *186*, 701–710. [CrossRef]
12. Czanikova, K.; Ilcikova, M.; Krupa, I.; Micusik, M.; Kasak, P.; Pavlova, E.; Mosnacek, J.; Chorvat, D.; Omastova, M. Elastomeric photo-actuators and their investigation by confocal laser scanning microscopy. *Smart Mater. Struct.* **2013**, *22*, 104001. [CrossRef]
13. Czanikova, K.; Krupa, I.; Ilcikova, M.; Kasak, P.; Chorvat, D.; Valentin, M.; Slouf, M.; Mosnacek, J.; Micusik, M.; Omastova, M. Photo-actuating materials based on elastomers and modified carbon nanotubes. *J. Nanophotonics* **2012**, *6*, 063522. [CrossRef]
14. Ilcikova, M.; Mrlik, M.; Sedlacek, T.; Doroshenko, M.; Koynov, K.; Danko, M.; Mosnacek, J. Tailoring of viscoelastic properties and light-induced actuation performance of triblock copolymer composites through surface modification of carbon nanotubes. *Polymer* **2015**, *72*, 368–377. [CrossRef]
15. Liang, J.J.; Xu, Y.F.; Huang, Y.; Zhang, L.; Wang, Y.; Ma, Y.F.; Li, F.F.; Guo, T.Y.; Chen, Y.S. Infrared-triggered actuators from graphene-based nanocomposites. *J. Phys. Chem. C* **2009**, *113*, 9921–9927. [CrossRef]
16. Ahir, S.V.; Squires, A.M.; Tajbakhsh, A.R.; Terentjev, E.M. Infrared actuation in aligned polymer–nanotube composites. *Phys. Rev. B* **2006**, *73*, 085420. [CrossRef]
17. Park, J.H.; Dao, T.D.; Lee, H.I.; Jeong, H.M.; Kim, B.K. Properties of graphene/shape memory thermoplastic polyurethane composites actuating by various methods. *Materials* **2014**, *7*, 1520–1538. [CrossRef]
18. Loomis, J.; King, B.; Burkhead, T.; Xu, P.; Bessler, N.; Terentjev, E.; Panchapakesan, B. Graphene-nanoplatelet-based photomechanical actuators. *Nanotechnology* **2012**, *23*, 045501. [CrossRef] [PubMed]
19. Feng, Y.Y.; Qin, M.M.; Guo, H.Q.; Yoshino, K.; Feng, W. Infrared-actuated recovery of polyurethane filled by reduced graphene oxide/carbon nanotube hybrids with high energy density. *ACS Appl. Mater. Interf.* **2013**, *5*, 10882–10888. [CrossRef] [PubMed]
20. Fan, X.M.; Khosravi, F.; Rahneshin, V.; Shanmugam, M.; Loeian, M.; Jasinski, J.; Cohn, R.W.; Terentjev, E.; Panchapakesan, B. MoS_2 actuators: Reversible mechanical responses of MoS_2–polymer nanocomposites to photons. *Nanotechnology* **2015**, *26*, 261001. [CrossRef] [PubMed]
21. Lei, Z.Y.; Zhu, W.C.; Sun, S.T.; Wu, P.Y. MoS_2-based dual-responsive flexible anisotropic actuators. *Nanoscale* **2016**, *8*, 18800–18807. [CrossRef] [PubMed]
22. Ilcikova, M.; Mrlik, M.; Sedlacek, T.; Chorvat, D.; Krupa, I.; Slouf, M.; Koynov, K.; Mosnacek, J. Viscoelastic and photo-actuation studies of composites based on polystyrene-grafted carbon nanotubes and styrene-*b*-isoprene–*b*–styrene block copolymer. *Polymer* **2014**, *55*, 211–218. [CrossRef]
23. Spitalsky, Z.; Danko, M.; Mosnacek, J. Preparation of functionalized graphene sheets. *Curr. Org. Chem.* **2011**, *15*, 1133–1150. [CrossRef]
24. Hui, C.M.; Pietrasik, J.; Schmitt, M.; Mahoney, C.; Choi, J.; Bockstaller, M.R.; Matyjaszewski, K. Surface-initiated polymerization as an enabling tool for multifunctional (nano-)engineered hybrid materials. *Chem. Mater.* **2014**, *26*, 745–762. [CrossRef]
25. Ilcikova, M.; Mosnacek, J.; Mrlik, M.; Sedlacek, T.; Csomorova, K.; Czanikova, K.; Krupa, I. Influence of surface modification of carbon nanotubes on interactions with polystyrene–*b*–polyisoprene-*b*-polystyrene matrix and its photo-actuation properties. *Polym. Adv. Technol.* **2014**, *25*, 1293–1300. [CrossRef]
26. Ilcikova, M.; Mrlik, M.; Sedlacek, T.; Slouf, M.; Zhigunov, A.; Koynov, K.; Mosnacek, J. Synthesis of photoactuating acrylic thermoplastic elastomers containing diblock copolymer-grafted carbon nanotubes. *ACS Macro Lett.* **2014**, *3*, 999–1003. [CrossRef]
27. Hummers, W.S.; Offeman, R.E. Preparation of graphitic oxide. *J. Am. Chem. Soc.* **1958**, *80*, 1339. [CrossRef]
28. Ilcikova, M.; Mrlik, M.; Spitalsky, Z.; Micusik, M.; Csomorova, K.; Sasinkova, V.; Kleinova, A.; Mosnacek, J. A tertiary amine in two competitive processes: Reduction of graphene oxide vs. Catalysis of atom transfer radical polymerization. *RSC Adv.* **2015**, *5*, 3370–3376. [CrossRef]

29. Mrlik, M.; Ilcikova, M.; Plachy, T.; Pavlinek, V.; Spitalsky, Z.; Mosnacek, J. Graphene oxide reduction during surface-initiated atom transfer radical polymerization of glycidyl methacrylate: Controlling electro-responsive properties. *Chem. Eng. J.* **2016**, *283*, 717–720. [CrossRef]
30. Yoon, J.T.; Lee, S.C.; Jeong, Y.G. Effects of grafted chain length on mechanical and electrical properties of nanocomposites containing polylactide-grafted carbon nanotubes. *Compos. Sci. Technol.* **2010**, *70*, 776–782. [CrossRef]
31. Cvek, M.; Mrlik, M.; Ilcikova, M.; Mosnacek, M.; Munster, L.; Pavlínek, V. Synthesis of silicone elastomers containing silyl-based polymer-grafted carbonyl iron particles: An efficient way to improve magnetorheological, damping, and sensing performances. *Macromolecules* **2017**, *50*, 2189–2200. [CrossRef]
32. Rabindranath, R.; Bose, H. On the mobility of iron particles embedded in elastomeric silicone matrix. *J. Phys. Conf. Ser.* **2013**, *412*, 012034. [CrossRef]

Paper II

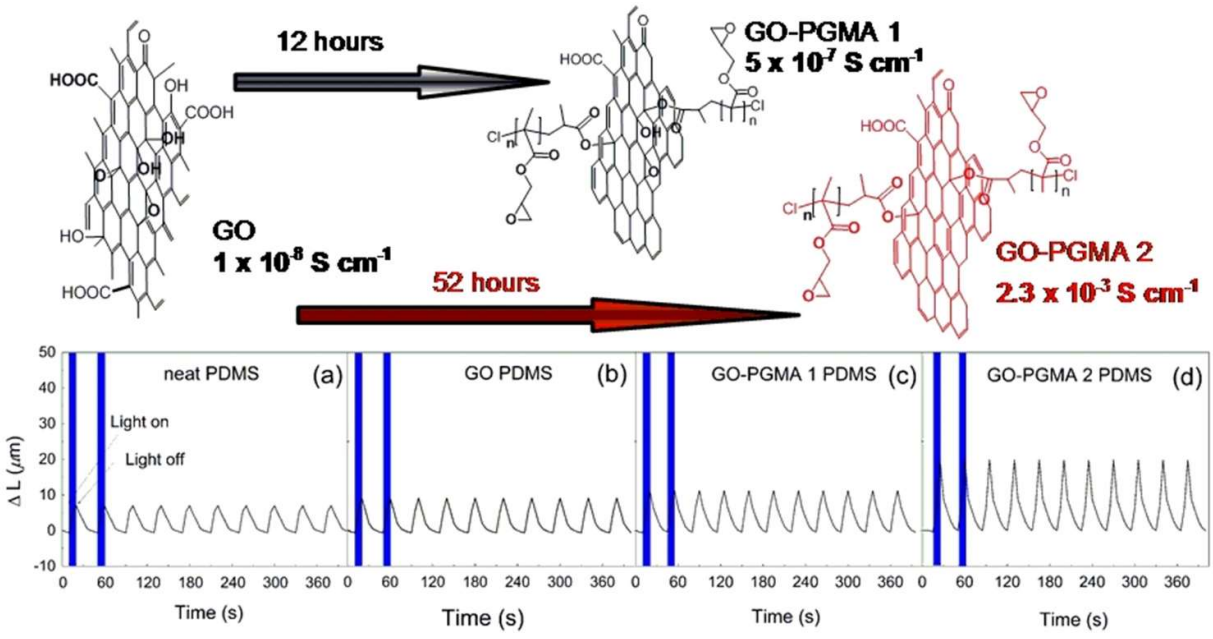
12 hours
GO-PGMA 1
5 x 10-7 S cm-1
GO
1 x 10-8 S cm-1
52 hours
GO-PGMA 2
2.3 x 10-3 S cm-1
HOOC
OH
COOH
HO
neat PDMS
(a)
GO PDMS
(b)
GO-PGMA 1 PDMS
(c)
GO-PGMA 2 PDMS
(d)
Light on
Light off
Δ L (μm)
Time (s)

polymers

MDPI

Article

Reversible Actuation Ability upon Light Stimulation of the Smart Systems with Controllably Grafted Graphene Oxide with Poly (Glycidyl Methacrylate) and PDMS Elastomer: Effect of Compatibility and Graphene Oxide Reduction on the Photo-Actuation Performance

Josef Osicka [1], Miroslav Mrlik [1], Marketa Ilcikova [2,*], Barbora Hanulikova [1], Pavel Urbanek [1], Michal Sedlacik [1,*] and Jaroslav Mosnacek [2,3]

1 Centre of Polymer Systems, University Institute, Tomas Bata University in Zlín, Trida T. Bati 5678, 760 01 Zlín, Czech Republic; osicka@utb.cz (J.O.); mrlik@utb.cz (M.M.); hanulikova@utb.cz (B.H.); urbanek@utb.cz (P.U.)

2 Polymer Institute, Slovak Academy of Sciences, Dúbravska cesta 9, 845 41 Bratislava, Slovakia; upolmosj@savba.sk

3 Centre for Advanced Materials Application, Slovak Academy of Sciences, Dúbravska cesta 9, 845 11 Bratislava, Slovakia

* Correspondence: upolmail@savba.sk (M.I.); msedlacik@utb.cz (M.S.); Tel.: +421-232-294-347 (M.I.); +420-576-038-027 (M.S.)

Received: 20 June 2018; Accepted: 26 July 2018; Published: 28 July 2018

Abstract: This study is focused on the controllable reduction of the graphene oxide (GO) during the surface-initiated atom transfer radical polymerization technique of glycidyl methacrylate (GMA). The successful modification was confirmed using TGA-FTIR analysis and TEM microscopy observation of the polymer shell. The simultaneous reduction of the GO particles was confirmed indirectly via TGA and directly via Raman spectroscopy and electrical conductivity investigations. Enhanced compatibility of the GO-PGMA particles with a polydimethylsiloxane (PDMS) elastomeric matrix was proven using contact angle measurements. Prepared composites were further investigated through the dielectric spectroscopy to provide information about the polymer chain mobility through the activation energy. Dynamic mechanical properties investigation showed an excellent mechanical response on the dynamic stimulation at a broad temperature range. Thermal conductivity evaluation also confirmed the further photo-actuation capability properties at light stimulation of various intensities and proved that composite material consisting of GO-PGMA particles provide systems with a significantly enhanced capability in comparison with neat GO as well as neat PDMS matrix.

Keywords: graphene oxide; reduction; SI-ATRP; photo-responsive material; light-stimuli material; dielectrics; poly (glycidyl methacrylate); dynamic mechanical analysis

1. Introduction

Smart materials belong to a group of matters. Such physical properties can be changed upon external stimulus i.e., electric [1–4] or magnetic field [5–8], pH [9–12], temperature [13–16], or light [17–20]. The systems exhibiting reversible photo-actuation and light-responsive properties are vital for the research community only during the last decade while the rest of the above mentioned properties have been part of the research community over the past 30 years. Therefore, there are still

many drawbacks in this topic like stability of the systems or even performance, which reversibly contracts or elongates the polymer composite sample upon light stimulation. Materials exhibiting this phenomenon can find utilization in various systems controlling the damping properties [21], sensing [22], or haptic displays [23]. Therefore, the broad applications belong to the field of electronic [24], civil engineering [25], or medicine [26], respectively.

In these applications, the graphene oxide (GO) particles as a part of smart systems were properly investigated due to their unique properties, i.e., good dispersibility in the surrounding media [27], possible post-functionalization [28], are easily reduced, and, therefore, provide tunability of the electrical conductivity [29]. There are various approaches regarding how to reduce the GO particles such as treatment with hydrazine [30], reduction in the acidic environment [31], or simultaneous reduction of GO during the surface-initiated atom transfer radical polymerization (SI-ATRP) [32].

Due to the high requirements in the above mentioned applications on the final material and from the mechanical and stability point of view, the utilization of poly (dimethyl siloxanes) PDMS is very frequent [33]. Such PDMS material can be either tailored by cross-linking density or using the addition of silicone oil and a curing agent. However, there is still a lack of compatibility of PDMS with common fillers such as MWCNT, graphene, or even GO and, therefore, such fillers need to be modified in order to improve compatibility and dispersibility as well as overall properties of prepared composite materials. There are various techniques of modification using surfactants [34], but such systems are rather instable or uncontrolled polymerization from the surface, which significantly changes the properties of filler [35] and, therefore, the SI-ATRP approach seems to be a very convenient method of surface modification using a variety of monomers [27,32,36,37] or copolymers [38], which significantly improves the compatibility while the basic physical properties such as mechanical or electrical are affected only negligibly.

Therefore, this article is focused on the SI-ATRP of glycidyl methacrylate (GMA) from the surface of GO particles in order to improve their compatibility with PDMS. Successful modification of GO by short polymer chains was proved using TEM and TGA-FTIR measurements. The compatibility, mechanical, dielectric, and photo-actuation properties were investigated when special aim was concentrated on the effect of light intensity on the final photo-actuation performance.

2. Materials and Methods

Graphite (powder, <20 μm, synthetic), sulfuric acid (H_2SO_4, 95%–98%), sodium nitrate ($NaNO_3$, ≥99%), potassium permanganate ($KMnO_4$, 97%), hydrogen peroxide (H_2O_2, 29.0–32.0 wt %), α-bromoisobutyryl bromide (BiBB, 98%), triethylamine (TEA, ≥99%), glycidyl methacrylate (GMA, 98%), ethyl α-bromoisobutyrate (EBiB, 98%), *N*,*N*,*N*′,*N*″,*N*″-pentamethyldiethylenetriamine (PMDETA, ≥99%), copper bromide (CuBr, ≥99%), anisole (99%), and diethyl ether (≥99%) were all purchased from Sigma Aldrich and were used as received.

The graphene oxide was fabricated from graphite powder by a modified Hummers method [39]. The product was separated in a high-speed centrifuge (Sorvall LYNX 4000, Thermo Scientific, Waltham, MA, USA) operating at 10,000 rpm for 20 min at 25 °C. The cleaning routine was based on the dispersion of the GO in 0.1 M HCl and their re–separation in a centrifugal field. The procedure was repeated with distilled water several times until the pH has reached a value of 7. Afterward, the particles were lyophilized in order to remove the residual amount of water after purification and remove the brown powder that was obtained. The initiator BiBB was immobilized, according to the procedure described in detail elsewhere [32]. Two various polymerizations from the surface of GO particles in order to prepare poly (glycidyl methacrylate)-modified GO (GO-PGMA and GO-PGMA-2), were performed by the following procedure. The molar ratio of reactants [GMA]:[EBiB]:[CuBr]:[PMDETA] was [100]:[1]:[1]:[4] and [100]:[1]:[1]:[2] while anisole (50 vol. %) was used as a solvent. The presence of oxygen was minimized by degassing the system by several freeze-pump-thaw cycles and after the last cycle by filling the system with argon. Lastly, the CuBr catalyst was added under argon flow and polymerization was carried out at 60 °C for 4 h and at 50 °C for 12 h for polymerizations performed

with 4:1 and 2:1 ratio of PMDETA to CuBr, respectively. The product was purified by filtration using DMF, acetone, and diethyl ether and dried using lyophilization.

^{1}H nuclear magnetic resonance (NMR) spectra were recorded at 25 °C using an instrument (400 MHz VNMRS Varian, Tokyo, Japan) with deuterated chloroform ($CDCl_3$) as a solvent. The ^{1}H NMR was used to determine the monomer conversion from the ratio of area of peaks assigned to PGMA to the area of peaks assigned to both PGMA and GMA (Figure 1). The molar mass and polydispersity ($Đ$) of PGMA chains were investigated using gel permeation chromatography (GPC) on the GPC instrument (PLGPC220, Agilent, Hachioji, Japan) equipped with GPC columns (Waters 515 pump, two PPS SDV 5 lm columns (diameter of 8 mm, length of 300 mm, 500 Å + 105 Å)) and a Waters 410 differential refractive index detector tempered to 30 °C. The neat GO and GO with a grafted PGMA polymer layer were observed using a transmission electron microscope (TEM, JEM-2100Plus, Jeol, Tokyo, Japan). The samples for the TEM analysis were prepared by dispersing the particles in acetone using mechanical stirring for 5 and 2 min of sonication and dropping the resultant suspension onto a copper grid. The Raman Shift (3 scans, resolution of 2 cm^{-1}) were collected on a Nicolet DXR (Nicolet, Rhinelander, WI, USA) using an excitation wavelength of 532 nm. The integration time was 30 s while the laser power on the surface was set to 1 mW. The powders under investigation were compressed to the form of pellets (diameter of 13 mm, thickness app 1 mm). The pellets were used for electrical conductivity measurements using a two-point method (Keithley 6517B, Cleveland, OH, USA). The contact angle (CA) values were evaluated from the static sessile drop method on the pellets carried out on a Surface Energy Evaluation system equipped with a CCD camera (Advex Instruments, Brno, Czech Republic). A droplet (5 μL) of PDMS was carefully dripped onto the surface and the CA value was recorded. The presented CA results are the average values from 10 independent measurements. The thermo-oxidation decomposition of the samples was on-line monitored using a thermogravimetric analyzer (TGA) operating in an oxygen atmosphere coupled with FTIR with a help of Nicolet iS10 equipped with TGA-IR module (Thermo Scientific, Waltham, MA, USA). In the Figure 2, the highlighted bands are those where the FTIR signal was collected in order to prove the presence of the various components in the GO-based powders.

The composites containing various amount of GO-based particles were prepared using the following standard procedure: PDMS (Sylgard 184, Atlanta, GA, USA) was mixed with silicone oil and subsequently a cross-linker was added in ratios of PDMS: silicone oil: cross-linker 7/3/1 and, lastly, 0.1 vol. % of the particles was added before the curing. In the case of the neat PDMS matrix, we further investigated the same ratio of PDMS in this paper. Silicone oil and a cross-linker was used but without the addition of the particles. In the case of all samples, the mixtures were degassed using a vacuum oven in the four cycles at 10 mbar at room temperature and then placed into the oven and cured at an elevated temperature set to 60 °C for 6 h.

The thermal conductivity was measured by one side contact method using the TCi model (C-Term Technologies, Vancouver, BC, Canada). The viscoelastic properties of both the nanocomposite and pure polymer matrix were studied through the dynamic mechanical analysis (DMA) in tensile mode. All measurements were performed at a linear viscoelastic region. The measurement was done at 1 Hz in the temperature range from −150 to 150 °C. To provide information about how the modification of the GO with PGMA grafts influences the strain of the materials, a dependence of the storage and loss moduli was plotted against the change in the length ΔL, i.e., parameter specified in the experimental photo-actuation investigations. The measurements were performed at 1 Hz and at 25 °C. The dielectric spectroscopy ranged from a temperature of −150 to 100 °C and ranged in frequency from 10^{-1} to 10^7 Hz, which were employed to investigate the polymer chains dynamics.

The glass transition process was evaluated through activation energies calculated from the Arrhenius equation (Equation (1)) in order to see the effect of modification on the relaxation processes in the PDMS based composites.

$$f_\beta = f_\infty \exp\left(\frac{E_a}{k_B T}\right), \quad (1)$$

where E_a is the activation energy, f_∞ is the pre-exponential factor, T is thermodynamic temperature, and k_B is the Boltzmann constant.

In order to properly investigate the polymer chains dynamics, the loss permittivity need to be recalculated to the loss modulus. This recalculation was based according to Equation (2) [40].

$$\begin{aligned} M^* &= \frac{1}{\varepsilon^*} \\ M' &= \frac{\varepsilon'}{\varepsilon'^2+\varepsilon''^2} \\ M'' &= \frac{\varepsilon''}{\varepsilon'^2+\varepsilon''^2} \end{aligned} \tag{2}$$

where ε* is complex permittivity and ε' and ε'' are relative permittivity and loss permittivity, respectively. M^* is the complex dielectric modulus and M' and M'' are storage and dielectric loss moduli, respectively.

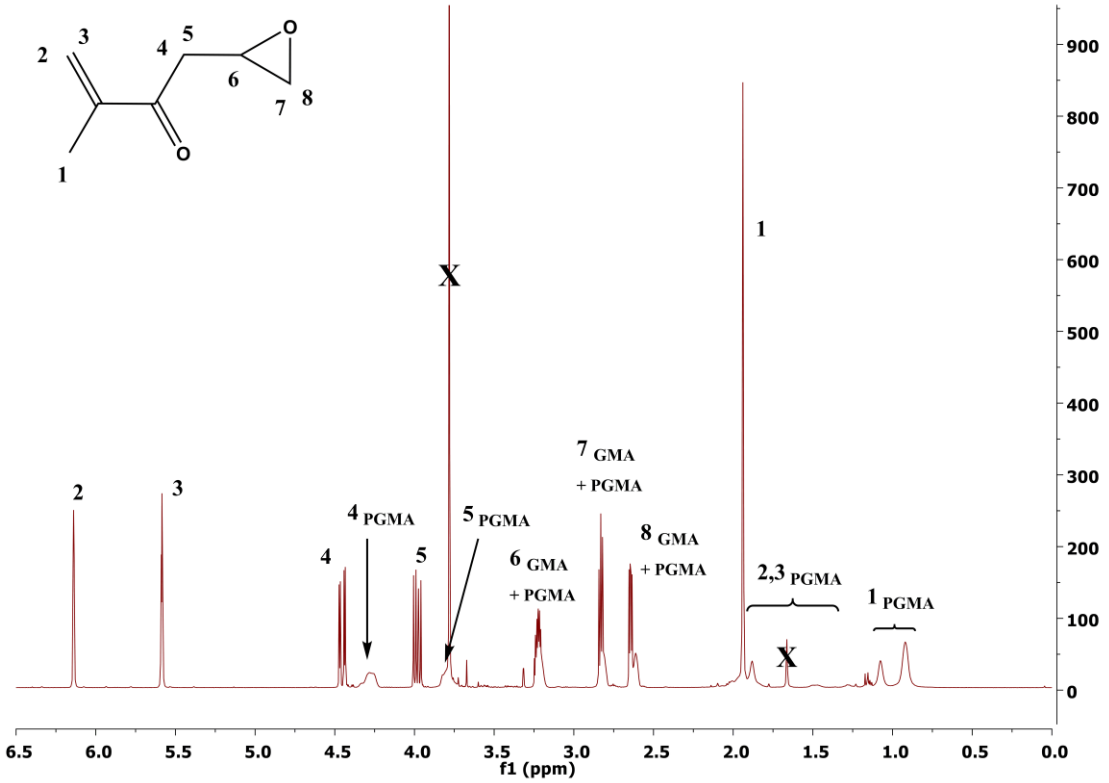

Figure 1. Representative ^{1}H NMR spectrum from filtered polymerization mixture of glycidyl methacrylate performed with [GMA]:[EBiB]:[CuBr]:[PMDETA] ratio of [100]:[1]:[1]:[4] at 60 °C for 4 h. The monomer conversion was 43%.

The photo-actuation ability of both the matrix and composite samples was investigated using thermal mechanical analysis (TMA, Mettler Toledo, Columbus, OH, USA), which was previously published [15]. Red LED diode (Luxeon Rebell, Philips, Amsterdam, the Netherlands) was used for irradiation. Irradiation was applied for 10 s at 627 nm with 6, 9, and 12 mW light source intensity under 10% pre-strain of the samples. The maximum value of actuation is characterized by a change in sample length during the exposition to light, $\Delta L = (L_0 - L)/L_0$, where L_0 is the length of non-irradiated sample and L is the length of an irradiated sample.

3. Results and Discussion

Successful polymerization of GMA from the surface of GO was confirmed by various techniques such as ^{1}H NMR, GPC, TEM, and TGA-FTIR. The conversion of GMA was calculated to be 43% and 46%, according to ^{1}H NMR spectra and the molar mass and Đ of PGMA chains determined from GPC were 5900 g·mol^{-1} and 1.28 and 6100 g·mol^{-1} and 1.26 for the GO-PGMA 1 and GO-PGMA 2, respectively, fit the experimental molar mass with the theoretical one. Furthermore, from the TEM investigation, the 2D nature of the neat GO particles (Figure 2a) can be clearly seen. Moreover, the 2D structure was also observed in the case of GO-PGMA while the presence of the PGMA chains exhibit rather flossy-like structures, which provided substantial coating for the GO particle (Figure 2b). The change in the reaction mixture for GO modification (Figure 2c) does not lead to a significant change in the morphology and provides nearly the same morphology than the previous one (Figure 2b).

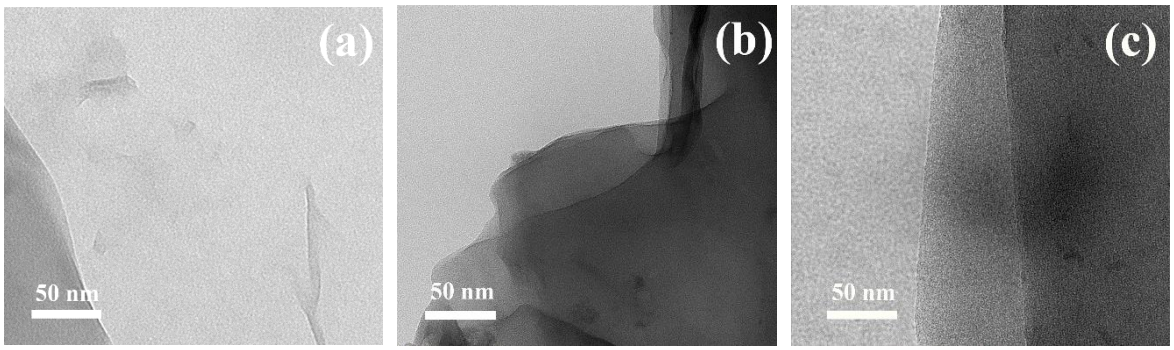

Figure 2. TEM images of (**a**) neat GO; (**b**) GO-PGMA; and (**c**) GO-PGMA-2.

The TGA-FTIR technique utilizing the on-line monitoring of the FTIR spectra during thermal decomposition of the neat GO (Figure 3a,b), GO with bonded initiator (Figure 3c,d), and GO-PGMA (Figure 3e,f) particles was employed to further prove the successful coating of GO with PGMA chains. In this case, the TGA spectra of the left side of Figure 3 correspond to the FTIR spectra on the right side of Figure 3. For the neat GO particles and GO with an initiator, the detailed description was already published elsewhere [41]. However, the following description is novel for GO-PGMA particles. It can be clearly seen that the particles peak around 200 °C, which corresponds to oxygen-containing groups that decrease as side information to prove the partial reduction of the GO-PGMA particles. Moreover, the presence of the successful coating is remarkable from Figure 3e when, in the range from 250 to 450 °C, we observed two peaks both corresponding to the thermal decomposition of PGMA. A similar range of PGMA decomposition was also found in the case of modification of carbonyl iron [42] as well as in the case of GO-PGMA modified through SI-ATRP where the mass loss in Figure 3e is very similar to the following reference [27]. In case of GO-PGMA-2, the TGA-FTIR scan looked nearly identical because, from the structural point of view, the FTIR spectra in Figure 3f represent the collection of the signal during the period highlighted in Figure 3e by a cyan color. Specific absorption bands were found at 1722 cm^{-1} (carbonyl), 1318 cm^{-1} C-O-C stretching, 2961, and 2791 cm^{-1} (alkyl vibrations). Furthermore, the sharp peak at 750 cm^{-1} is based on an epoxy ring absorption and, therefore, confirms the presence of PGMA polymer chains grafted on the surface of GO.

Graphene oxide reduction is a very important factor from its applicability point of view. If the material has a higher electric conductivity, the thermal conductivity is higher. The thermal energy redistribution in the sample is a crucial factor for the final photo-actuation performance. In addition, the composite material upon its deformation can show a sensing capability only if certain resistivity of the material is reached. Therefore, the high conductivity of the final composite is very important. This is similarly observed in the study by Georgousiss et al. [43]. Therefore, the conductivity and Raman spectroscopy (Figure 4) were investigated to prove the degree of reduction of GO and variously reduced GO-PGMA particles. The intensities ratios (I_D/I_G) were found to be 0.9 for neat GO (Figure 4a)

and 1.08 and 1.26 for GO-PGMA 1 (Figure 4b) and GO-PGMA 2 (Figure 4c) corresponding to the determined conductivities of 1.2×10^{-8}, 5×10^{-7}, and 2.3×10^{-3} S·cm^{-1}, respectively. The ratios indicate a significant and controllable reduction during the SI-ATRP process, which is very promising for further industrial applications.

Compatibility of the filler with a matrix is a crucial factor for improvement of the physical as well as mechanical properties of the final composite material. Inhomogeneity present in the sample due to the weak compatibility can be mainly responsible for mechanical instabilities during a repeatable mechanical load or, in the case of materials with desired electrical or thermal conductivities, can lead to their suffered performances. Therefore, the contact angle values of PDMS drops, as the elastomeric matrix used in this study, onto the surface of pellets prepared from the neat GO or GO-PGMA particles, which were investigated (Figure 5). It can be clearly seen that the contact angle of neat GO was determined to be 49.9° ± 3.2°, which showed relatively poor compatibility while the modification of the GO with short polymer chains of PGMA decreased the contact angle to 40.1° ± 1.3° and, therefore, improved the wettability between the PDMS and GO-PGMA surface due to the presence of the aliphatic polymer backbone. In this case, the influence of various conductivities was not proven and contact angles were in the range of error. However, the contacts angles were not so low as was previously found by our research group for PMMA or PBMA grafts [36].

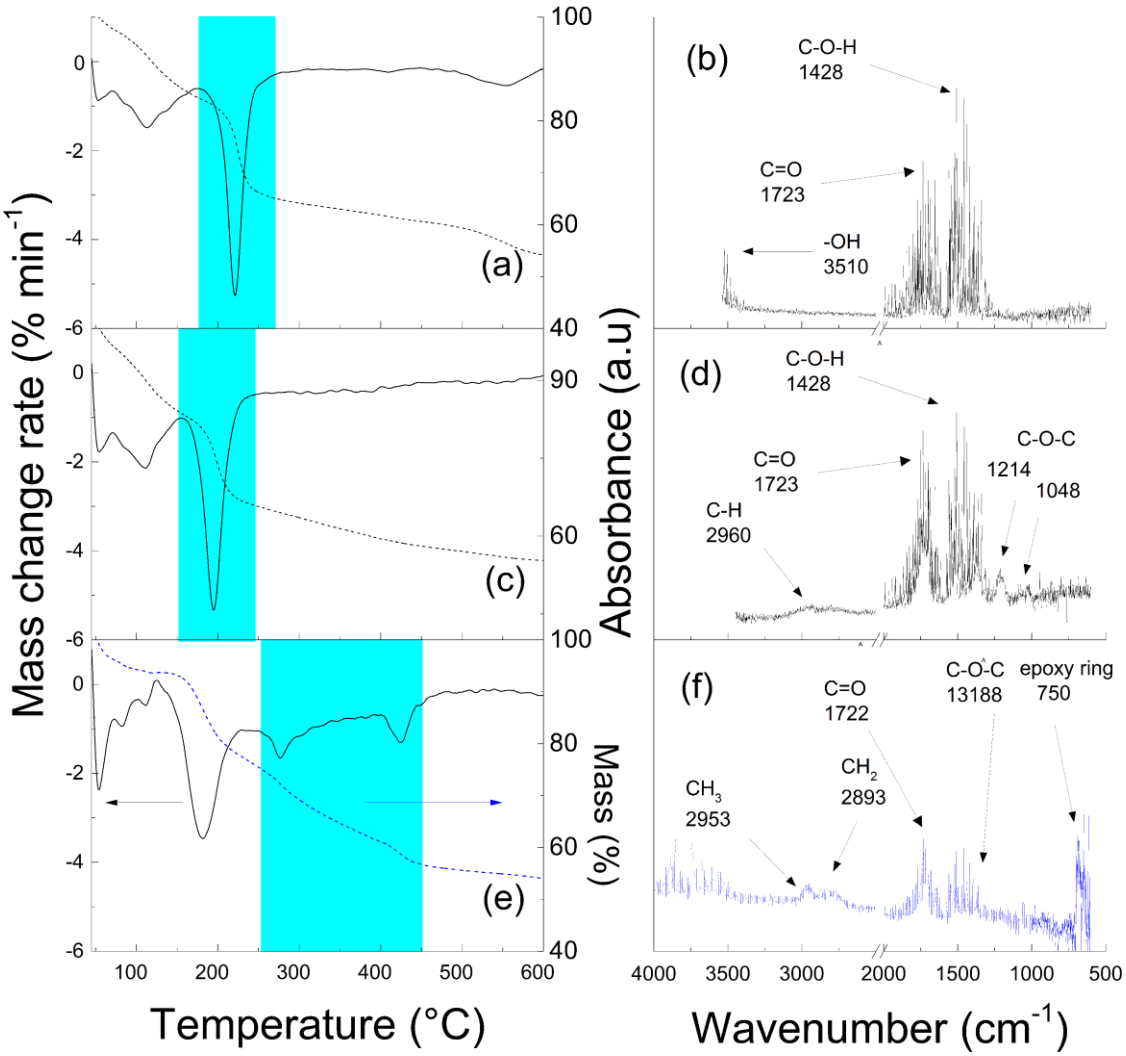

Figure 3. TGA analysis (**a**,**c**,**e**) with on-line monitoring of the FTIR spectra (**b**,**d**,**f**) for neat GO (**a**,**b**); GO-iniciator, and (**c**,**d**) and GO-PGMA (**e**,**f**) particles.

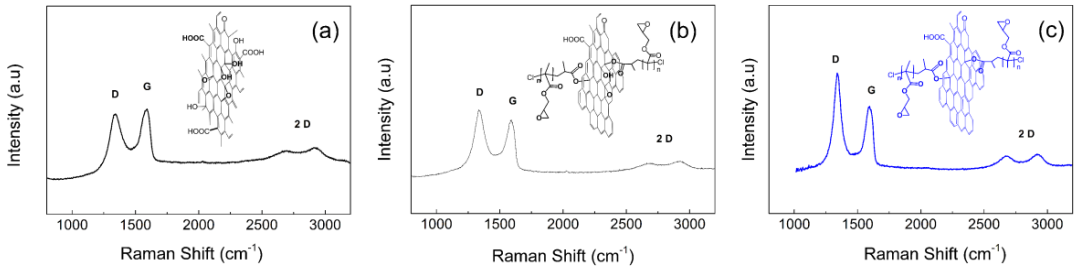

Figure 4. Raman spectra of the neat GO (**a**) GO-PGMA 1; (**b**) GO-PGMA 2; and (**c**) particles and corresponding chemical structures.

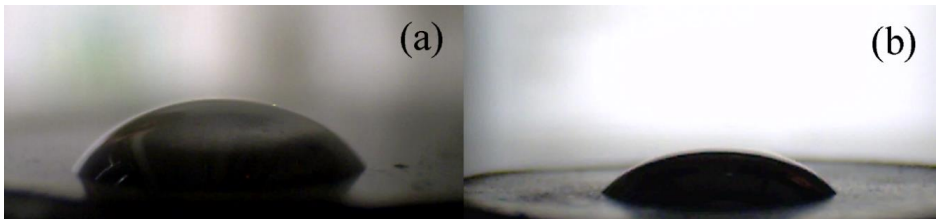

Figure 5. Images from CCD camera of the 5 µL PDMS droplets on the neat GO (**a**) and GO-PGMA (**b**).

In order to show how the optical properties of the composites were changed after adding various fillers, the images of neat PDMS as well as the GO-based composites were performed (Figure 6a). It can be seen that the best optical properties had a neat PDMS. However, the modification using the SI-ATRP approach provided the composites with better dispersed filler in comparison to the neat GO due to the fact that neat GO/PDMS composites seem to be of higher transparency with relatively big agglomerates and less uniform filler dispersion compared to the GO-PGMA grafted particles. In addition, the change of the contact angles between the water and composites is nearly negligible and is more affected by the modification than the time of storage (Figure 6b). This means that the properties that were changing over 7 days did so negligibly. The contact angle for neat as-prepared PDMS and after 7 days of storage is 105.4° and 105.1°, respectively. Similar results were found for other composites where the as-prepared GO-PGMA 1 after 7 days of storage show contact angles of 98.7° and 98.2°, respectively. The longer grafts provided composites with a slightly lower contact angle of 97.4° and 96.8° for as-prepared GO-PGMA 2 and after 7 days of storage, respectively, due to the higher amount of the hydrophilic epoxy groups presented on the GO-PGMA 2 particles surface. The lower contact angle was observed for neat GO, which was expected due to the presence of hydroxyl, carboxyl, and epoxy groups on its surface. Therefore, showing contact angle of 87.7° and 87.1° for as-prepared GO composite after 7 days of the storage, respectively.

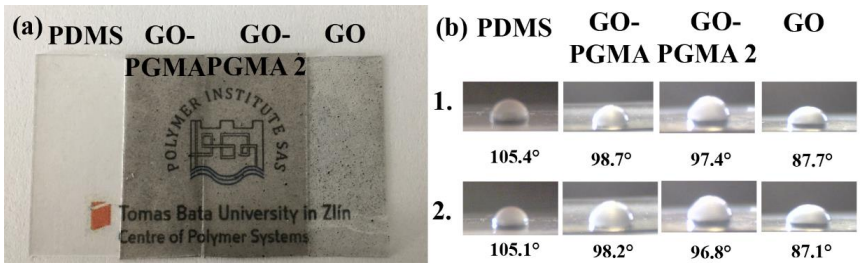

Figure 6. (**a**) Images of the neat PDMS and prepared composites and (**b**) Images from CCD camera of the 5 µL water droplets on the neat PDMS and various composites. Line 1 represents measurements for as-prepared samples while line 2 represents the measurements of the samples after 7 days of storage at RT.

Investigations of dielectric properties (Figure 7) is very important due to the fact that, with the help of measurement in a broad temperature range and frequency-dependent permittivity, it is possible to calculate E_a of the glass transition and T_g, which provides information about the polymer chain flexibility in the presence of GO particles. In our study, however, the prepared composites exhibited a rather strong electrical response to the applied electric field and, therefore, obtained ε' and ε'' exhibited electrode polarization and were not suitable for E_a calculation [40]. Therefore, the expression of M' and M'' was used, which was mainly M'' according to Equation (2). Therefore, this quantity was also used for the interpretation of the dielectric spectra in Figure 5. Here the peak around −120 °C indicating the presence of T_g can be seen for all investigated samples.

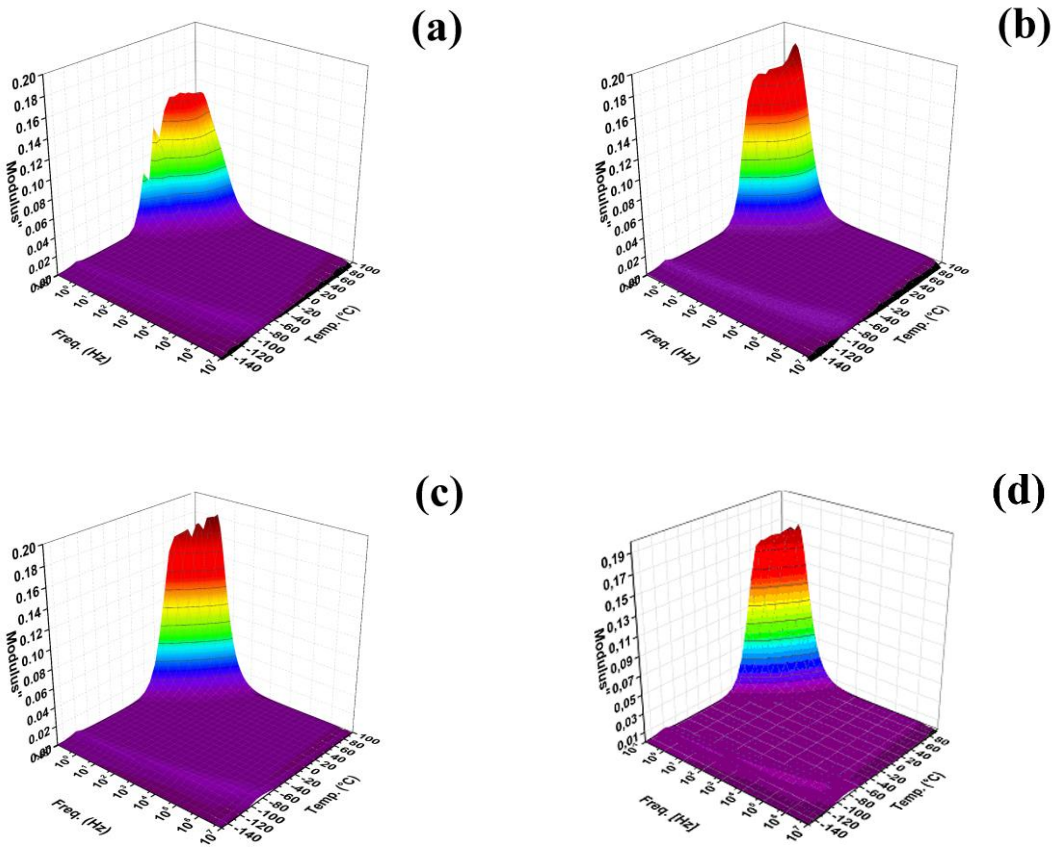

Figure 7. 3D plots of the dielectric properties of the neat PDMS matrix, (**a**) neat GO-PDMS; (**b**) GO-PGMA 1; (**c**) and GO-PGMA 2; (**d**) All at 0.1 vol. % content in PDMS.

From the position of the maxima of this peak at various temperatures, the E_a of T_g was calculated according to Equation (1) and results are listed in Table 1. It can be clearly seen that the highest E_a of 45.70 kJ·mol^{-1} was found for neat PDMS by following the neat GO composite with E_a of 36.57 kJ·mol^{-1}. The sample GO-PGMA 1 with 0.1 volume percentage of particles of lower conductivity possess only a slight decrease in E_a showing an improved PDMS chain mobility after modification while the sample GO-PGMA 2 with same particle loading. However, with significantly higher conductivity possesses significantly better chain mobility and, lastly, the lowest E_a of 23.80 kJ·mol^{-1} further enhanced the photo-actuation capability. These results indicate that the presence of the GO-PGMA particles in the composite significantly improves the flexibility of the PDMS chains due to the fact that the energy necessary for the polymer chain movement is lower. As it will be shown below, these results were also confirmed by the investigation of DMA and photo-actuation performance since the results from these experiments well-correlates with these dielectric investigations.

Table 1. Activation energies of a glass transition process for pure PDMS and PDMS composites with variously conducting particles.

Sample Code	E_a (kJ·mol^{-1}) of T_g (−120 °C)
pure PDMS	45.70
0.1 vol % neat GO/PDMS	36.57
0.1 vol % GO-PGMA 1/PDMS	31.32
0.1 vol % GO-PGMA 2/PDMS	23.80

Dynamic mechanical properties (Figure 8) are one of the most crucial factors influencing the applicability of materials as photo-actuation systems. Reversible contraction/elongation of the sample by light stimulation is a rather dynamic process and, therefore, investigation upon dynamic conditions is very important. As can be seen in Figure 8a, the storage moduli below T_g were nearly the same for all investigated samples. The first difference can be seen above T_g when the lowest storage modulus was obtained for neat PDMS and was followed by the GO-PGMA sample. The highest values were observed for samples containing neat GO particles. A similar situation occurs above the melting region when the neat GO possessed the highest storage modulus. This observation can be explained by possible covalent bonding between the PDMS and hydroxyl groups of GO particles [44]. Since the amount of the hydroxyl groups significantly decreased due to both the modification with PGMA chains and the reduction of the GO (clearly seen from Figures 3 and 4), the mechanical response is mostly based on the good compatibility of the GO-PGMA particles with the PDMS. From the temperature dependence of the tan δ (Figure 8b), it can be seen that the peak of tan δ for the sample containing GO-PGMA decreased when compared with pure PDMS or PDMS filled with neat GO, which indicated enhanced compatibility of GO-PGMA with the PDMS matrix. Yet, the absolute value of tan δ after all transitions was higher for GO-PGMA than for PDMS matrix and PDMS containing neat GO due to the fact that physical entanglements of PGMA short polymer chains provide more flexible structure than in the case of GO with possible covalent bonding to the PDMS. Composites consisting of various GO-PGMA with different conductivities show nearly the same mechanical behavior. The differences were in the range of error. Therefore, only the one consisting of GO-PGMA particles with higher conductivities are shown in Figure 8. Therefore, it can be stated that GO-PGMA/PDMS composite provides a system with enhanced damping and also with improved flexibility of the composite system, which well-correlates with dielectric studies and which is in the same time highly suitable for the photo-actuation point of view.

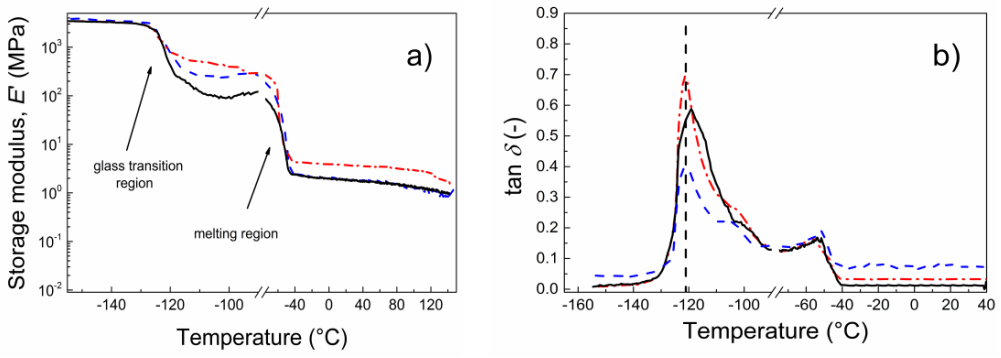

Figure 8. Dependence of the storage modulus (**a**) and tan δ (**b**) for broad temperature range for neat PDMS (black solid line) and for PDMS composites containing 0.1 vol % of neat GO (red dash dot line) and GO-PGMA 2 (blue dashed line).

In order to investigate the mechanical properties of the prepared composites, dependence on the change in the length ΔL in the range of potential photo-actuation on the viscoelastic moduli were measured. Various natures of the filler can provide the system with multiple mechanical performances

at the strain deformation obtained during light-stimulation. As can be seen in Figure 9, the composite consisting of the neat GO particles has the highest values of the storage modulus. However, the significant drop is visible at lower deformations. However, the GO-PGMA-based composites show lower values, which corresponds to their softer nature and higher possible elongation. According to the performed measurements, it can be expected that GO-PGMA composites will provide systems with better photo-actuation performance due to more suitable mechanical properties.

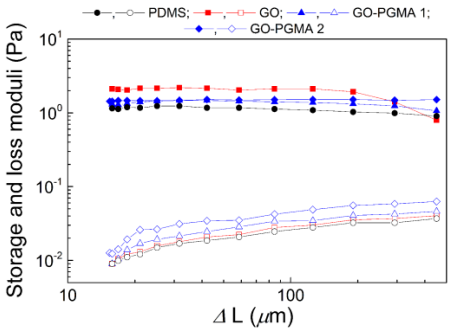

Figure 9. Dependence of the storage (solid symbols) and loss (open symbols) moduli on the change in deformation upon dynamic tensile testing at 1 Hz and 25 °C.

According to the previous study [45], the thermal conductivity is another crucial parameter affecting the photo-actuation performance. As can be seen from Table 2, the pure PDMS matrix has thermal conductivity of 0.071 $W \cdot m \cdot K^{-1}$. It increases with the addition of filler for both investigated samples. Due to the improved compatibility of GO particles with the PDMS matrix by PGMA chains grafted on the GO surface, these composites with GO-PGMA exhibited further improvement of thermal conductivity compared with the composite based on neat GO (Table 2). Therefore, the composite sample containing GO-PGMA particles could provide significant contribution to the enhanced photo-actuation capabilities due to the improved heat redistribution within the sample.

Table 2. Thermal conductivity of pure PDMS and PDMS composites with various fillers.

Sample Code	Thermal Conductivity ($W \cdot m \cdot K^{-1}$)
pure PDMS	0.071
0.1 vol % neat GO/PDMS	0.144
0.1 vol % GO-PGMA-1/PDMS	0.152
0.1 vol % GO-PGMA-2/PDMS	0.161

In order to confirm the photo-actuation ability of the GO-PGMA/PDMS composite, the photo-actuation performance in this case expressed as the change in the length ΔL was investigated (Figure 10). It can be seen that there was only a slight increase of the photo-actuation performance for PDMS containing neat GO compared with the neat PDMS provided that ΔL is 9.1 and 7.1 μm, respectively. The situation was considerably different in the case of the sample containing GO-PGMA particles (Figure 10c,d). The ΔL after irradiation reached a value of 20.2 μm, which is nearly three times higher than that obtained for the neat PDMS matrix (Figure 10a) and more than two times higher than that for PDMS composite with neat GO particles (Figure 10b). This significant enhancement is caused by several factors: (i) the particles has better wettability to PDMS and, therefore, better compatibility of the filler with the matrix, (ii) the presence of PGMA prevents the additional cross-links presented in the PDMS or GO/PDMS providing the system with more flexible structure, and (iii) increased electrical conductivity due to GO reduction during the SI-ATRP modification of GO leading to the enhanced thermal conductivity. The first and the third factors are responsible for more effective heat transport and homogeneous heat redistribution. The second mentioned factor ensures good flexibility, which is very important for reversible actuation and positively influences the overall performance.

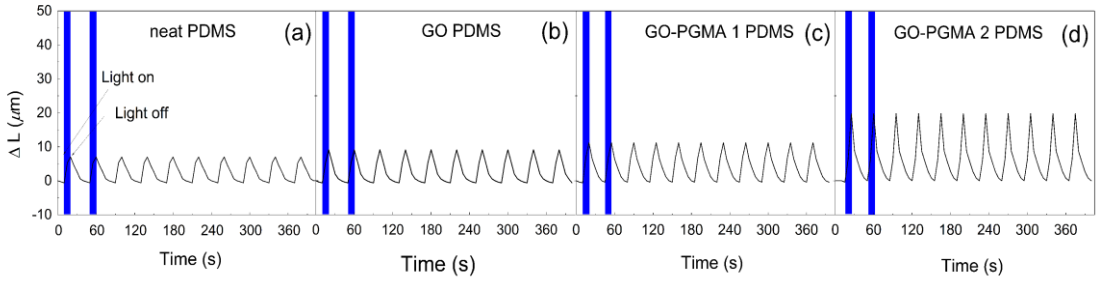

Figure 10. Photo-actuation performance of pure PDMS (**a**) and PDMS composites containing 0.1 vol.% of neat GO; (**b**) GO-PGMA-1; (**c**) and GO-PGMA-2 (**d**) at 6 mW irradiation intensity.

With increased intensity of the radiation, the difference between the investigated systems became even more pronounced. First, it should be mentioned that for neat PDMS, the changes were negligibly affected by the increasing intensity (results are not presented). The PDMS composite containing neat GO showed only a slight increase of Δ*L* in the line 9.1, 10.7, and 12.5 μm for 6, 9, and 12 mW, respectively (Figure 11).

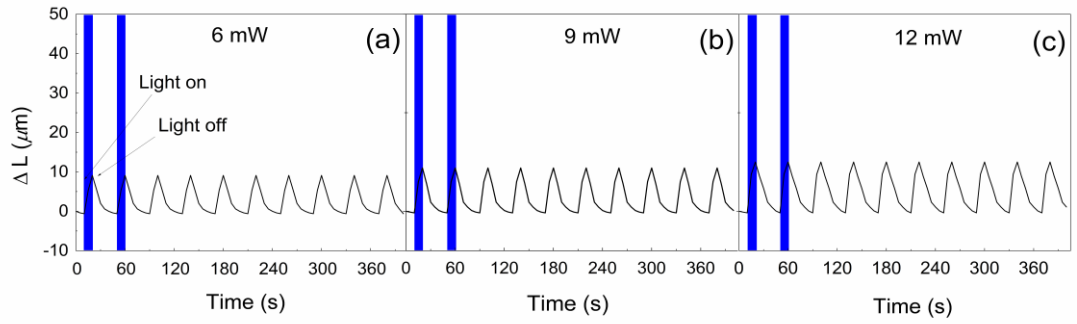

Figure 11. Photo-actuation performance of GO/PDMS composite at (**a**) 6 mW; (**b**) 9 mW; and (**c**) 12 mW irradiation intensity.

However, the PDMS containing GO-PGMA showed significant enhancement in photo-actuation performance with ΔL in the line 20.2, 30.2, and 36.7 μm for 6, 9, and 12 mW, respectively (Figure 12). The main reason for this behavior is possible covalent interactions of the neat GO and PDMS already observed from DMA investigations. Therefore, it can be stated than the developed composite system based on the PDMS matrix containing GO nanoparticles simultaneously reduced and grafted with PGMA chains provided the reversible photo-actuation phenomenon and has excellent mechanical properties in a dynamic mode, which is highly promising for their potential applications.

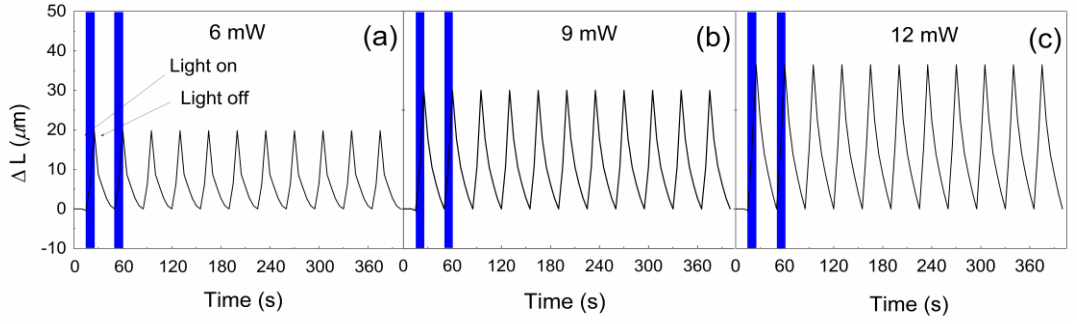

Figure 12. Photo-actuation performance of GO-PGMA 2/PDMS composite at (**a**) 6 mW; (**b**) 9 mW; and (**c**) 12 mW irradiation intensity.

4. Conclusions

In this paper, the successful grafting of the PGMA on the surface of the GO particles was performed by SI-ATRP and confirmed using TGA-FTIR and TEM investigations. Simultaneous reduction of GO during SI-ATRP was proven by Raman spectroscopy and electrical conductivity measurements. The enhanced compatibility of PDMS with GO after its modification with PGMA chains was confirmed by the contact angle measurements of PDMS drops on the GO and GO-PGMA pellets. Lower E_a of T_g of PDMS chains in the GO-PGMA/PDMS composite calculated from dielectric measurements compared with neat PDMS or GO/PDMS composite pointed to higher polymer chain dynamics thanks to the incorporation of GO-PGMA nanoparticles. Important mechanical performance upon dynamic conditions was investigated using DMA at a broad temperature range and it was found that GO surface modification provides the materials with enhanced damping properties, which positively affects the photo-actuation performance. Lastly, the photo-actuation capability measurements showed significantly improved performance of GO-PGMA-based composites due to the improved dispersibility, enhanced flexibility, and increased thermal conductivity. All these aspects provided the system with very promising performance and with values suitable for real-life applications.

Author Contributions: Conceptualization, M.M. and J.M. Methodology, M.I. Formal Analysis, J.O., M.M., M.I., and M.S. Investigation, J.O., M.M., B.H., P.U., and M.S. Writing-Original Draft Preparation, J.O., M.M., M.I., and J.M.. Writing-Review & Editing, M.S.

Funding: This research was funded by the Czech Science Foundation (no. 16-20361Y) for financial support. This work was also supported by the Ministry of Education, Youth and Sports of the Czech Republic-program NPU I (LO1504). Authors M.I. and J.M. gratefully acknowledge APVV-15-0545 and APVV-14-0891 for financial support. The TGA-FTIR results obtained in this article were possibly collected using the device brought from the financial support of Operational Program Research and Development for Innovations co-funded by the European Regional Development Fund (ERDF) and national budget of the Czech Republic within the framework of project CPS-strengthening research capacity (no. CZ.1.05/2.1.00/19.0409).

Conflicts of Interest: The authors declare no conflict of interest.

References

1. Ilcikova, M.; Mrlik, M.; Babayan, V.; Kasak, P. Graphene oxide modified by betaine moieties for improvement of electrorheological performance. *RSC Adv.* **2015**, *5*, 57820–57827. [CrossRef]
2. Jun, C.S.; Kwon, S.H.; Choi, H.J.; Seo, Y. Polymeric Nanoparticle-Coated Pickering Emulsion-Synthesized Conducting Polyaniline Hybrid Particles and Their Electrorheological Study. *ACS Appl. Mater. Interfaces* **2017**, *9*, 44811–44819. [CrossRef] [PubMed]
3. Mosse, A. Gossamer timescapes: A design-led investigation into electro-active and light responsive textiles for the home. *Smart Mater. Struct.* **2018**, *27*, 074009. [CrossRef]
4. Peng, L.; Liu, Y.; Huang, J.N.; Li, J.H.; Gong, J.H.; Ma, J.H. Microfluidic fabrication of highly stretchable and fast electro-responsive graphene oxide/polyacrylamide/alginate hydrogel fibers. *Eur. Polym. J.* **2018**, *103*, 335–341. [CrossRef]
5. Mrlik, M.; Ilcikova, M.; Cvek, M.; Pavlinek, V.; Zahoranova, A.; Kronekova, Z.; Kasak, P. Carbonyl iron coated with a sulfobetaine moiety as a biocompatible system and the magnetorheological performance of its silicone oil suspensions. *RSC Adv.* **2016**, *6*, 32823–32830. [CrossRef]
6. Han, S.; Choi, J.; Seo, Y.P.; Park, I.J.; Choi, H.J.; Seo, Y. High-Performance Magnetorheological Suspensions of Pickering-Emulsion-Polymerized Polystyrene/Fe_3O_4 Particles with Enhanced Stability. *Langmuir* **2018**, *34*, 2807–2814. [CrossRef] [PubMed]
7. Deng, L.; Jia, W.P.; Zheng, W.; Liu, H.; Jiang, D.G.; Li, Z.M.; Tian, Y.; Zhang, W.L.; Liu, J.Q. Hierarchically magnetic Ni-Al binary layered double hydroxides: Towards tunable dual electro/magneto-stimuli performances. *J. Ind. Eng. Chem.* **2018**, *58*, 163–171. [CrossRef]
8. Nakayama, M.; Kajiyama, S.; Kumamoto, A.; Nishimura, T.; Ikuhara, Y.; Yamato, M.; Kato, T. Stimuli-responsive hydroxyapatite liquid crystal with macroscopically controllable ordering and magneto-optical functions. *Nat. Commun.* **2018**, *9*, 568. [CrossRef] [PubMed]

9. Mrlík, M.; Špírek, M.; Al-Khori, J.; Ahmad, A.A.; Mosnaček, J.; AlMaadeed, M.A.; Kasák, P. Mussel-mimicking sulfobetaine-based copolymer with metal tunable gelation, self-healing and antibacterial capability. *Arabian J. Chem.* **2017**. [CrossRef]
10. Chen, W.; Ma, Y.; Pan, J.M.; Meng, Z.H.; Pan, G.Q.; Sellergren, B. Molecularly Imprinted Polymers with Stimuli-Responsive Affinity: Progress and Perspectives. *Polymers* **2015**, *7*, 1689–1715. [CrossRef]
11. Curcio, M.; Mauro, L.; Naimo, G.D.; Amantea, D.; Cirillo, G.; Tavano, L.; Casaburi, I.; Nicoletta, F.P.; Alvarez-Lorenzo, C.; Iemma, F. Facile synthesis of pH-responsive polymersomes based on lipidized PEG for intracellular co-delivery of curcumin and methotrexate. *Colloid Surf. B Biointerfaces* **2018**, *167*, 568–576. [CrossRef] [PubMed]
12. Kang, W.L.; Zhao, Y.L.; Wang, P.X.; Li, Z.; Hou, X.Y.; Huang, Z.T.; Yang, H.B. Rheological behavior and mechanism of pH-responsive wormlike micelle variations induced by isomers of phthalic acid. *Soft Matter* **2018**, *14*, 4445–4452. [CrossRef] [PubMed]
13. Zahoranova, A.; Mrlik, M.; Tomanova, K.; Kronek, J.; Luxenhofer, R. ABA and BAB Triblock Copolymers Based on 2-Methyl-2-oxazoline and 2-*n*-Propyl-2-oxazoline: Synthesis and Thermoresponsive Behavior in Water. *Macromol. Chem. Phys.* **2017**, *218*, 1700031. [CrossRef]
14. Zhang, N.; Luxenhofer, R.; Jordan, R. Thermoresponsive Poly(2-Oxazoline) Molecular Brushes by Living Ionic Polymerization: Modulation of the Cloud Point by Random and Block Copolymer Pendant Chains. *Macromol. Chem. Phys.* **2012**, *213*, 1963–1969. [CrossRef]
15. Xiu, M.M.; Kang, Q.; Tao, M.L.; Chen, Y.; Wang, Y. Thermoresponsive AIE supramolecular complexes in dilute solution: Sensitively probing the phase transition from two different temperature-dependent emission responses. *J. Mater. Chem. C* **2018**, *6*, 5926–5936. [CrossRef]
16. Jerca, F.A.; Jerca, V.V.; Anghelache, A.M.; Vuluga, D.M.; Hoogenboo, R. Poly(2-isopropenyl-2-oxazoline) as a versatile platform towards thermoresponsive copolymers. *Polym. Chem.* **2018**, *9*, 3473–3478. [CrossRef]
17. Ilcikova, M.; Mosnacek, J.; Mrlik, M.; Sedlacek, T.; Csomorova, K.; Czanikova, K.; Krupa, I. Influence of surface modification of carbon nanotubes on interactions with polystyrene-*b*-polyisoprene-*b*-polystyrene matrix and its photo-actuation properties. *Polym. Adv. Technol.* **2014**, *25*, 1293–1300. [CrossRef]
18. Kobatake, S.; Takami, S.; Muto, H.; Ishikawa, T.; Irie, M. Rapid and reversible shape changes of molecular crystals on photoirradiation. *Nature* **2007**, *446*, 778–781. [CrossRef] [PubMed]
19. Zhang, T.; Sheng, L.; Liu, J.N.; Ju, L.; Li, J.H.; Du, Z.; Zhang, W.R.; Li, M.J.; Zhang, S.X.A. Photoinduced Proton Transfer between Photoacid and pH-Sensitive Dyes: Influence Factors and Application for Visible-Light-Responsive Rewritable Paper. *Adv. Funct. Mater.* **2018**, *28*, 1705532. [CrossRef]
20. Du, L.; Xu, Z.Y.; Fan, C.J.; Xiang, G.; Yang, K.K.; Wang, Y.Z. A Fascinating Metallo-Supramolecular Polymer Network with Thermal/Magnetic/Light-Responsive Shape-Memory Effects Anchored by Fe_3O_4 Nanoparticles. *Macromolecules* **2018**, *51*, 705–715. [CrossRef]
21. Li, Y.C.; Li, J.C.; Li, W.H.; Samali, B. Development and characterization of a magnetorheological elastomer based adaptive seismic isolator. *Smart Mater. Struct.* **2013**, *22*, 035005. [CrossRef]
22. Mannsfeld, S.C.B.; Tee, B.C.K.; Stoltenberg, R.M.; Chen, C.; Barman, S.; Muir, B.V.O.; Sokolov, A.N.; Reese, C.; Bao, Z.N. Highly sensitive flexible pressure sensors with microstructured rubber dielectric layers. *Nat. Mater.* **2010**, *9*, 859–864. [CrossRef] [PubMed]
23. Godman, N.P.; Kowalski, B.A.; Auguste, A.D.; Koerner, H.; White, T.J. Synthesis of Elastomeric Liquid Crystalline Polymer Networks via Chain Transfer. *ACS Macro Lett.* **2017**, *6*, 1290–1295. [CrossRef]
24. Anderson, I.A.; Gisby, T.A.; McKay, T.G.; O'Brien, B.M.; Calius, E.P. Multi-functional dielectric elastomer artificial muscles for soft and smart machines. *J. Appl. Phys.* **2012**, *112*, 041101. [CrossRef]
25. Li, Y.C.; Li, J.C.; Tian, T.F.; Li, W.H. A highly adjustable magnetorheological elastomer base isolator for applications of real-time adaptive control. *Smart Mater. Struct.* **2013**, *22*, 095020. [CrossRef]
26. Robinson, S.S.; O'Brien, K.W.; Zhaob, H.; Peele, B.N.; Larson, C.M.; Murray, B.C.M.; van Meerbeek, I.M.; Dunham, S.N.; Shepherd, R.F. Integrated soft sensors and elastomeric actuators for tactile machines with kinesthetic sense. *Extreme Mech. Lett.* **2015**, *5*, 47–53. [CrossRef]
27. Mrlik, M.; Ilcikova, M.; Plachy, T.; Pavlinek, V.; Spitalsky, Z.; Mosnacek, J. Graphene oxide reduction during surface-initiated atom transfer radical polymerization of glycidyl methacrylate: Controlling electro-responsive properties. *Chem. Eng. J.* **2016**, *283*, 717–720. [CrossRef]

28. Steurer, P.; Wissert, R.; Thomann, R.; Mulhaupt, R. Functionalized Graphenes and Thermoplastic Nanocomposites Based upon Expanded Graphite Oxide. *Macromol. Rapid Commun.* **2009**, *30*, 316–327. [CrossRef] [PubMed]
29. Marcano, D.C.; Kosynkin, D.V.; Berlin, J.M.; Sinitskii, A.; Sun, Z.Z.; Slesarev, A.; Alemany, L.B.; Lu, W.; Tour, J.M. Improved Synthesis of Graphene Oxide. *ACS Nano* **2010**, *4*, 4806–4814. [CrossRef] [PubMed]
30. Park, S.; An, J.; Potts, J.R.; Velamakanni, A.; Murali, S.; Ruoff, R.S. Hydrazine-reduction of graphite- and graphene oxide. *Carbon* **2011**, *49*, 3019–3023. [CrossRef]
31. Pei, S.F.; Zhao, J.P.; Du, J.H.; Ren, W.C.; Cheng, H.M. Direct reduction of graphene oxide films into highly conductive and flexible graphene films by hydrohalic acids. *Carbon* **2010**, *48*, 4466–4474. [CrossRef]
32. Ilcikova, M.; Mrlik, M.; Spitalsky, Z.; Micusik, M.; Csomorova, K.; Sasinkova, V.; Kleinova, A.; Mosnacek, J. A tertiary amine in two competitive processes: Reduction of graphene oxide vs. catalysis of atom transfer radical polymerization. *RSC Adv.* **2015**, *5*, 3370–3376. [CrossRef]
33. Peraza-Hernandez, E.A.; Hartl, D.J.; Malak, R.J.; Lagoudas, D.C. Origami-inspired active structures: A synthesis and review. *Smart Mater. Struct.* **2014**, *23*, 094001. [CrossRef]
34. Czanikova, K.; Krupa, I.; Ilcikova, M.; Kasak, P.; Chorvat, D.; Valentin, M.; Slouf, M.; Mosnacek, J.; Micusik, M.; Omastova, M. Photo-actuating materials based on elastomers and modified carbon nanotubes. *J. Nanophotonics* **2012**, *6*, 063522. [CrossRef]
35. Kuila, T.; Bose, S.; Mishra, A.K.; Khanra, P.; Kim, N.H.; Lee, J.H. Chemical functionalization of graphene and its applications. *Prog. Mater. Sci.* **2012**, *57*, 1061–1105. [CrossRef]
36. Osicka, J.; Ilcikova, M.; Mrlik, M.; Minarik, A.; Pavlinek, V.; Mosnacek, J. The Impact of Polymer Grafting from a Graphene Oxide Surface on Its Compatibility with a PDMS Matrix and the Light-Induced Actuation of the Composites. *Polymers* **2017**, *9*, 264. [CrossRef]
37. Ilcikova, M.; Mrlik, M.; Sedlacek, T.; Chorvat, D.; Krupa, I.; Slouf, M.; Koynov, K.; Mosnacek, J. Viscoelastic and photo-actuation studies of composites based on polystyrene-grafted carbon nanotubes and styrene-*b*-isoprene-*b*-styrene block copolymer. *Polymer* **2014**, *55*, 211–218. [CrossRef]
38. Ilcikova, M.; Mrlik, M.; Sedlacek, T.; Slouf, M.; Zhigunov, A.; Koynov, K.; Mosnacek, J. Synthesis of Photoactuating Acrylic Thermoplastic Elastomers Containing Diblock Copolymer-Grafted Carbon Nanotubes. *ACS Macro Lett.* **2014**, *3*, 999–1003. [CrossRef]
39. Zhang, W.L.; Liu, Y.D.; Choi, H.J.; Kim, S.G. Electrorheology of Graphene Oxide. *ACS Appl. Mater. Interfaces* **2012**, *4*, 2267–2272. [CrossRef] [PubMed]
40. Mrlik, M.; Moucka, R.; Ilcikova, M.; Bober, P.; Kazantseva, N.; Spitalsky, Z.; Trchova, M.; Stejskal, J. Charge transport and dielectric relaxation processes in aniline-based oligomers. *Synth. Met.* **2014**, *192*, 37–42. [CrossRef]
41. Mrlik, M.; Cvek, M.; Osicka, J.; Moucka, R.; Sedlacik, M.; Pavlinek, V. Surface-initiated atom transfer radical polymerization from graphene oxide: A way towards fine tuning of electric conductivity and electro-responsive capabilities. *Mater. Lett.* **2018**, *211*, 138–141. [CrossRef]
42. Cvek, M.; Mrlik, M.; Ilcikova, M.; Plachy, T.; Sedlacik, M.; Mosnacek, J.; Pavlinek, V. A facile controllable coating of carbonyl iron particles with poly(glycidyl methacrylate): A tool for adjusting MR response and stability properties. *J. Mater. Chem. C* **2015**, *3*, 4646–4656. [CrossRef]
43. Georgousis, G.; Pandis, C.; Kalamiotis, A.; Georgiopoulos, P.; Kyritsis, A.; Kontou, E.; Pissis, P.; Micusik, M.; Czanikova, K.; Kulicek, J.; et al. Strain sensing in polymer/carbon nanotube composites by electrical resistance measurement. *Compos. Part B Eng.* **2015**, *68*, 162–169. [CrossRef]
44. Rabindranath, R.; Bose, H. On the mobility of iron particles embedded in elastomeric silicone matrix. In Proceedings of the 13th International Conference on Electrorheological Fluids and Magnetorheological Suspensions, Ankara, Turkey, 2–6 July 2012; Unal, H.I., Ed.; Iop Publishing Ltd.: Bristol, UK, 2013.
45. Feng, Y.Y.; Qin, M.M.; Guo, H.Q.; Yoshino, K.; Feng, W. Infrared-Actuated Recovery of Polyurethane Filled by Reduced Graphene Oxide/Carbon Nanotube Hybrids with High Energy Density. *ACS Appl. Mater. Interfaces* **2013**, *5*, 10882–10888. [CrossRef] [PubMed]

Paper III

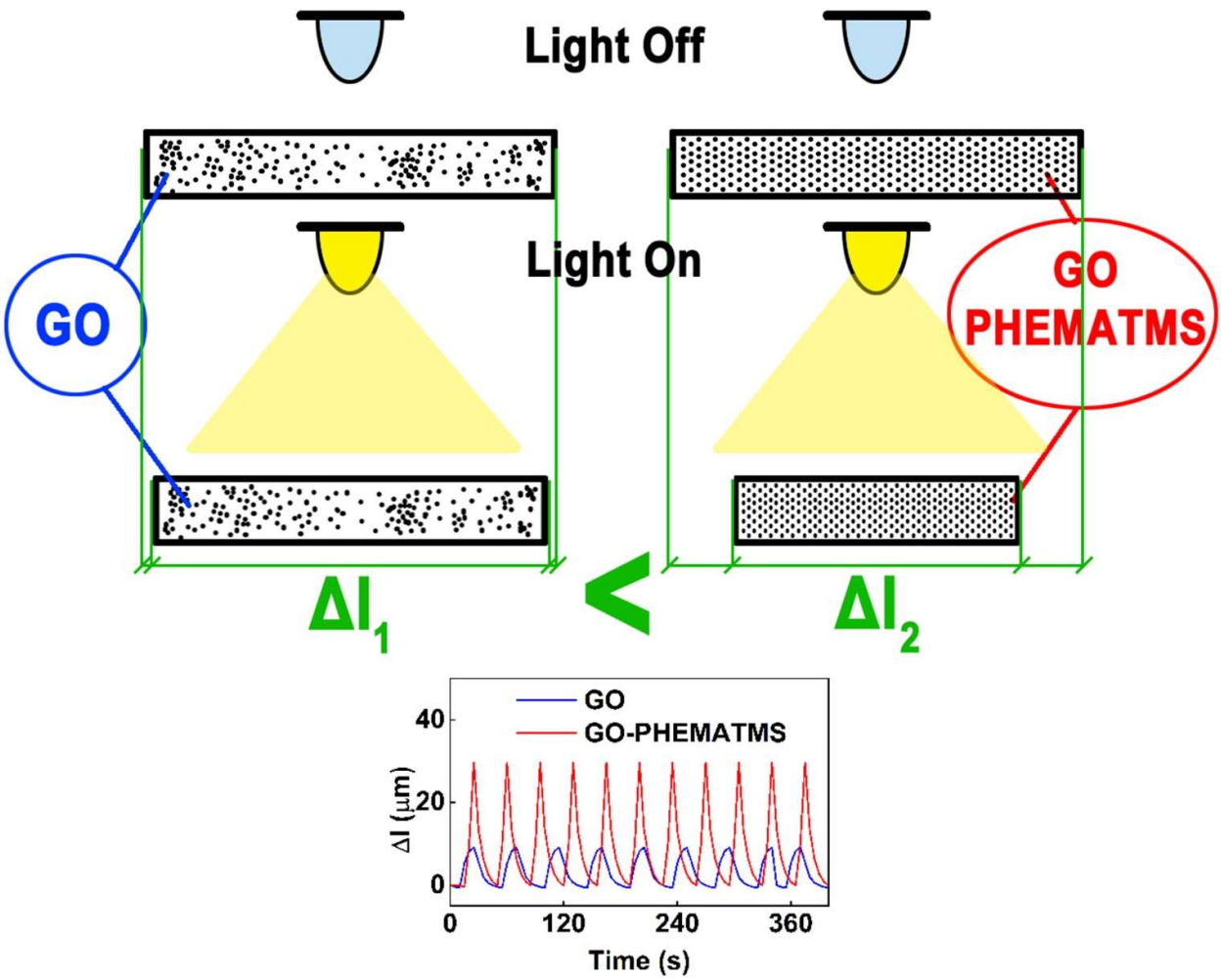
Light Off
Light On
GO
GO
PHEMATMS
ΔI1
<
ΔI2
GO
GO-PHEMATMS
ΔI (μm)
40
20
0
0
120
240
360
Time (s)

polymers

MDPI

Article

Light-Induced Actuation of Poly(dimethylsiloxane) Filled with Graphene Oxide Grafted with Poly(2-(trimethylsilyloxy)ethyl Methacrylate)

Josef Osicka [1], Miroslav Mrlik [1,*], Markéta Ilčíková [2], Lukas Munster [1], Pavel Bazant [1], Zdenko Špitalský [2] and Jaroslav Mosnáček [2,3,*]

1 Centre of Polymer Systems, University Institute, Tomas Bata University in Zlin, Trida T. Bati 5678, 760 01 Zlin, Czech Republic; osicka@utb.cz (J.O.); munster@utb.cz (L.M.); bazant@utb.cz (P.B.)
2 Polymer Institute, Slovak Academy of Sciences, Dubravska cesta 9, 845 41 Bratislava, Slovakia; marketa.ilcikova@savba.sk (M.I.); upolspiz@savba.sk (Z.Š.)
3 Centre for Advanced Materials Application, Slovak Academy of Sciences, Dubravska cesta 9, 845 45 Bratislava, Slovakia
* Correspondence: mrlik@utb.cz (M.M.); jaroslav.mosnacek@savba.sk (J.M.); Tel.: +420-576-038-027 (M.M.); +421-2-3229-4353 (J.M.)

Received: 28 August 2018; Accepted: 21 September 2018; Published: 24 September 2018

Abstract: This study serves to combine two approaches into one single step, to achieve a significant improvement of the light-induced actuation capabilities. Graphene oxide (GO) is an inert material, from the electrical and thermal conductivity point of view, and is incompatible with the usually-used poly(dimethylsiloxane) (PDMS) matrix. During surface-modification by surface-initiated atom transfer radical polymerization, the GO was transformed into a conducting and compatible material with the PDMS showing enormous light-induced actuation capability. The GO surface-modification with poly(2-(trimethylsilyloxy)ethyl methacrylate) (PHEMATMS) chains was confirmed by transmission electron microscopy and thermogravimetric analysis, with an on-line monitoring of gasses using FTIR. The improved compatibility was elucidated using contact angle and dielectric properties measurements. The PHEMATMS shell was investigated using gel permeation chromatography and nuclear magnetic resonance. The improved electric conductivity was measured using the four-point probe method and by Raman spectroscopy. The very important mechanical properties were elucidated using dynamic mechanical analysis, and with the help of thermo-mechanic analysis for the light-induced actuation. The excellent actuation capabilities observed, with changes in the length of around 0.8% at 10% pre-strain, are very promising from the point of view of applications.

Keywords: light-induced actuation; SI-ATRP; graphene oxide; reduction; dielectrics; dynamic mechanical analysis

1. Introduction

Materials capable of changing its dimensions, upon encountering certain external stimulus, reversibly belongs to the group of smart materials [1,2]. Such deformation can be controlled using various stimuli such as electric [3,4] or magnetic field [5,6], humidity [7,8], temperature [9,10], and light [11–13]. From these stimuli, only the humidity, temperature and light-induced deformation provide a non-contact deformation, thus, creating various very-specific applications [14,15].

Materials that show a light-induced capability usually consist of two phases, the filler, and the polymer matrix. The former includes mainly organic [16,17] and carbon-based fillers [18–20], while the latter can be formed by various systems. The most frequent matrix is poly(dimethylsiloxane)

elastomer (PDMS) [20], but in some cases, the thermoplastic elastomers [13], polyurethanes [21], or rubber compounds [22] have been successfully applied.

In order to obtain materials with sufficient performance, the stiffness of the matrix is a crucial parameter [20]. There are various methods of providing a material with lower stiffness and improved elongation, such as addition of the low molecular weight liquids [18] into the matrices, optimizing the amount of cross-linking agent, in the case of chemically cross-linked systems [6], or designing the chemical composition of the thermoplastic elastomers by the means of a length of hard and soft segments [13].

In the case of filler, the crucial parameter is the absorption of light with a wavelength of the utilized light source [23], a good compatibility with the matrix ensuring maximal heat transfer to the matrix and proper dispersion, in the matrix, providing an enhanced thermal conductivity, and homogeneous distribution of the heat within the matrix [24].

Several techniques have been proposed to fulfill the mentioned recommendations. These include a physical modification of the filler surface by using surfactants, [25], covalent modification of the filler with low molecular weight compounds or polymeric chains compatible with polymer matrix [26], and in situ grafting of the filler, during the synthesis of the polymer matrix [13].

In our preceding study, we have shown the influence of the structure of the polymer chains—such as, poly(methyl methacrylate) (PMMA), poly(*n*-butyl methacrylate) (PBMA), and poly(glycidyl methacrylate) (PGMA) which are grafted onto the surface of the graphene oxide (GO) particles—on the final actuation capability of the PDMS-based photo-actuators [18,27]. Additionally, the effect of the filler concentration [18] and the polymer chain length [27] has already been investigated.

In this study, in order to further improve the compatibility with the polymer matrix, the poly(2-(trimethylsilyloxy)ethyl methacrylate) (PHEMATMS) was grafted from the surface of GO particles and mixed with PDMS and a certain amount of silicon oil, to improve the flexibility of the matrix. Successful modification of GO surface was confirmed using transmission electron microscopy and thermogravimetric analysis, with on-line monitoring of gasses, using FTIR. The compatibility was elucidated using contact angle investigations and dielectric properties. Mechanical performance and light-induced actuation were investigated by the means of dynamic mechanical analysis and modified thermo-mechanical analysis, respectively. The application of the surface-initiated atom transfer radical polymerization (SI-ATRP) technique for grafting of the PHEMATMS onto the GO surface, can provide partially reduced and polymer-modified GO with an improved compatibility for the PDMS matrix, leading toward an excellent light-induced actuation, especially for filler concentrations as low as 1 vol.%. According to our knowledge, utilizing silane-based grafts on the surface of GO and mix them into the PDMS elastomer, for an improvement of the light-induced deformations, has not been published.

2. Materials and Methods

2.1. Materials

Graphite (powder, <20 μm, synthetic) as a precursor of GO; sulfuric acid (H_2SO_4, reagent grade, 95–98%), sodium nitrate ($NaNO_3$, ACS reagent, ≥99%), potassium permanganate ($KMnO_4$, 97%) and hydrogen peroxide (H_2O_2, ACS reagent, 29–32 wt % H_2O_2 basis) were used as chemical agents for the GO sheets formation. GO particles were fabricated by the modified Hummers method from graphite powder, as was described previously [28]. α-Bromoisobutyryl bromide (BiBB, 98%) was as an initiator, linked onto the GO surface and the triethyleneamine (TEA, ≥99%), as a proton trap. The GO sheets were modified with atom transfer radical polymerization (ATRP) initiator as described previously [29]. 2-(trimethylsilyloxy)ethyl methacrylate (HEMATMS, 99%), ethyl α-bromoisobutyrate (EBiB, 98%), *N*,*N*,*N*′,*N*″,*N*″-pentamethyldiethylenetriamine (PMDETA, ≥99%), copper bromide (CuBr, ≥99%), and anisole (99%) were used as a monomer, sacrificial initiator, ligand, catalyst, and solvent, respectively, for the ATRP. Diethyl ether (ACS reagent, anhydrous, ≥99%) was used to dry the semi and the final

product. All chemicals were purchased from Sigma Aldrich (St. Louis, MO, USA). For the polymer matrix, polydimethyl siloxane Silgard 184 (PDMS) from Dow Corning (Midland, MI, USA), and dried silicone oil M200 from Lukosiol (Kolin, Czech Republic) were used. Tetrahydrofuran (THF, p.a.) dried by flakes of sodium (99.9%), dimethyl formamide (DMF, p.a.), acetone (p.a.), ethanol (absolute anhydrous, p.a.), toluene (p.a.), and hydrochloric acid (HCl, 35%, p.a.) were obtained from Penta Labs (Prague, Czech Republic). Deionized water (DW) was used in all the experiments.

2.2. Surface Initiated Atom Transfer Radical Polymerization

The initiator–modified GO sheets (1 g) were put into a Schlenk flask and evacuated and backfilled with argon, three times. HEMATMS (146.6 mmol, 32 mL), EBiB (1.466 mmol, 0.215 mL), PMDETA (5.864 mmol, 1.22 mL), and anisole (32 mL) were pre-purged with argon, at least for 10 min each, and added into the flask, under an argon flow. The system was degassed by three freeze–pump–thaw cycles and finally filled with argon. The catalyst CuBr (1.466 mmol, 0.2103 g) was added to the frozen system under a gentle argon flow. The molar ratio of the reactants [HEMATMS]:[EBiB]:[CuBr]:[PMDETA] was [100]:[1]:[1]:[4]. Anisole was used as a solvent in an amount of 50 vol %. The flask with the polymerization mixture was immersed in a 60 °C preheated, silicone oil bath, to initiate the polymerization process, and stirred at this temperature for two hours. Finally, the polymerization was stopped by exposing the mixture to air. The product, GO–PHEMATMS, was filtered, cleaned by the DMF (2 × 200 mL) and acetone (2 × 200 mL), then dried by diethyl ether (2 × 100 mL).

2.3. Elastometric Matrix Preparation

The polymer matrix was prepared by mixing the PDMS, silicone oil (SO), and curing agent in a volume ratio of 8:2:1. The matrix was filled by GO–PHEMATMS, in concentrations of 0.1 vol %, 0.5 vol %, and 1 vol %, and properly homogenized using a combination of ultra-sonication (UPS-400, Ultra Autosonic, Maharahstra, India) and mechanical stirring with a glass stick. This mixture was poured into a teflon-lined mold and evacuated in order to eliminate the presence of air bubbles. Then the mold was placed in an oven for two hours, at 60 °C, to fully cross-link the PDMS-based samples.

2.4. Analyses

The modification of the GO with an initiator and the PHEMATMS chains was proved by FTIR (ATR) Nicolet 6700 (Thermo Scientific, Madison, WI, USA), transmission electron microscopy JEOL JEM 2100 (JEOL, Tokyo, Japan), and Raman spectroscopy Nicolet DXR (Thermo Scientific, USA). The molar mass and dispersity ($Đ$) of PHEMATMS chains were investigated using a gel permeation chromatography (GPC) on the GPC instrument (PL-GPC220, Agilent, Hachioji, Japan), equipped with GPC columns (Waters 515 pump, two PPS SDV 5 μm columns (diameter of 8 mm, length of 300 mm, 500 Å + 105 Å)), and a Waters 410 differential refractive index detector tempered to 30 °C. THF dried over KOH was used as a solvent with a polystyrene calibration. The ^{1}H NMR was used to determine the monomer conversion from the ratio of an area of the peak at 3.88 ppm, assigned to the PHEMATMS to the sum of an area of the peaks at 3.88 and 4.08 ppm, where the second one was assigned to the HEMATMS (Figure 1). Contact angle measurement (CA) was evaluated from the static sessile drop method carried out on a Surface Energy Evaluation system, equipped with a CCD camera (Advex Instruments, Brno, Czech Republic). The dielectric properties were measured by Broadband Dielectric Impedance Analyzer (Novocontrol, Montabaur, Germany), in the frequency range of 0.01 Hz to 10 MHz, and temperature range of −150 to 100 °C, using a standard sample cell BDCS 140. The viscoelastic properties of both the nanocomposites and pure polymer matrix were studied by a dynamic mechanical analysis (DMA), in a shear mode.

The glass transition process was evaluated through activation energies calculated from an Arrhenius equation (Equation (1)), in order to see the effect of the modification on the relaxation processes, in the PDMS-based composites:

$$f_\beta = f_\infty \exp\left(\frac{E_a}{k_B T}\right), \tag{1}$$

where E_a is the activation energy, f_∞ is the pre-exponential factor, T is the thermodynamic temperature, and k_B is Boltzmann constant.

In order to properly investigate the polymer chains dynamics, the loss permittivity needed to be recalculated to the loss modulus. This recalculation was performed according to Equation (2),

$$\begin{aligned} M^* &= \frac{1}{\varepsilon^*} \\ M' &= \frac{\varepsilon'}{\varepsilon'^2+\varepsilon''^2} \\ M'' &= \frac{\varepsilon''}{\varepsilon'^2+\varepsilon''^2} \end{aligned} \tag{2}$$

where ε^* is the complex permittivity, ε' and ε'' are relative permittivity and loss permittivity, respectively. M^*, M', and M'' are complex, storage, and loss dielectric moduli, respectively.

The light-induced actuation ability of both the matrix and nanocomposite was investigated using a thermal mechanical analysis (TMA, Mettler Toledo, Langacher, Switzerland), using a process similar to that in Reference [19]. Samples in the form of stripes with dimensions of 15 mm in length, 2.5 mm in width, and 0.26 mm in thickness were irradiated using a red LED diode (Luxeon Rebel, Philips, Amsterdam, The Netherlands). Irradiation was applied for 10 s, at 627 nm, with 6, 9, and 12 mW light source intensity, under 10% pre-strain of the samples. Maximum value of the actuation was characterized by a change in the sample length, during an exposure to light, $\Delta L = (L_0 - L)/L_0$, where L_0 is the length of a non-irradiated sample mounted between the clamps (10 mm), and L is the length of the irradiated sample. Actuation describes a material's ability to undergo reversible shape changes in response to an external light stimulus.

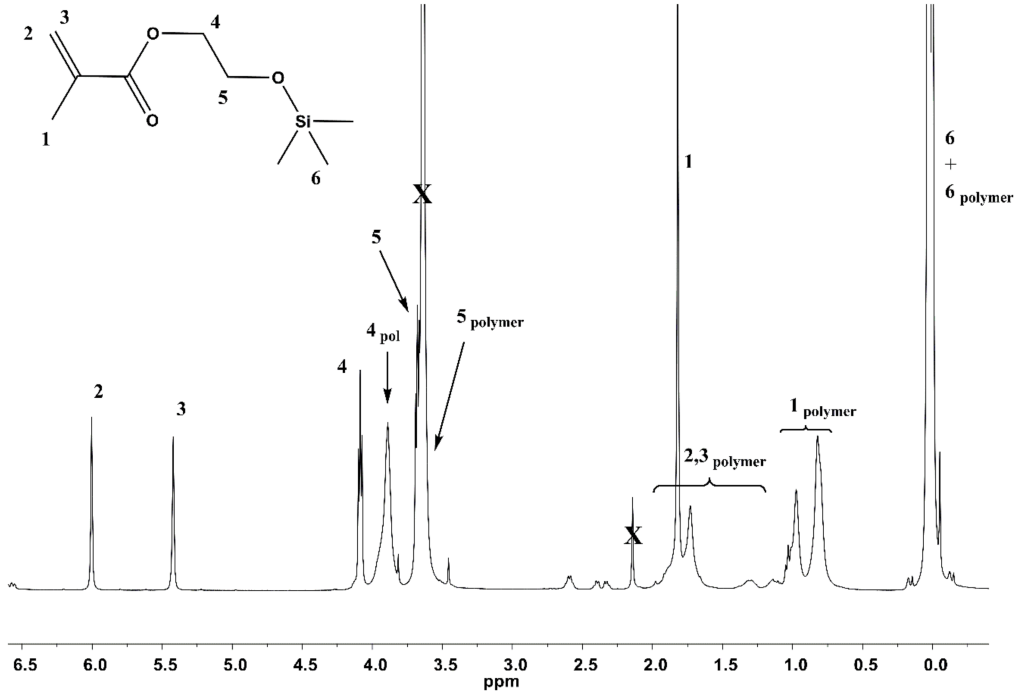

Figure 1. Representative ^{1}H NMR spectrum from filtered polymerization mixture of poly(2-(trimethylsilyloxy)ethyl methacrylate) (PHEMATMS).

3. Results

The presence of an excess of sacrificial initiator, as compared to initiator bonded onto the GO surface, allowed us to follow the polymerization and to determine the molecular characteristics of the polymer, using GPC, and the monomer conversion, using the NMR spectroscopy (Figure 1). Based on the assumption of the simultaneous growing the polymer chains, in bulk, and from the surface [30], it was found that molar mass and dispersity of the PHEMATMS chains grafted onto the GO surface were 12,600 g·mol^{-1} and 1.19, respectively. The monomer conversion after 2 h of polymerization was 67%. A good correlation of the molar mass with the theoretical one (13,750 g·mol^{-1}), calculated from the monomer:sacrificial initiator ratio, and the monomer conversion, as well as the narrow dispersity, confirmed a good control of the ATRP process. The polymerization procedure for comparing the effect of the various grafts on the overall physical properties of the PDMS/hybrid-based composites, was similar to that used in our previous studies [18,27], with regards to the targeting of the PHEMATMS molar mass. It was also found in our preceding study [6], that compatibility with the surrounding matrix was not significantly changed when the molar mass of the grafted polymer chains was over 12,000 g·mol^{-1}.

The successful growth of the polymer chains from the GO surface was confirmed using TEM and TGA, with an online-connected FTIR. As can be seen in Figure 2, the GO was synthesized with considerable exfoliation and only a few layers of GO sheets could be visible in Figure 2a. After the polymerization, the GO particles were analyzed, and certain polymer layers could be observed (Figure 2b) as a floss-like layer with a darker tone than that of a neat GO, and confirmed the presence of polymer chains.

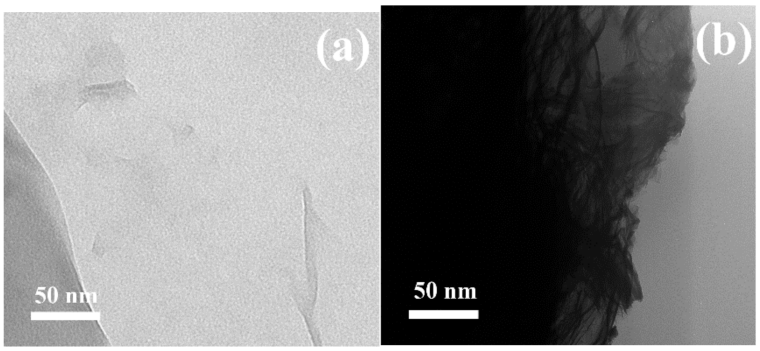

Figure 2. TEM images of (**a**) neat Graphene oxide (GO), (**b**) Graphene oxide grafted with poly(2-(trimethylsilyloxy)ethyl methacrylate) (GO–PHEMATMS).

In order to further confirm the presence of the covalently bonded PHEMATMS shell on the GO surface, the TGA spectra with the FTIR online monitoring of the volatile products produced during the TGA of the GO (Figure 3a,b), initiator-modified GO (Figure 3c,d), and GO–PHEMATMS (Figure 3e,f) particles were analyzed. Properly described decomposition of the neat GO and GO-I has already been published elsewhere [18,27]. In addition to the peak corresponding to the oxygen-containing groups (which was the case for the GO–PHEMATMS shifted to lower temperatures (peak below 200 °C), as compared to the GO and initiator-modified GO), the TGA of the GO–PHEMATMS was characteristic with two more peaks at 270 °C and 330 °C. These peaks corresponded to the volatile products of the thermal degradation of the PHEMATMS chains from the GO surface. The gas phase produced at these critical temperatures range was analyzed using an FTIR (Figure 3f). The FTIR spectra analysis showed the absorption bands typical for methacrylates, as have already been described during the use of this technique [18,27]. Additional peaks at 1207 and 1067 cm^{-1}, corresponding to the Si–C and Si–O stretching vibrations, respectively, were also observed and were connected to the trimethylsilyloxyethyl moieties. These results clearly showed the presence of covalently-bonded PHEMATMS on the surface of the GO particles.

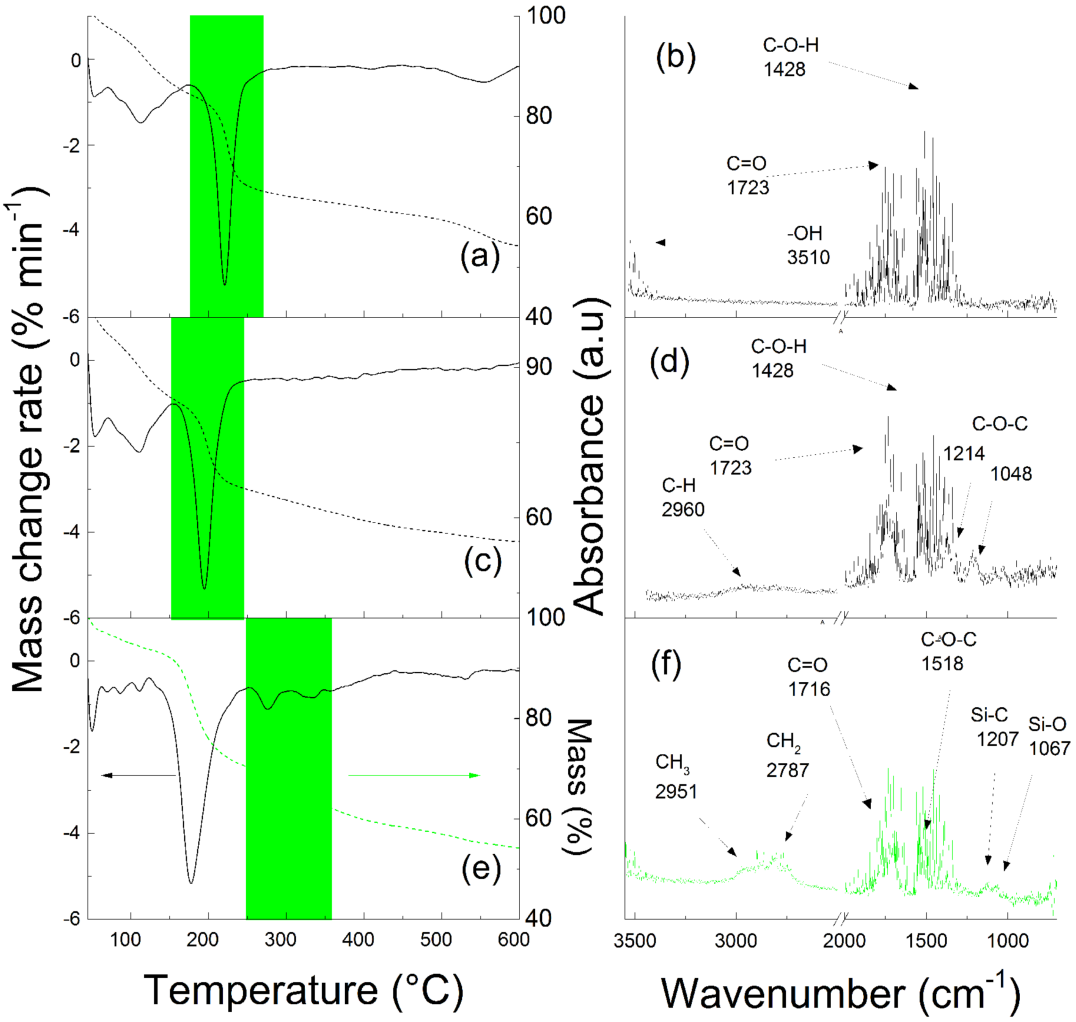

Figure 3. TGA analysis (**a**,**c**,**e**) with on-line monitoring of volatile degradation products from the green marked temperature range by the FTIR spectra (**b**,**d**,**f**) for a neat GO (**a**,**b**), GO-initiator and (**c**,**d**) and GO–PHEMATMS (**e**,**f**) particles.

In addition to surface modification of the GO, the SI-ATRP approach also provided a simultaneous reduction of the GO surface, as was invented and properly described by Ilcikova et.al. [31]. The degree of reduction could be tailored by the reaction time and the ligand concentration. In this case, the reaction was carried out for two hours and therefore a just negligible GO reduction was obtained. Such a reduction was confirmed by the conductivity measurements, as well as by the change in the I_D/I_G peaks ratio in the Raman spectra. The peak ratios were 0.9 and 1.09 for the neat GO (Figure 4a) and the GO–PHEMATMS (Figure 4b), respectively, with conductivities of 1.2×10^{-8} and 6×10^{-7} S·cm^{-1}, respectively.

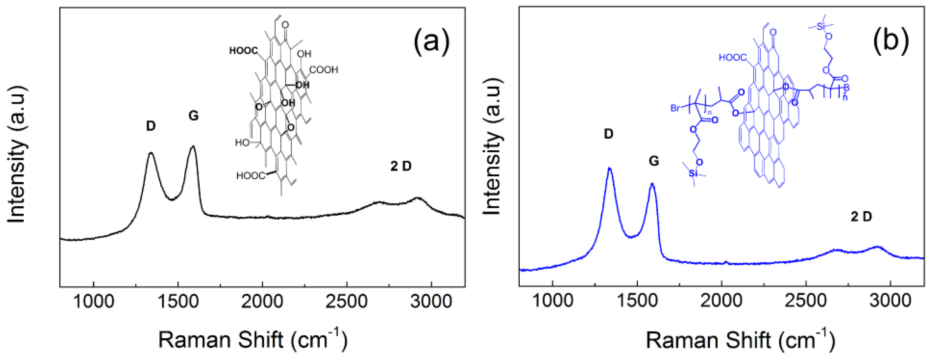

Figure 4. Raman spectra of the neat GO (**a**) and GO-PHEMATMS (**b**) particles and corresponding chemical structures.

Compatibility between the filler and the polymer matrix was a crucial parameter to obtain an excellent photo-actuation capability. Therefore, the contact angle investigations were performed between the GO or the GO–PHEMATMS pellet and a drop of the PDMS elastomer. As can be seen in Figure 5a, the neat GO surface showed a contact angle of 49.9° ± 3.2°, indicating only partial wettability and thus only a slight compatibility with the PDMS. On the contrary, the GO–PHEMATMS showed improvement, and in fact, excellent wettability with the PDMS, as proved by the contact angle value of 26.3° ± 3.0°. The wettability observed for the GO–PHEMATMS was also the lowest, in comparison with GO grafted with other types of polymers, where contact angle values of 40.1° ± 1.3° were described for the GO modified with PGMA [27], 38.7° ± 2.7° for PMMA, and 28.7° ± 2.7° for PBMA chains. Such significantly improved compatibility serves a very promising dispersibility of the filler, due to the compatible grafts of the PHEMATMS with the PDMS and can also predict the excellent light-induced material deformation.

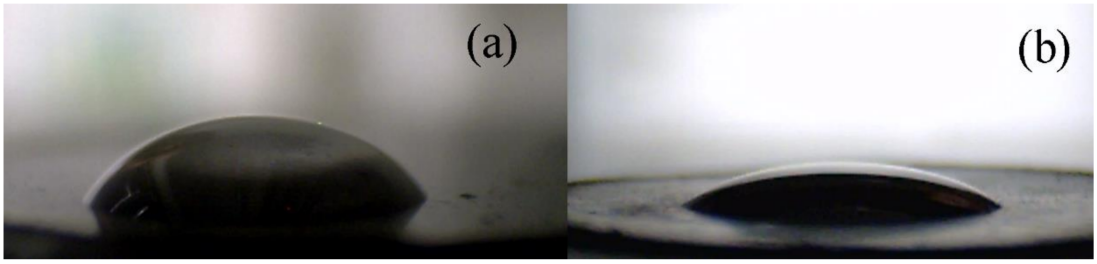

Figure 5. Images from a CCD camera of the 5 µL poly(dimethylsiloxane) (PDMS) droplets on the neat GO (**a**) and the GO-PHEMATMS (**b**).

Dielectric properties are very often used as tools for investigation of polymer chain dynamics. In this case, the polymer chain flexibility was a crucial factor influencing the light-induced deformation. Therefore, the dielectric loss modulus was plotted against the temperature and the frequency, as a 3D plot, to see the differences in the dielectric behavior (Figure 6).

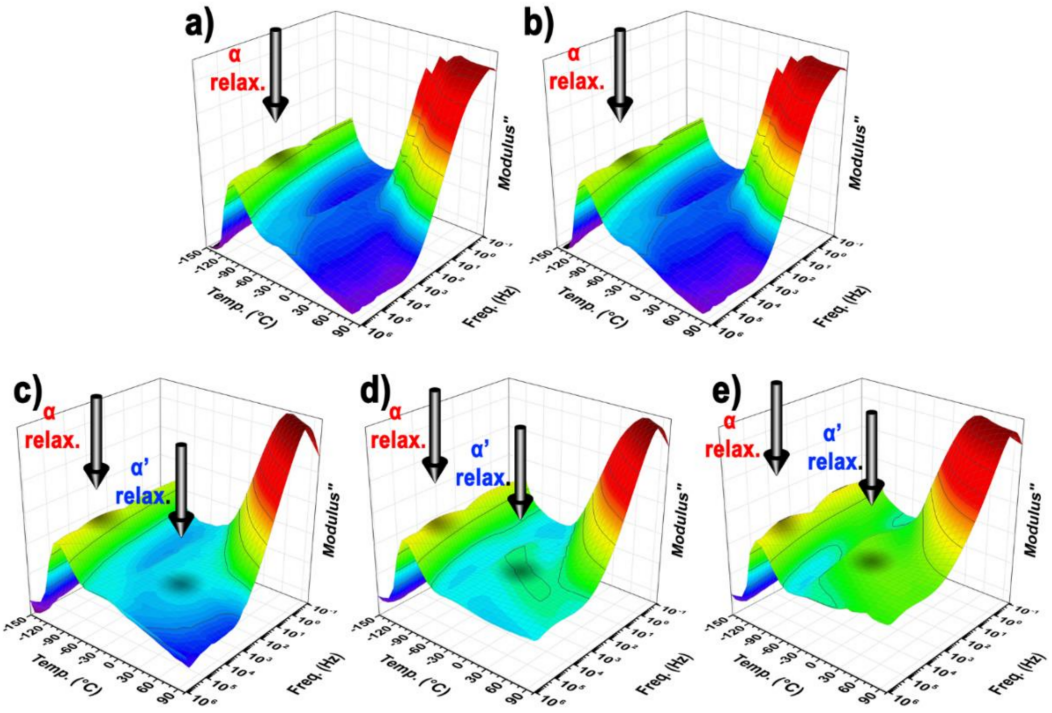

Figure 6. 3D plots of the dielectric properties of the neat PDMS matrix (**a**), and PDMS matrix filled with GO (**b**), 0.1 vol % GO–PHEMATMS (**c**), 0.5 vol % GO–PHEMATMS (**d**) and 1 vol % GO–PHEMATMS (**e**).

The flexibility of the polymer matrix was given by two factors, the mobility of the main chain characterized by an α relaxation, corresponding to T_g, and the side chains mobility characterized by α′ relaxation, indicating how the entanglements of the side chains got stiff. Therefore, both relaxations were investigated using the Arhenius equation (Equation (1)). The activation energy of α relaxation (Table 1) was significantly shifted to lower values, from 45.57 kJ·mol^{-1} to 22.01 kJ·mol^{-1}, after the PHEMATMS grafting, indicating an improved flexibility of the polymer matrix. However, for the side chains flexibility, α′ relaxation, was much more influenced and was clearly visible only for the composites containing the GO–PHEMATMS (Figure 6). Such flexibility was also confirmed by an activation energy decrease from 19.96 kJ·mol^{-1} and 19.09 kJ·mol^{-1} for the neat matrix and composite-containing GO, respectively, to values below 11 kJ mol^{-1}, determined for the composites containing the various GO–PHEMATMS loadings (Table 1).

Table 1. Activation energies of glass transition process for pure PDMS and various PDMS composites. Filler content is in vol %.

Sample Name	Ea α′ (kJ·mol^{-1})	Ea α (kJ·mol^{-1})
PDMS	19.96	45.70
PDMS/GO 0.1%	19.04	36.57
PDMS/GO-PHEMATMS 0.1%	10.7	22.01
PDMS/GO-PHEMATMS 0.5%	9.23	21.3
PDMS/GO-PHEMATMS 1%	9.09	20.1

The light-induced deformation of the materials was a reversible process and could also be classified as a cyclic deformation process. Therefore, a dynamic mechanical analysis of the neat matrix and various composites was performed. From the mechanical point of view, the GO–PHEMATMS composites showed the lowest values of elastic modulus, due to the significantly increased flexibility of the main, as well as the side polymer chains (Figure 7a). This could also be clearly seen from Figure 7b, where the peak of the T_g had shifted 15 °C toward lower temperatures, than those of the neat polymer

matrix and the nanocomposite-containing unmodified GO. Additionally, the crystalline phase was found to have shifted significantly, with a melting point at a lower temperature. On the other hand, the composite containing GO–PHEMATMS exhibited excellent damping performance with tan delta values of around 0.2, which was classified as a good material for damping applications [6].

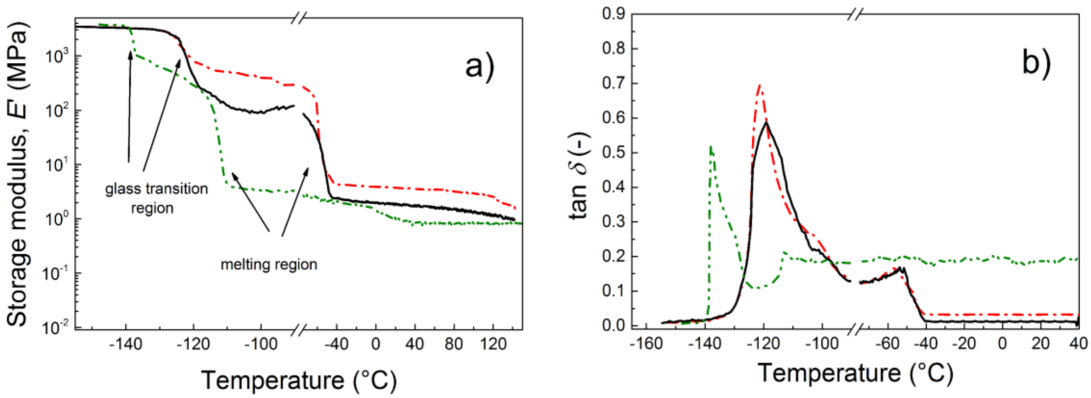

Figure 7. Dependence of the storage modulus (**a**) and tan δ (**b**) for a broad temperature range for a neat PDMS (black solid line), and for PDMS composites containing 0.1 vol % of either the neat GO (red dash–dot line) or the GO–PHEMATMS (green dash–dot–dot line).

The above-mentioned investigations indicated the significantly enhanced flexibility of the polymer composite due to the grafting of the GO surface with the PHEMATMS chains, and thus, the excellent compatibility with the PDMS. The light-induced deformation studies clearly confirmed these results. As can be seen in Figure 8, the neat PDMS matrix, as well as the composite containing the unmodified GO, showed very poor actuation ability. On the other hand, the composite containing the same vol % of the GO–PHEMATMS exhibited a four times higher actuation-ability, reaching a ΔL of 34 μm. For comparison, this value was significantly higher than that recently determined for the composites containing the same vol % of GO–PMMA, GO–PBMA, and GO–PGMA, with ΔL values of 9.4, 11.8, and 20.2 μm, respectively [18,27]. In addition, if the concentration of the GO–PHEMATMS filler increased, the ability of the actuation was also significantly improved (Figure 9), reaching values of 55 μm and 75 μm, for 0.5 vol % and 1 vol % of GO-PHEMATMS, respectively. That is, more than six times higher actuation values than those obtained for the composites containing unmodified GO. This superior result was mainly caused by the enormously improved compatibility of the GO–PHEMATMS with the matrix, the proper filler dispersion within the matrix, and the improved flexibility of the matrix in the presence of GO–PHEMATMS.

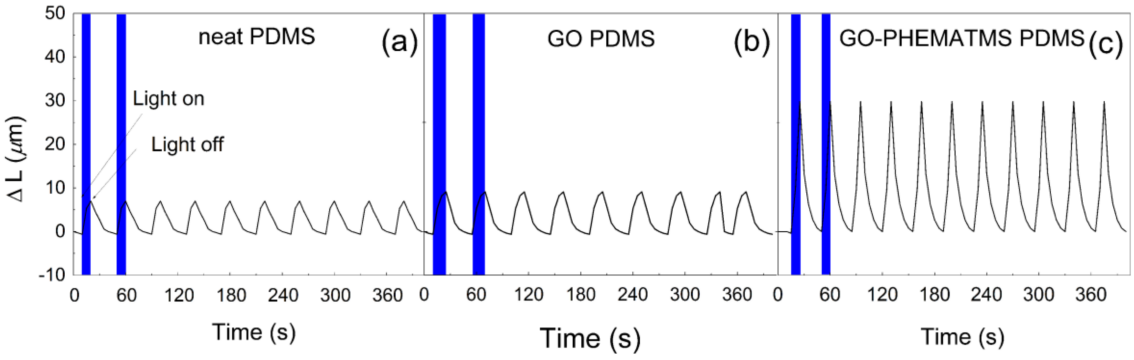

Figure 8. Light-induced deformation capability of pure PDMS (**a**), PDMS composites containing 0.1 vol % of GO (**b**), and GO–PHEMATMS (**c**) under the application of irradiation, with an intensity of 6 mW.

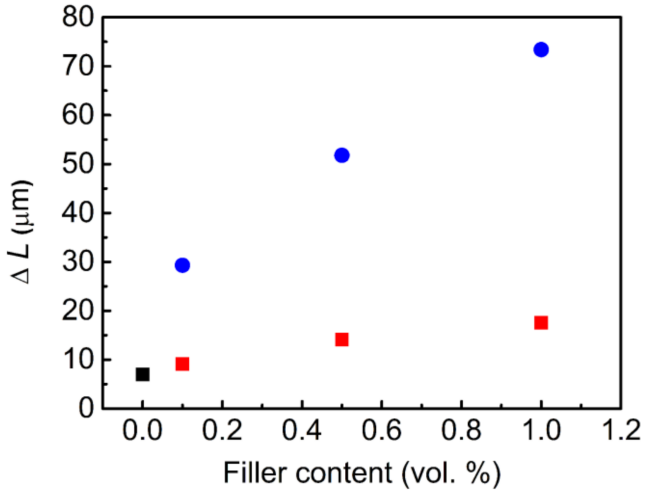

Figure 9. Dependence of the filler content on the change in length, for pure PDMS matrix (black squares), PDMS composites containing unmodified GO (red squares), and GO-PHEMATMS (blue circles). Error bars are within the size of the symbols.

In these studies, the PDMS was partially softened using an additional amount of SO. However, in order to increase the elasticity and softening of the PDMS matrix, the decreased ratio between the matrix and the curing agent could also be used, as already mentioned in the introduction. Furthermore, the actuation capability was strongly dependent on the matrix stiffness, therefore, the utilization of the hydrogel matrix could also be very effective [32], and will be planned for our future studies, in order to further improve the light-induced actuation of the polymeric materials.

4. Conclusions

Surface initiated atom transfer radical polymerization was used for the surface modification of GO nanoparticles with poly(2-(trimethylsilyloxy)ethyl methacrylate) (PHEMATMS) chains, with a molar mass of approximately 12,500 g·mol^{-1}. The surface modification was confirmed by TEM and TGA-FTIR. Partial reduction of the GO surface during the polymerization process led to the slight increase of the conductivity from I_D/I_G 1.2 × 10^{-8} to 6 × 10^{-7} S·cm^{-1}, and change of the I_D/I_G peaks ratio in Raman spectra, from 0.9 for the neat GO to 1.09 for the GO–PHEMATMS. Modification of the GO surface provided a significant improvement in the wettability of the GO surface by the PDMS matrix, as was proved by the contact angle value, which was as low as 26°. This improved compatibility, also dramatically affected the mobility of both the main chains and the side chains. This could be observed by the dielectric measurements which showed a substantial decrease in the activation energies of both α and α' relaxation processes, which dropped by half, as compared to a pure matrix or composites containing unmodified GO. This could be explained by the effective plasticizing effect of the PHEMATMS chains on the PDMS matrix, thanks to their high wettability. Thus, mechanical properties of the composite containing GO–PHEMATMS were also markedly affected by the increased mobility of the PDMS chains, leading to the decrease of both T_g and the melting point, by approximately 15 °C and 50 °C, respectively. On the contrary, the damping factor substantially increased after the modification of the GO surface by the PHEMATMS chains. All these results also positively affected the targeted property of the investigated composites, i.e., their actuation performance. The change in the length of the sample, during the light-induced actuation, was found to be four times higher for the composites containing 0.1 vol %, of the GO–PHEMATMS, as compared to the pure PMDS or composites containing the same content of the unmodified GO. Moreover, the actuation ability of the composites containing the GO–PHEMATMS was also significantly enhanced, as compared to all previously published composites, containing GO modified with various polymer chains. Such superior actuation performance is very promising for the application of these materials in

various smart systems, sensors, and can be generally utilized in many processes where the non-contact stimulation is a benefit.

Author Contributions: Conceptualization, M.M. and J.M.; Methodology, M.I.; Formal Analysis, J.O., M.M., M.I., L.M., P.B. and Z.Š.; Investigation, J.O., M.M., M.I. and Z.Š.; Writing-Original Draft Preparation, J.O., M.M., M.I. and J.M.

Funding: This research was funded by the Czech Science Foundation (No. 16-20361Y). This work was also supported by the Ministry of Education, Youth and Sports of the Czech Republic—program NPU I (LO1504). M.I. and J.M. gratefully acknowledge to APVV-15-0545 and APVV-14-0891 for financial support.

Conflicts of Interest: The authors declare no conflict of interest.

References

1. Yetisen, A.K.; Martinez-Hurtado, J.L.; Uenal, B.; Khademhosseini, A.; Butt, H. Wearables in medicine. *Adv. Mater.* **2018**, *30*, 1706910. [CrossRef] [PubMed]
2. Bisoyi, H.K.; Urbas, A.M.; Li, Q. Soft materials driven by photothermal effect and their applications. *Adv. Opt. Mater.* **2018**, *6*, 21. [CrossRef]
3. He, K.; Wen, Q.K.; Wang, C.W.; Wang, B.X.; Yu, S.S.; Hao, C.C.; Chen, K.Z. A facile synthesis of hierarchical flower-like TiO_2 wrapped with MoS_2 sheets nanostructure for enhanced electrorheological activity. *Chem. Eng. J.* **2018**, *349*, 416–427. [CrossRef]
4. Stejskal, J.; Bober, P.; Trchova, M.; Horsky, J.; Walterova, Z.; Filippov, S.K.; Plachy, T.; Mrlik, M. Oxidation of pyrrole with p-benzoquinone to semiconducting products and their application in electrorheology. *New J. Chem.* **2018**, *42*, 10167–10176. [CrossRef]
5. Hu, T.; Xuan, S.H.; Ding, L.; Gong, X.L. Stretchable and magneto-sensitive strain sensor based on silver nanowire-polyurethane sponge enhanced magnetorheological elastomer. *Mater. Des.* **2018**, *156*, 528–537. [CrossRef]
6. Cvek, M.; Mrlik, M.; Ilcikova, M.; Mosnacek, J.; Munster, L.; Pavlinek, V. Synthesis of silicone elastomers containing silyl-based polymer grafted carbonyl iron particles: An efficient way to improve magnetorheological, damping, and sensing performances. *Macromolecules* **2017**, *50*, 2189–2200. [CrossRef]
7. Zhang, W.Z.; Wang, L.F.; Sun, K.; Luo, T.; Yu, Z.Z.; Pan, K. Graphene-based janus film with improved sensitive response capacity for smart actuators. *Sens. Actuators B Chem.* **2018**, *268*, 421–429. [CrossRef]
8. Wang, T.P.; Li, M.T.; Zhang, H.; Sun, Y.Y.; Dong, B. A multi- responsive bidirectional bending actuator based on polypyrrole and agar nanocomposites. *J. Mater. Chem. C* **2018**, *6*, 6416–6422. [CrossRef]
9. Zahoranova, A.; Mrlik, M.; Tomanova, K.; Kronek, J.; Luxenhofer, R. Aba and bab triblock copolymers based on 2-methyl-2-oxazoline and 2-n-propyl-2-oxazoline: Synthesis and thermoresponsive behavior in water. *Macromol. Chem. Phys.* **2017**, *218*, 12. [CrossRef]
10. Shah, A.; Malik, M.S.; Khan, G.S.; Nosheen, E.; Iftikhar, F.J.; Khan, F.A.; Shukla, S.S.; Akhter, M.S.; Kraatz, H.B.; Aminabhavi, T.M. Stimuli-responsive peptide-based biomaterials as drug delivery systems. *Chem. Eng. J.* **2018**, *353*, 559–583. [CrossRef]
11. Li, M.; Wang, Y.; Chen, A.P.; Naidu, A.; Napier, B.S.; Li, W.Y.; Rodriguez, C.L.; Crooker, S.A.; Omenetto, F.G. Flexible magnetic composites for light-controlled actuation and interfaces. *Proc. Natl. Acad. Sci. USA* **2018**, *115*, 8119–8124. [CrossRef] [PubMed]
12. Toshchevikov, V.; Petrova, T.; Saphiannikova, M. Kinetics of ordering and deformation in photosensitive azobenzene lc networks. *Polymers* **2018**, *10*, 20. [CrossRef]
13. Ilcikova, M.; Mrlik, M.; Sedlacek, T.; Slouf, M.; Zhigunov, A.; Koynov, K.; Mosnacek, J. Synthesis of photoactuating acrylic thermoplastic elastomers containing diblock copolymer-grafted carbon nanotubes. *ACS Macro Lett.* **2014**, *3*, 999–1003. [CrossRef]
14. Hu, Y.; Wu, G.; Lan, T.; Zhao, J.J.; Liu, Y.; Chen, W. A graphene-based bimorph structure for design of high performance photoactuators. *Adv. Mater.* **2015**, *27*, 7867–7873. [CrossRef] [PubMed]
15. Yang, Y.K.; Zhan, W.J.; Peng, R.G.; He, C.G.; Pang, X.C.; Shi, D.; Jiang, T.; Lin, Z.Q. Graphene-enabled superior and tunable photomechanical actuation in liquid crystalline elastomer nanocomposites. *Adv. Mater.* **2015**, *27*, 6376–6381. [CrossRef] [PubMed]
16. Pennacchio, F.A.; Fedele, C.; De Martino, S.; Cavalli, S.; Vecchione, R.; Netti, P.A. Three-dimensional microstructured azobenzene-containing gelatin as a photoactuable cell confining system. *Acs Appl. Mater. Interfaces* **2018**, *10*, 91–97. [CrossRef] [PubMed]

17. Li, C.; Yun, J.H.; Kim, H.; Cho, M. Light propagation and photoactuation in densely cross-linked azobenzene-functionalized liquid-crystalline polymers: Contribution of host and concerted isomerism. *Macromolecules* **2016**, *49*, 6012–6020. [CrossRef]
18. Osicka, J.; Ilcikova, M.; Mrlik, M.; Minarik, A.; Pavlinek, V.; Mosnacek, J. The impact of polymer grafting from a graphene oxide surface on its compatibility with a pdms matrix and the light-induced actuation of the composites. *Polymers* **2017**, *9*, 14. [CrossRef]
19. Ilcikova, M.; Mrlik, M.; Sedlacek, T.; Doroshenko, M.; Koynov, K.; Danko, M.; Mosnacek, J. Tailoring of viscoelastic properties and light-induced actuation performance of triblock copolymer composites through surface modification of carbon nanotubes. *Polymer* **2015**, *72*, 368–377. [CrossRef]
20. Loomis, J.; King, B.; Burkhead, T.; Xu, P.; Bessler, N.; Terentjev, E.; Panchapakesan, B. Graphene-nanoplatelet-based photomechanical actuators. *Nanotechnology* **2012**, *23*, 10. [CrossRef] [PubMed]
21. Koerner, H.; Price, G.; Pearce, N.A.; Alexander, M.; Vaia, R.A. Remotely actuated polymer nanocomposites—Stress-recovery of carbon-nanotube-filled thermoplastic elastomers. *Nat. Mater.* **2004**, *3*, 115–120. [CrossRef] [PubMed]
22. Afzal, A.; Kausar, A.; Siddiq, M. Review highlighting physical prospects of styrenic polymer and styrenic block copolymer reinforced with carbon nanotube. *Polym. Plast. Technol. Eng.* **2017**, *56*, 573–593. [CrossRef]
23. Ilcikova, M.; Mrlik, M.; Sedlacek, T.; Chorvat, D.; Krupa, I.; Slouf, M.; Koynov, K.; Mosnacek, J. Viscoelastic and photo-actuation studies of composites based on polystyrene-grafted carbon nanotubes and styrene-b-isoprene-b-styrene block copolymer. *Polymer* **2014**, *55*, 211–218. [CrossRef]
24. Feng, Y.Y.; Qin, M.M.; Guo, H.Q.; Yoshino, K.; Feng, W. Infrared-actuated recovery of polyurethane filled by reduced graphene oxide/carbon nanotube hybrids with high energy density. *Acs Appl. Mater. Interfaces* **2013**, *5*, 10882–10888. [CrossRef] [PubMed]
25. Czanikova, K.; Torras, N.; Esteve, J.; Krupa, I.; Kasak, P.; Pavlova, E.; Racko, D.; Chodak, I.; Omastova, M. Nanocomposite photoactuators based on an ethylene vinyl acetate copolymer filled with carbon nanotubes. *Sens. Actuators B* **2013**, *186*, 701–710. [CrossRef]
26. Mrlik, M.; Ilcikova, M.; Sedlacik, M.; Mosnacek, J.; Peer, P.; Filip, P. Cholesteryl-coated carbonyl iron particles with improved anti-corrosion stability and their viscoelastic behaviour under magnetic field. *Colloid Polym. Sci.* **2014**, *292*, 2137–2143. [CrossRef]
27. Osicka, J.; Mrlik, M.; Ilcikova, M.; Hanulikova, B.; Urbanek, P.; Sedlacik, M.; Mosnacek, J. Reversible actuation ability upon light stimulation of the smart systems with controllably grafted graphene oxide with poly (glycidyl methacrylate) and pdms elastomer: Effect of compatibility and graphene oxide reduction on the photo-actuation performance. *Polymers* **2018**, *10*, 832. [CrossRef]
28. Mrlik, M.; Cvek, M.; Osicka, J.; Moucka, R.; Sedlacik, M.; Pavlinek, V. Surface-initiated atom transfer radical polymerization from graphene oxide: A way towards fine tuning of electric conductivity and electro-responsive capabilities. *Mater. Lett.* **2018**, *211*, 138–141. [CrossRef]
29. Mrlik, M.; Ilcikova, M.; Plachy, T.; Moucka, R.; Pavlinek, V.; Mosnacek, J. Tunable electrorheological performance of silicone oil suspensions based on controllably reduced graphene oxide by surface initiated atom transfer radical polymerization of poly(glycidyl methacrylate). *J. Ind. Eng. Chem.* **2018**, *57*, 104–112. [CrossRef]
30. Yoon, J.T.; Lee, S.C.; Jeong, Y.G. Effects of grafted chain length on mechanical and electrical properties of nanocomposites containing polylactide-grafted carbon nanotubes. *Compos. Sci. Technol.* **2010**, *70*, 776–782. [CrossRef]
31. Ilcikova, M.; Mrlik, M.; Spitalsky, Z.; Micusik, M.; Csomorova, K.; Sasinkova, V.; Kleinova, A.; Mosnacek, J. A tertiary amine in two competitive processes: Reduction of graphene oxide vs. Catalysis of atom transfer radical polymerization. *Rsc Adv.* **2015**, *5*, 3370–3376. [CrossRef]
32. Ma, C.X.; Le, X.X.; Tang, X.L.; He, J.; Xiao, P.; Zheng, J.; Xiao, H.; Lu, W.; Zhang, J.W.; Huang, Y.J.; et al. A multiresponsive anisotropic hydrogel with macroscopic 3d complex deformations. *Adv. Funct. Mater.* **2016**, *26*, 8670–8676. [CrossRef]

Paper IV

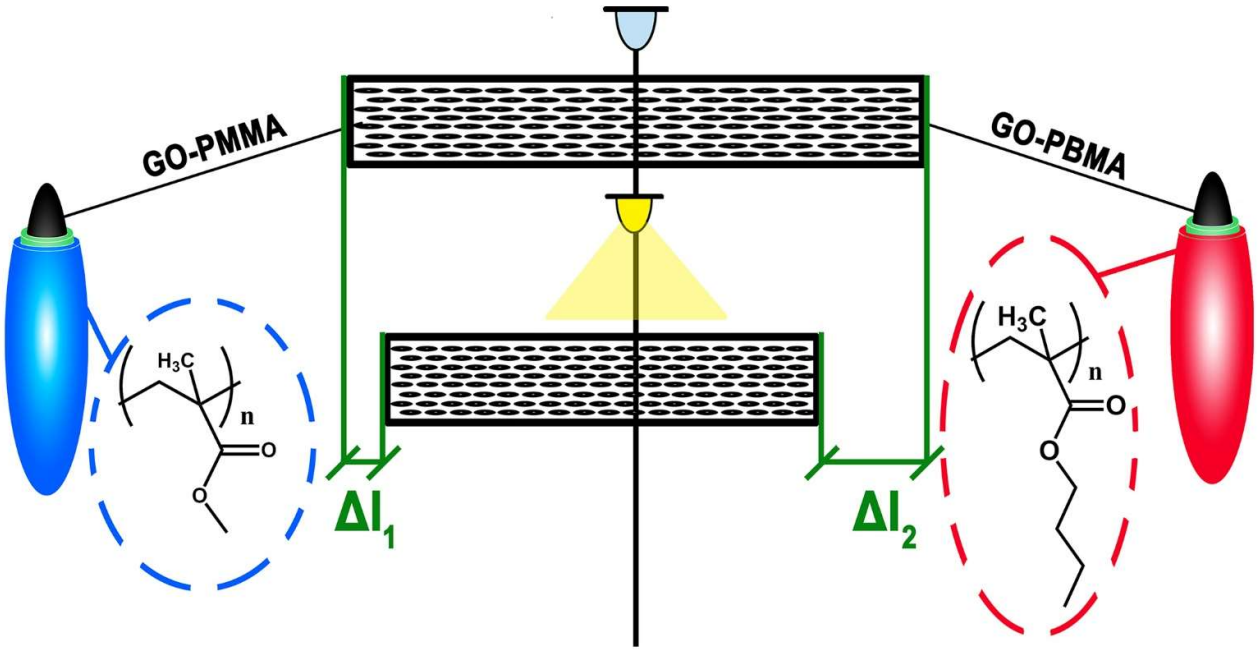

Reactive and Functional Polymers 148 (2020) 104487

Contents lists available at ScienceDirect

Reactive and Functional Polymers

journal homepage: www.elsevier.com/locate/react

Controllably coated graphene oxide particles with enhanced compatibility with poly(ethylene-co-propylene) thermoplastic elastomer for excellent photo-mechanical actuation capability

Josef Osicka[a], Miroslav Mrlik[a,*], Marketa Ilcikova[b,c], Igor Krupa[d,**], Patrik Sobolčiak[d], Tomáš Plachý[a], Jaroslav Mosnáček[b,e,***]

[a] Centre of Polymer Systems, University Institute, Tomas Bata University in Zlin, Trida T. Bati 5678, 760 01 Zlin, Czech Republic
[b] Polymer Institute, Slovak Academy of Sciences, Dubravska cesta 9, 845 41 Bratislava 45, Slovakia
[c] Department of Chemistry, Lodz University of Technology, Institute of Polymer and Dye Technology, 90 924 Lodz, Poland
[d] Center for Advanced Materials, Qatar University, P. O. Box 2713, Doha, Qatar
[e] Centre for Advanced Materials Application, Slovak Academy of Sciences, Dúbravska cesta 9, 845 11 Bratislava, Slovakia

ARTICLE INFO

Keywords:
Graphene oxide
ATRP
Compatibility
Vistamaxx
Grafting
Stimuli responsive properties

ABSTRACT

This paper reports the utilization of the controllable coating via SI-ATRP technique as a promising approach for controlling stimuli-responsive capabilities of graphene oxide (GO) based nanocomposites. Various polymer brushes with controlled molar mass and narrow dispersity were grown from the surface of GO particles. Modification of GO with poly(methyl methacrylate) and poly(*n*-butyl methacrylate) was proved by transmission electron microscopy, thermogravimetric analysis with online FTIR recording and finally by X-ray photoelectron spectroscopy (XPS). Densities of GO-based materials were investigated and conductivity measurements showed the increase values. XPS and Raman shift was used to confirm the GO particles reduction. A compatibility of the filler with propylene-based elastomer was elucidated by melt rheology. The light-induced actuation capability was investigated on composite samples to show, that polymer hybrid particles based on GO have better compatibility with the polymer matrix and thus their proper dispersibility was significantly improved. In addition the plasticizing effect of the short polymer grafts present on the GO filler surface has the crucial impact on the matrix stiffness and thus the ability of composite material to reversibly respond to the external light stimulation.

1. Introduction

The photomechanical actuators (also known as photo-actuators) are a class of smart materials that can alter their dimensions or undergo mechanical motion when exposed to photons (light emission). Absorption of the energy from photons leads to a contract or a generation of a certain mechanical motion of polymeric chains [1,2], which is called photo-actuation. Photo-actuators are kind of promising materials thanks to their wireless actuation. Such behavior can be utilized in many applications, in which a transformation of optical-to-mechanical energy is required or beneficial. Thus, photo-actuating systems are mainly used as various motors [3], as smart curtains [4], systems reproducing biomimetic motions [5], *etc*. One of the most important class from the application point of view are photo-thermal actuators, which are uniform composite systems consisting of a flexible elastomeric matrix and various functional fillers promoting interactions with photons [2]. Carbon particles such as carbon nanotubes (CNTs) [1,3], graphene oxide [1,6], graphene [7,8] *etc.,* are extensively used as fillers in these systems thanks to their excellent both thermal and mechanical properties. Their utilization increases absorption of the energy from photons [9] and, thus, promotes an overall photomechanical performance of the photo-actuators.

In the most of composite systems, the distribution of particles in the matrix plays an important role in overall performance of the composite together with its photo-actuation performance. It has been shown that the photo-actuating systems based on neat multi-walled CNTs (MWCNTs) exhibited deterioration of the elastic properties of the matrix as confirmed by dynamic mechanic analysis [10]. On the other hand, modification of MWCNTs with polystyrene brushes led to the systems, which preserves flexibility and exhibited sufficient

* Correspondence to: M. Mrlík, Centre of Polymer Systems, University Institute, Tomas Bata University in Zlin, Trida T. Bati 5678, 760 01 Zlin, Czech Republic
** Corresponding author.
*** Correspondence to: J. Mosnáček, Polymer Institute, Slovak Academy of Sciences, Dubravska cesta 9, 845 41 Bratislava 45, Slovakia.
E-mail addresses: mrlik@utb.cz (M. Mrlik), igor.krupa@qu.edu.qa (I. Krupa), jaroslav.mosnacek@savba.sk (J. Mosnáček).

https://doi.org/10.1016/j.reactfunctpolym.2020.104487
Received 20 September 2019; Received in revised form 9 January 2020; Accepted 10 January 2020
Available online 11 January 2020
1381-5148/

phototactuation of polystyrene-*b*-polyisoprene-*b*-polystyrene nanocomposites [10]. Graphene itself, due to its strong aggregation tendency, usually exhibits inhomogeneous distribution within a polymer matrix and, therefore, using of GO is commonly preferred. The presence of functional groups (hydroxyl, epoxy and carbonyl) on the GO surface can be utilized for further modification to target compatibility with wide range of polymer matrices [11]. We have recently introduced [12–14] a surface-initiated atom transfer radical polymerization (SI-ATRP) as a promising approach for GO surface modification enabling to tune its properties with controlled mechanism of the reaction. SI-ATRP approach can be effectively used for preparation of polymer hybrids enables exact control of polymer architecture including molar mass of the polymers, uniformity of polymer chain length, grafting density, and chain composition [15,16]. The surface modification enables the proper filler dispersion, homogenous distribution of the filler within the surrounding polymer, which is crucial for its final performance. Osicka et al. has recently used SI-ATRP for coating of GO particles with poly (glycidyl methacrylate) (PGMA)[17], poly(methyl methacrylate) (PMMA), and poly(*n*-butyl methacrylate) (PBMA)[18] polymers in form of short brushes. The PMMA and PBMA, compared to neat GO, the increased wettability of the grafted GO hybrids with poly(dimethyl siloxane) matrix was reported. It led to improved particles dispersion and distribution of the filler resulting in increased thermal conductivities of their composites. Thermal conductivity is one of the crucial factor affecting photo-actuation effect [19] and such systems, i.e. containing PMMA and PBMA modified GO, have therefore exhibited more significant photo-actuation effect with the maximum value of the actuation around 35 μm under particles loading of 1 wt.% [18]. Also in the case of PGMA brushes the grafted GO-based systems exhibited increased photo-actuation effect together with higher thermal conductivity. It is worth to note, that better dispersion and homogeneous distribution of the particles within the polymer matrix achieved through modification of GO benefits overall performance of these composites.

In this study the GO-polymer hybrids were used for the first time for preparation of photo-mechanical actuators based on a poly(propylene-*co*-ethylene) matrix possessing thermoplastic elastomer properties. The poly(propylene-*co*-ethylene) copolymer was chosen as a polymer matrix, due to its easy processing conditions, proper elasticity, long-term stability and enhanced chemical resistance. The GO was grafted with two types of polymer brushes, namely PMMA and PBMA. The effect of presence and type of polymer grafts was investigated using rheological investigations showing better insight into the interactions between GO-based particles and poly(propylene-*co*-ethylene) copolymer. Finally, photo-actuation performance showed that incorporation of the GO-polymer hybrids into the polymeric matrix led to the enhancement in determined value of actuations and thus significantly increased capability of the system.

2. Experimental part

2.1. Materials

The sacrificial initiator methyl 2-bromopropionate 98 %, initiator for direct covalent bonding 2-Bromopropionyl bromide 97 %, ATRP ligand *N,N,N′,N″,N″*-pentamethyldiethylenetriamine (PMDETA) 98 %, copper bromide (CuBr) 97 % and anisole 98%, were utilized without further purification. Methyl methacrylate 98%, *n*-butyl methacrylate 98% were purified by passing through a basic alumina before the use in order to remove a stabilizer. Triethylamine (Et_3N) 98 % and tetrahydrofuran (THF) were dried overnight using sodium cubes. All chemical were bought from Sigma Aldrich, USA Graphite in form of fine powder 40 μm (Sigma Aldrich, USA) was used as received. Dimethylformamid p.a., acetone p.a. and diethylether p.a. (LachNer, Gemany) were all used as received. Poly(propylene-*co*-ethylene) copolymer (Vistamaxx^{TM} 6202, ExxonMobil, USA) contains (85 wt.%) and (15 wt.%) of isotactic propylene and random ethylene units, respectively. Vistamaxx has following characteristics such as melt flow index (MFI) 7.4 g/10 min and polymer density 0.861 g·cm^{-3}). GO and GO modified with ATRP initiator (GO-I) were prepared similarly as was already published [18,20,21] (see ESI).

2.2. Grafting of PMMA and PBMA from GO surface

General procedure for polymer modification of GO surface was as follows: 1.5 g of GO-I was put into the special type of flask (Schlenk type) with volume of 100 mL containing a magnetic bar for stirring. Then, the flask was three times filled inert atmosphere and evacuated and followed by addition of anisole (30 mL) pre-purged with inert gas. Then ethyl α-bromoisobutyrate, as a sacrificial initiator with same molarity as CuBr were added. Further, PMDETA was added in 4-fold molar excess to the sacrificial initiator. The corresponding monomer (30 mL) in 100 molar excess to sacrificial initiator was bubbled with inert gas and transferred to the flask. To avoid the presence of oxygen the four F-T-P cycles were completed. Finally, CuBr was put into the flask under inert atmosphere, when the reaction mixture was frozen. The polymerization was performed at 70 °C for 2 h. To stop the reaction, Schlenk flask was opened and additional 15 mL of anisole have been added. Compositions of performed reactions were analyzed and summarized in the Table 1 together with the monomer conversion (based on ^{1}H NMR spectra), M_n and dispersity ($Đ$) elucidated by GPC. The reaction mixtures including the GO-based powder were filtered using following procedure. The powders were firstly dispersed in 100 mL of DMF, then filtrated using 0.44 μm PTFE filter and followed by washing with acetone (100 mL). Such procedure was repeated for three times. Finally, the powders were washed with diethyl ether (100 mL) to remove all residuals.

2.3. Composites preparation

The composites consisting of the neat or polymers modified GO particles and Vistamaxx matrix were mixed using Brabender (Duisburg, Germany). The device has three heating zones all operating at temperature 190 °C, The components (filler, matrix) were added within one minute and whole compounding time was four minutes at speed 50 rpm.

2.4. Characterization methods

Molar mass (M_n) and dispersity ($Đ$) of synthesized polymer brushes

Table 1
Composition of the polymerization mixture in molar ratios and characterization of the polymers.

Sample name	Monomer	Initiator	PMDETA	CuBr	M_n[a] (g mol^{-1})	$Đ$[a]	Conversion[b] (%)
GO-PMMA	100	1	4	1	6800	1.18	89
GO-PBMA	100	1	4	1	5800	1.21	41

[a] According to the GPC and recalculation using Mark-Houwink parameters.
[b] According to the ^{1}HNMR

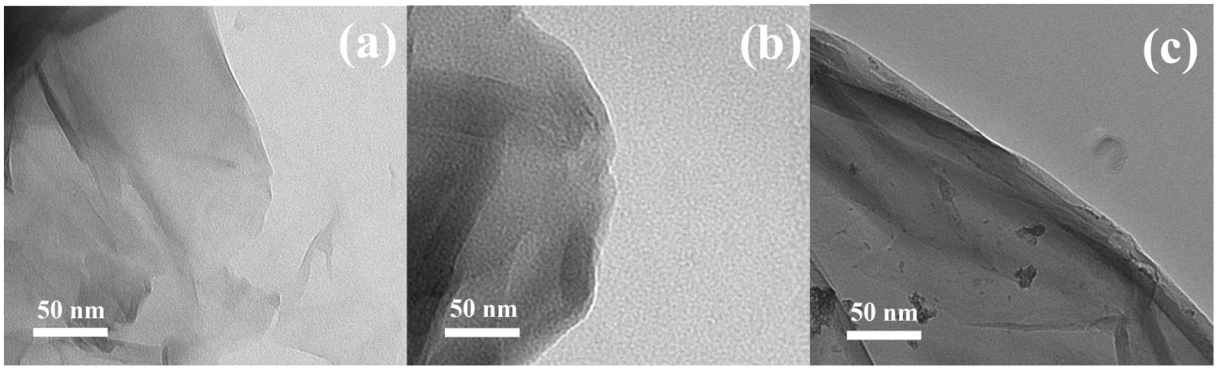

Fig. 1. TEM micrographs of the neat GO sheet(a), GO with PMMA brushes (b), and GO-PBMA brushes (c).

were investigated by GPC, PL-GPC220 (Agilent, Japan) using polystyrene calibration and anisole as an internal standard. The resulting molar masses of poly(methyl methacrylate) (PMMA) and poly(*n*-butyl acrylate) (PBA) were recalculated using Mark-Houwink parameters for PS ($K = 16.0{\cdot}10^{-5}$ dL g^{-1}, $\alpha = 0.700$) [22], for PBA ($K = 11.0{\cdot}10^{-5}$ dL g^{-1}, $\alpha = 0.723$) and for PMMA ($K = 12.8 \times 10^{-5}$ dL·g^{-1} and $\alpha = 0.690$).[23] Conversions of the monomers were calculated from ^{1}H NMR signals obtained from measurements VNMRS Varian spectrometer, 400 MHz at 25 °C, and $CDCl_3$ was used as a solvent. The chemical composition of neat and polymers modified GO was measured using Nicolet iS10 (Thermo Scientific, USA) connected to the TGA (TA, instruments), where the decomposed components were individually analyzed. The Raman shift was investigated from 3 scans (resolution of 2 cm^{-1}) using a Nicolet DXR (Nicolet, USA). The individual layers of the GO and GO-polymer hybrids were analyzed using transmission electron microscopy (TEM) (Philips CM12, Nederlands). The XPS analysis chamber was evacuated approximately 6×10^{-8} Pa. The samples were excited by X-rays over a 400 μm^2 spot area with monochromatic Al Kα1,2 radiation at 1486.6 eV. All the spectra were referenced to the main C 1s peak of the carbon atoms, which was assigned a value of 284.8 eV. Samples for electrical conductivity in form of powder, were pressed on the hydraulic press (H-62, Trystom, Czech Republic). Then current responses have been evaluated using electrometer (Keithley 6517B, USA) and 10 measurement were used to provide final value. In order identify the density of the GO-based samples, the pellets were weight on air and in decane using Sartorius R 160P balances (Sartorius AG, Germany). The thermal conductivity was measured by one side contact method using TCi model (C-term Technologies, Canada)

The rheological characteristics of composites were measured utilizing rheometer Physica (MCR502, Anton Paar, Austria) connected to Peltier heating/cooling fixture and parallel-plate geometry (PP25). Samples in form of discs with thickness of 1 mm were elucidated. Firstly, the linear viscoelastic region was investigated. Then to avoid the sample slippage, the constant 0.3 N force was applied. Finally the frequency sweep in the range from 10^{-1} to 10^{1} Hz was performed. Final, values used in the figures are average values obtained from three individual measurements. In order to investigate the photo-responsive properties of neat polymer matrix and prepared nanocomposites in form of fibre mats the thermo-mechanical analyzer (TMA) (Mettler Toledo) [16]. The photo-actuation performance is ability of the material shows the reversible contraction and elongation upon irradiation with light source having 627 nm wavelength and intensity of 6 mW, 9 mW and 12 mW. Temperature during the measurement was checked by external sensor and during whole investigation was 25 °C ± 0.4 °C.

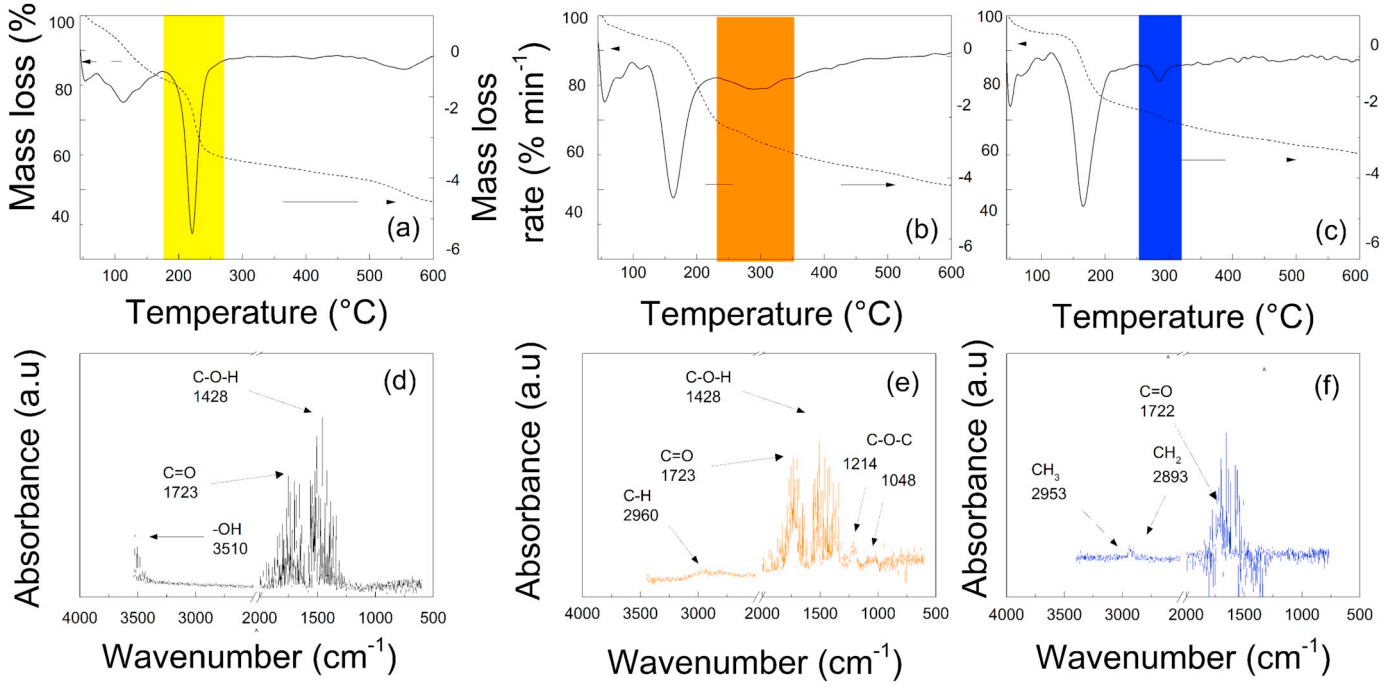

Fig. 2. TGA-FTIR online monitoring of the neat GO (a, d), GO-PMMA (b, e) and GO-PBMA (c, f) particles.

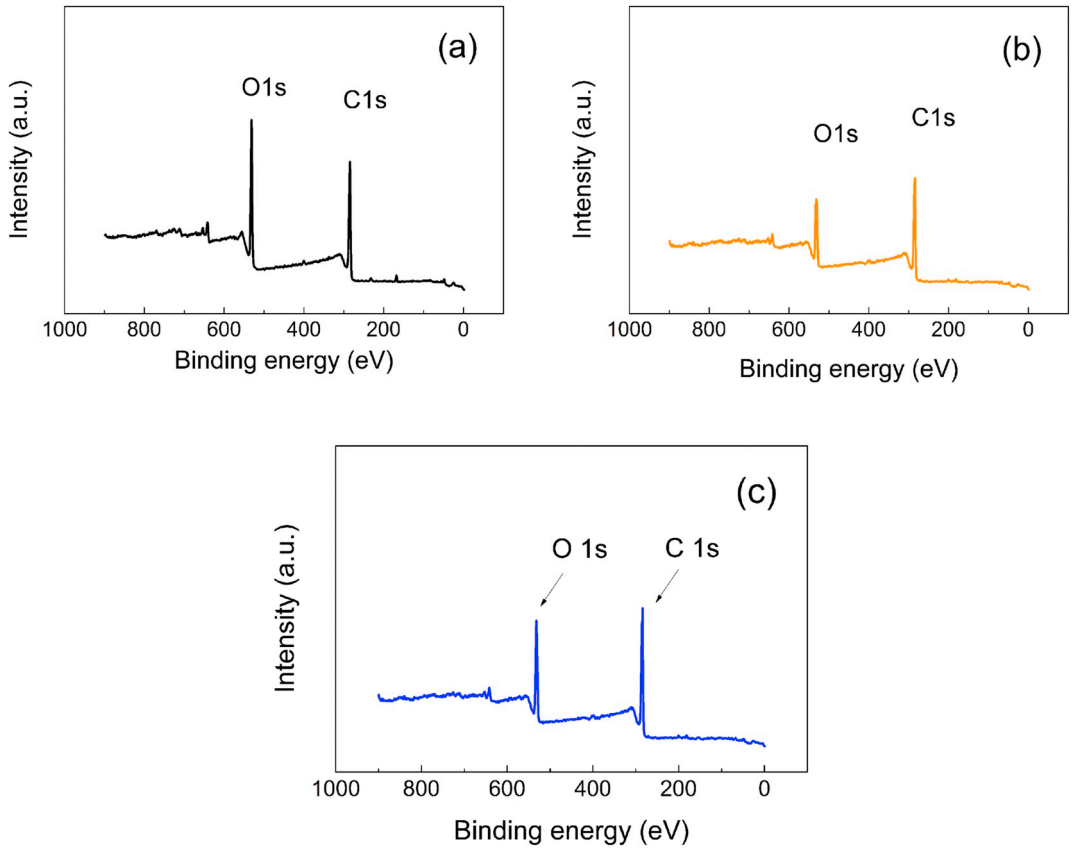

Fig. 3. XPS spectra of neat GO (a), GO-PMMA brushes (b) and GO-PBMA brushes (c).

3. Results and discussion

The coating of the GO polymer hybrids was successfully performed and reaction mixture based on sacrificial initiator was analyzed using GPC and ^{1}H NMR. The ratio of the individual components and characterization of the final polymers are presented in Table 1. Here, the polymers with narrow *Đ* were obtained as a result of good control over the polymerization process. Finally, the GPC traces of both modifications can be seen in Fig. S1 (ESI).

TEM images were investigated to get information about exfoliation of neat GO as well as GO-polymers hybrids. As can be in Fig. 1a the neat GO has several layers and exhibits expected 2D structure. SI-ATRP provides well-precise and controlled polymerization conditions with progressive growing the polymer chains from the GO surface and thus the 2D structure is retained for both GO-PMMA and GO-PBMA (Fig. 1b and 1c, respectively). The flossy-like appearance confirms the grafting of GO surface by very thin polymer layer.

The investigation of the chemical composition of GO-based samples was performed using FTIR monitoring of the gas phase created during decomposition process of TGA. As can be seen in the Fig. 2a (neat GO), the main drop between 150–300 °C correspond to the stretching from hydroxyl and cabonyl moieties at 3510 cm^{-1} and 1723 cm^{-1}. In addition in-plane bending vibration signal of C-OH from carboxyl pendant was observed at 1423 cm^{-1}. Controllable coating of GO sheets with short brushes shifted the release of oxygen moieties to lower temperatures. Furthermore, the decomposition of the polymers can be visible above 220 °C (Fig. 2b and c). For GO-PMMA the FTIR collected at the temperature range of 220–350 °C showed strong signals from stretching vibrations of carbonyl groups at about 1731 cm^{-1} and from C—H moieties at wavenumbers range of 1250–1550 cm^{-1} (Fig. 2e). In addition, new signals from stretching of alkyl moieties and bending of C—O—C moieties appeared at 2600–3000 cm^{-1} and also 1000–1200 cm^{-1}, respectively, confirming presence of PMMA. Comparable signals were observed in FTIR spectra of degradation products collected at the temperature range of 220–380 °C from TGA of GO-PBMA (Fig. 2f), when PBMA moieties shows decomposition at higher temperatures. with the difference of shifting of the release of the groups from PBMA to the higher temperatures. Moreover, also the grafting density in both cases GO-PMMA as well as GO-PBMA were calculated according to the reference [15] and it was found that the grafting density was 0.83 chain/nm^2 and 0.6 chain/nm^2, respectively.

To further prove the covalent bonding of the polymer chains on GO surface the XPS spectra were measured and investigated (Fig. 3, Table 1). Following the successful coating with PMMA and PBMA chains, a clear increase in C/O ratio could be observed due to higher carbon content in the polymers. This is more pronounced for PBMA where longer aliphatic chain is present. Moreover, increased content of sp^2 accompanied by decreased content of sp^3 hybridized form indicates

Table 2
Surface element content (atomic %) of neat GO and GO-polymers hybrids.

Sample name	C1s	O1s	C1s sp^2	C1s sp^3	C1s C-O	C1s C=O	C1s O-C=O	C1s/O1s
GO	66.7	33.3	26.7	28.4	32.3	9.0	3.6	2.00
GO-PMMA	69.1	30.9	31.4	26.2	30.9	8.3	3.2	2.24
GO-PBMA	70.9	29.1	36.5	25.3	27.5	7.7	3.0	2.43

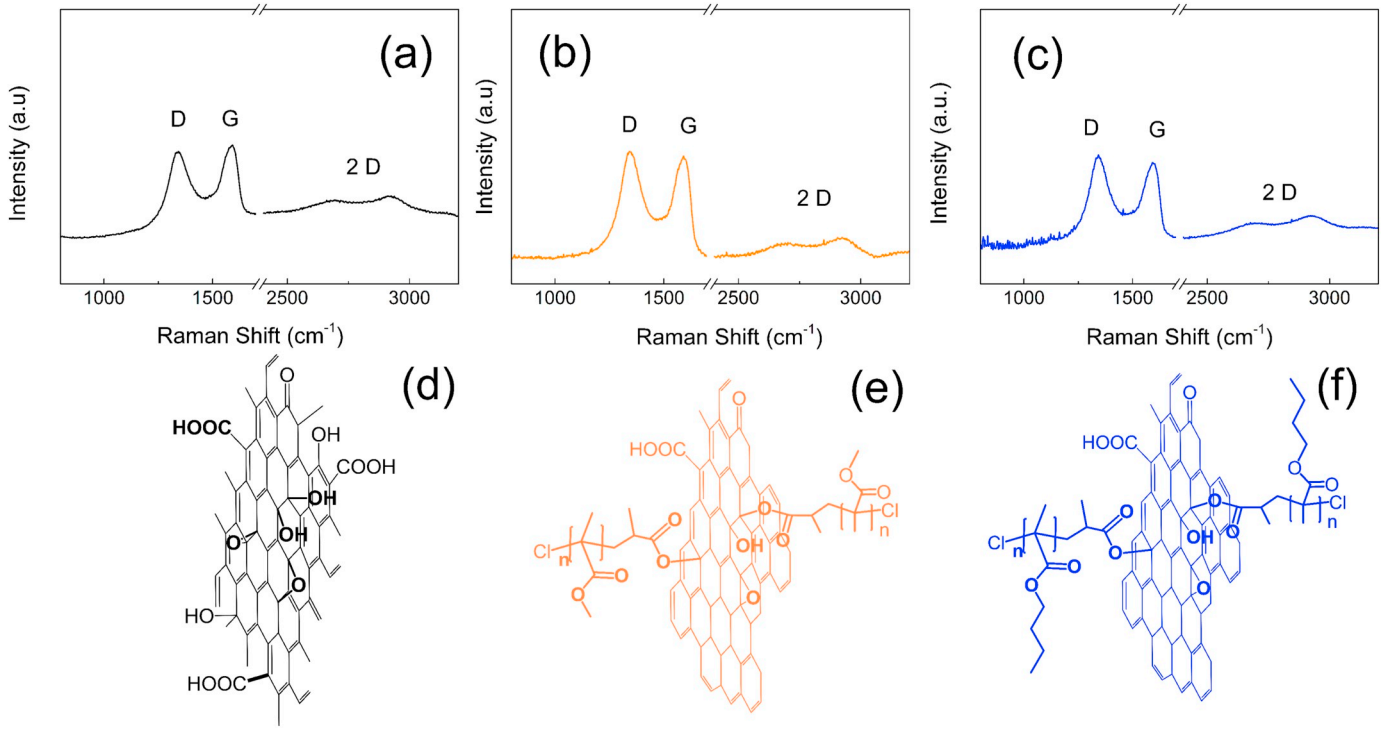

Fig. 4. Raman spectra of the neat GO (a), GO-PMMA (b) and GO-PBMA (c) and their schematic illustatrions for GO (d). GO-PMMA (e) and GP-PBMA (f).

Table 3
Conductivities and densities of neat GO and GO-modified particles.

Sample name	Conductivity (S cm^{-1})	Density (g cm^{-3})
Neat GO	$1.2 \cdot 10^{-8}$	2.68
GO-PMMA	$6.3 \cdot 10^{-8}$	2.53
GO-PBMA	$2.1 \cdot 10^{-7}$	2.34

that the reduction of GO surface took place as well, as will be further confirmed also by Raman shift and conductivity measurements (Table 2).

3.1. Reduction of the GO particles by SI-ATRP approach

From the Raman spectra (Fig. 4a–c) is clearly shown that 2D structure of GO is negligibly affected by both polymer modifications (Fig. 4e and f), while the considerable reduction of the GO surface was reached. This reduction was elucidate according to the calculations of the peak intensities those corresponding to sp^2 and sp^3 hybridization and are marked I_D and I_G, respectively. This ratio is for neat GO 0.90 and for GO-PMMA 1.05 and GO-PBMA 1.08, showing usual increase when reduction of the GO surface takes place.

The comparative method for GO reduction evaluation is next to the abovementioned Raman, electric conductivity investigation those well-correlates with Raman reuslts. Electric conductivity increased from 1.2×10^{-8} S cm^{-1} for neat GO, slightly increased to 6.3×10^{-8} S cm^{-1} for GO-PMMA and 2.1×10^{-7} S cm^{-1} for GO-PBMA. This is in good agreement with previously reported simultaneous partial GO surface reduction during controllable modification process. The controllable coating of graphene oxide surface by polymer chains was finally also confirmed by change of the GO density, which is decreased due to the certain polymer layer on the GO particles. Densities for investigated samples are summarized in the Table 3.

3.2. Compatibility between the GO-polymer particles and Vistamaxx matrix

The investigation of the viscoelastic properties at certain frequency range provide crucial information about compatibility of the modified GO sheets with the Vistamaxx copolymer It can be seen that neat Vistamaxx has cross-over point at 4.47 Hz (Fig. 5a), while for the composite containing neat GO particles cross-over point is 3.3 Hz (Fig. 5b) showing increases values of both moduli and reinforcing effect. For GO-PMMA and GO-PBMA grafted sheets cross-over points can be visible at 6.1 Hz and 6.30 Hz, respectively, because of the short grafted brushes on the GO surface, providing the plasticizing effect for such composite in Vistamaxx matrix (Fig. 5c and d)). Similar results were observed for other thermoplastic elastomers [24,25]. The presence of the short polymer chains is highly beneficial in the case of our system, because it also significantly enhances flexibility of the composite [10]. Both these factors, i.e. better compatibility and higher flexibility, indicate that GO-polymer based composites should provide enhanced photo-actuation capability, the property which is investigated below.

3.3. Thermal conductivity

Thermal conductivity is very crucial factor for the material actuation upon light stimulation, due to the fact that, absorbed light from the source need to the redistributed within the whole sample and thus provide significantly improved actuation capability [19]. Table 4 shows the values of the thermal conductivity of various elastomeric composite samples. As was already confirmed by Raman spectroscopy and electric conductivity investigations, the electric conductivity of these system, increasing, which is also in correlation with thermal conductivity, which increased from 0.089 for neat matrix to 0.156, 0.196 and 0.202 W mK^{-1} for GO-filled, GO-PMMA and GO-PBMA filled elastomeric composites, respectively. Such increment is very promising from the photo-actuation point of view and will be further presented in the section below.

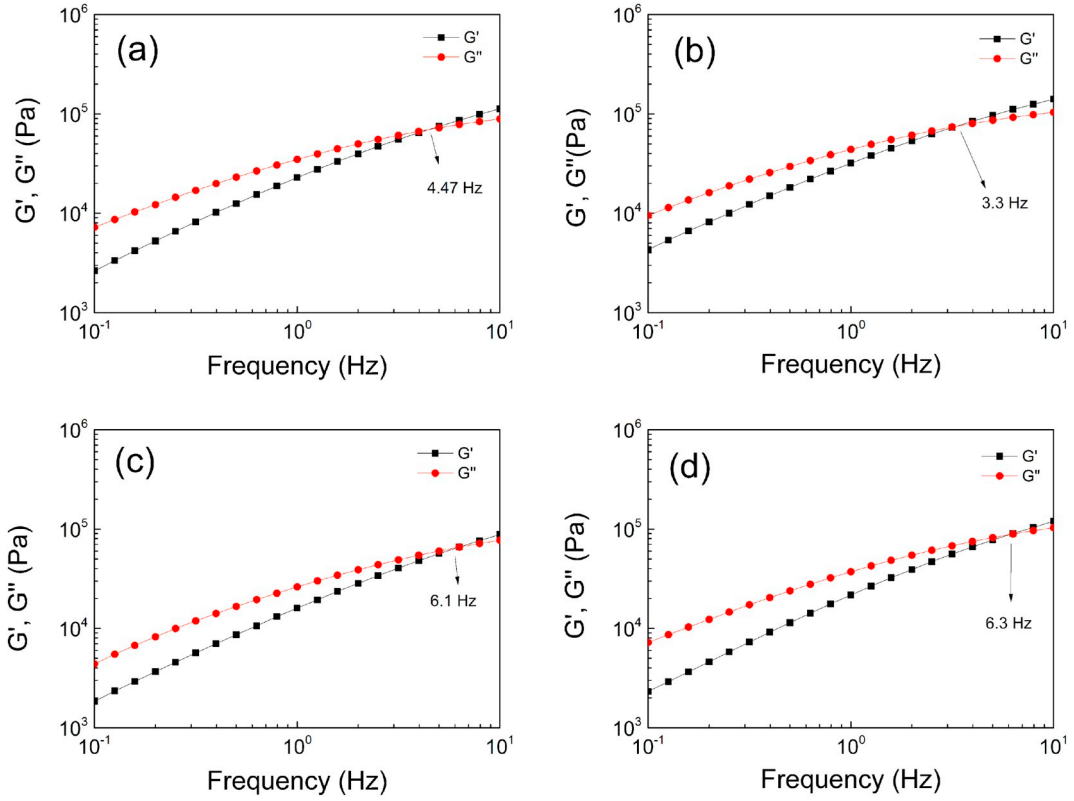

Fig. 5. Frequency dependence of storage, G′, and loss G″ moduli for neat Vistamaxx (a), and composites based on neat GO (b), GO-PMMA (c) and GO-PBMA (d) measured at 110 °C.

Table 4
Thermal conductivity of neat Vistamaxx and composites with GO-PMMA and GO-PBMA

Sample code	Thermal conductivity (W mK^{-1})
Neat Vistamaxx	0.089
0.1 vol.% GO	0.156
0.1 vol.% GO-PMMA	0.196
0.1 vol.% GO-PBMA	0.202

3.4. Light-induced actuation capability

Light -induced actuation capabilities of the prepared samples were investigated similarly as in our previous papers [17,18], here also the effect of the GO coating on the actuation performance has been determined. Impact of the light intensity as well as filler loading in case of the most promising system was deeply elucidated. As is shown in Fig. 6, the neat Vistamaxx exhibit certain value of actuation, however the final actuation value, *ΔL*, was 12.0 μm with very long recovery time reaches nearly 30 s. Photo-actuation performance was nearly doubled for

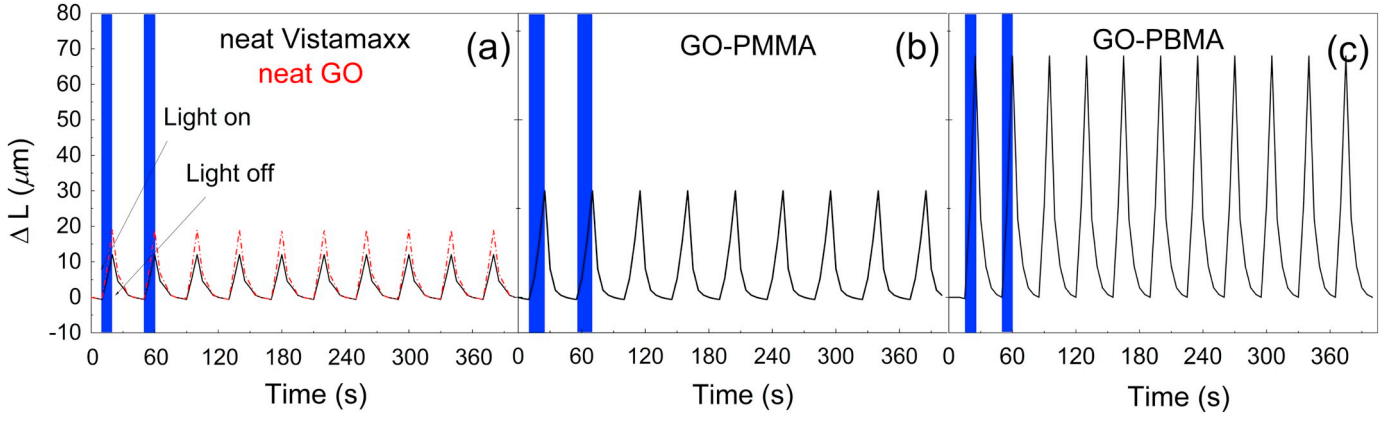

Fig. 6. Photo-actuation performance of neat Vistamaxx (black solid line) and composite contaning 0.1 vol. % of neat GO (red dash-dot line) (a), GO-PMMA (b), and GO-PBMA (c) at light intensity of 6 mW. (For interpretation of the references to color in this figure legend, the reader is referred to the web version of this article.)

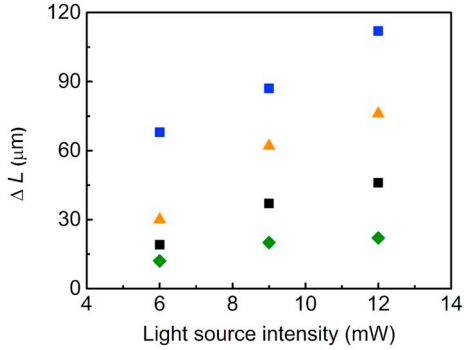

Fig. 7. Dependence of the change in the length on the light source power for neat Vistamaxx matrix (green diamonds) and composites containing 0.1 vol. % of neat GO (black squares), GO-PMMA (orange triangles) and GO-PBMA (blue squares). Height of the symbols are corresponding to the error bars of the measurement. (For interpretation of the references to color in this figure legend, the reader is referred to the web version of this article.)

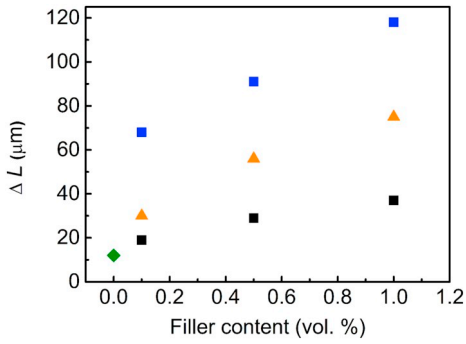

Fig. 8. Dependence of the change in the length on the filler content for neat Vistamaxx matrix (green diamonds) and vistamaxx elastomers with GO particles (black squares), GO-PMMA (orange triangles) and GO-PBMA (blue squares) at light intensity of 6 mW. Height of the symbols are corresponding to the error bars of the measurement. (For interpretation of the references to color in this figure legend, the reader is referred to the web version of this article.)

composite with neat GO particles (0.1 vol. %) due to ability of GO to absorb the light and the enhanced thermal conductivity of GO composite. After addition of 0.1 vol.% of GO-PMMA sheets, the absolute value of actuation reaches 30 μm while time to reach the initial length decreased to 25 s. More pronounced improvement can be seen for composite sample with GO-PBMA sheets, where absolute maximum value reaches 68 μm, and showing very similar recovery time as previous modification (25 s). The crucial factor which can be assign for significantly improved actuation performance is improved compatibility of polymer hybrids of GO and short PMMA and PBMA polymer brushes with Vistamaxx and also partial plasticizing effect on the matrix and improved heat transition within the samples causing easier and more proper shape recovery.

Further the impact of light source intensity on the photo-actuation capability in case of Vistamaxx-based composites was elucidated and can be clearly seen in Fig. 7. Generally, the change in the length increasing when the light source intensity increases. From this point of view the composites with GO-PBMA sheets, were investigated, due to the fact that exhibit the best actuation performance at 6 mW. However if the light intensity was increased to 12 mW, the actuation performance reaches 110 μm, what is about 8 times higher value than for neat Vistamaxx. The neat Vistamaxx as well as composite containing neat GO and GO-PMMA shows certain saturation of the photo-actuation properties, since the increment of the change in the length is slightly decreasing with increasing light source power. This is not a case of composite containing GO-PBMA particle; this composite has similar change in the length increment with increasing light source power and at highest power provide unsaturated system. At this point can be stated that significantly increased flexibility of the composite system can be assigned to the presence of short polymer brushes, which finally contribute to the considerable enhancement of actuation performance [24–26]. The GO modification also significantly improved the compatibility with Vistamaxx matrix providing samples with proper filler distribution improving the final thermal conductivity and thus the transformation of the energy from light to mechanical movement. GO-based systems showed in this study have comparably higher actuation performance in comparison to CNTs, carbon black, GO or graphene nanoplatelets (2 wt.%) in the PDMS composites. Those samples exhibit only 25 μm actuation recalculated to our conditions [27].

Increasing the filler content from 0.1 vol. % to 0.5 and 1 vol. % led to increased photo-actuation capabilities, while the course was different for individual systems based on the type of dispersed particles (Fig. 8). Change in the length for GO-based composites reached 29 μm at 0.5 vol. % and just slightly increased for 1 vol. % to 37 μm. Similarly, for the composite with GO-PMMA particles the increment in the change in the length with particles concentration was not linear but slightly saturates and reached values of 56 μm and 75 μm for 0.5 and 1 vol. %, respectively. The highest photo-actuation performance was again discovered for samples including GO-PBMA polymer hydrides. As can be seen the change in the length increment is still linear and suggests that further filler loading could be effective and actuation performance could be higher than obtained for 0.5 and 1 vol. %, 91 μm and 118 μm, which is high enough for application as a part of tactile displays. These results confirm the previous findings, that flexibility of the matrix together with proper filler dispersion and enhanced thermal conductivity are crucial factor influencing the photo-actuation capability.

4. Conclusions

This study is dealing with the influence of the modification of the GO particles on the photo-actuation performance of the thermoplastic elastomer matrix. The SI-ATRP approach was utilized for grafting of PMMA and PBMA chains from the GO sheets accompanied with controllable reduction. The grafting was proved using TEM, GPC, ^{1}H NMR, TGA-FTIR and XPS. The partial GO reduction was confirmed with Raman shift, electric conductivity investigations and XPS. The improved interactions between of the GO- based polymer brushes with Vistamaxx was proved by melt rheology investigation where the crossover point was shifted to the higher frequencies and showed enhanced compatibility. Finally the photo-actuation studies showed the excellent length change values of 120 μm for 6 mW at 1 vol.% of GO-PBMA loading and nearly 110 μm at 12 mW for only 0.1 vol.% of GO-PBMA loading. This photo-actuation capability is significantly higher than obtained previously for other similar systems. Thus it has to be concluded that the approach reported here is very promising for further investigation and possible increased filler loading can further enhance the photo-actuation capability.

Authors declaration

None.

Declaration of Competing Interest

None.

Acknowledgement

This research was funded by Qatar University Collaborative High Impact Grant QUHI-CENG-18/19-1. The findings achieved herein are solely the responsibility of the authors. Authors also gratefully thanks to the Grant Agency of the Czech Republic (no. 16-20361Y) for financial

support. This work was also supported by the Ministry of Education, Youth and Sports of the Czech Republic – program NPU I (LO1504). This study was also performed during the implementation of the project Building-up Centre for advanced materials application of the Slovak Academy of Sciences, ITMS project code 313021T081 supported by Research & Innovation Operational Programme funded by the ERDF. JM also acknowledge for financial support to project VEGA 2/0129/19. This article (specify by the fact) was also written with support of Operational Program Research and Development for innovations co-funded by the European Regional Development Fund (ERDF) and national budget of Czech Republic, within the framework of project CPS - strengthening research capacity (reg. number: CZ.1.05/2.1.00/19.0409). M. I. also thank to National Science Centre, Poland for the financial support through POLONEZ project number UMO-2016/23/P/ST5/02131. This project is carried out under POLONEZ program which has received funding from the European Unions's Horizon 2020 research and innovation programme under Marie Sklodowska-Curie grant agreement. No 665778.

Appendix A. Supplementary data

Supplementary data to this article can be found online at https://doi.org/10.1016/j.reactfunctpolym.2020.104487.

References

[1] Y. Hu, G. Wu, T. Lan, J.J. Zhao, Y. Liu, W. Chen, A graphene-based bimorph structure for design of high performance photoactuators, Adv. Mater. 27 (2015) 7867, https://doi.org/10.1002/adma.201502777.
[2] Y. Hu, Z. Li, T. Lan, W. Chen, Photoactuators for direct optical-to-mechanical energy conversion: from nanocomponent assembly to macroscopic deformation, Adv. Mater. 28 (2016) 10548, https://doi.org/10.1002/adma.201602685.
[3] X. Zhang, Z.B. Yu, C. Wang, D. Zarrouk, J.W.T. Seo, J.C. Cheng, A.D. Buchan, K. Takei, Y. Zhao, J.W. Ager, J.J. Zhang, M. Hettick, M.C. Hersam, A.P. Pisano, R.S. Fearing, A. Javey, Photoactuators and motors based on carbon nanotubes with selective chirality distributions, Nat. Commun. 5 (2014) 82983, https://doi.org/10.1038/ncomms3983.
[4] P. Leeladhar, J.P.S. Raturi, Sunlight-driven eco-friendly smart curtain based on infrared responsive graphene oxide-polymer photoactuators, Sci. Rep. 8 (2018) 93687, https://doi.org/10.1038/s41598-018-21871-3.
[5] Y. Hu, J.Q. Liu, L.F. Chang, L.L. Yang, A.F. Xu, K. Qi, P. Lu, G. Wu, W. Chen, Y.C. Wu, Electrically and sunlight-driven actuator with versatile biomimetic motions based on rolled carbon nanotube bilayer composite, Adv. Funct. Mater. 27 (2017) 101704388, https://doi.org/10.1002/adfm.201704388.
[6] D. Kim, H.S. Lee, J. Yoon, Highly bendable bilayer-type photo-actuators comprising of reduced graphene oxide dispersed in hydrogels, Sci. Rep. 6 (2016) 1020921, https://doi.org/10.1038/srep20921.
[7] L.L. Yang, K. Qi, L.F. Chang, A.F. Xu, Y. Hu, H. Zhai, P. Lu, A powerful dual-responsive soft actuator and photo-to-electric generator based on graphene microgasbags for bioinspired applications, J. Mater. Chem. B 6 (2018) 9, https://doi.org/10.1039/c8tb01222a.
[8] P. Leeladhar, A. Raturi, J.P.S. Kumar, Graphene-polydimethylsiloxane/chromium bilayer-based flexible, reversible, and large bendable photomechanical actuators, Smart Mater. Struct. 26 (2017) 9095030, https://doi.org/10.1088/1361-665X/aa7a49.
[9] L. Yu, H.F. Yu, Light-powered tumbler movement of graphene oxide/polymer nanocomposites, ACS Appl. Mater. Interfaces 7 (2015) 3834, https://doi.org/10.1021/am508970k.
[10] M. Ilcikova, M. Mrlik, T. Sedlacek, D. Chorvat, I. Krupa, M. Slouf, K. Koynov, J. Mosnacek, Viscoelastic and photo-actuation studies of composites based on polystyrene-grafted carbon nanotubes and styrene-b-isoprene-b-styrene block copolymer, Polymer 55 (2014) 211, https://doi.org/10.1016/j.polymer.2013.11.031.
[11] R. Rohini, P. Katti, S. Bose, Tailoring the interface in graphene/thermoset polymer composites: a critical review, Polymer *70* (2015) A17, https://doi.org/10.1016/j.polymer.2015.06.016.
[12] M. Mrlik, M. Ilcikova, T. Plachy, R. Moucka, V. Pavlinek, J. Mosnacek, Tunable electrorheological performance of silicone oil suspensions based on controllably reduced graphene oxide by surface initiated atom transfer radical polymerization of poly(glycidyl methacrylate), J. Ind. Eng. Chem. 57 (2018) 104.
[13] M. Mrlik, M. Ilcikova, T. Plachy, V. Pavlinek, Z. Spitalsky, J. Mosnacek, Graphene oxide reduction during surface-initiated atom transfer radical polymerization of glycidyl methacrylate: Controlling electro-responsive properties, Chem. Eng. J. 283 (2016) 717, https://doi.org/10.1016/j.cej.2015.08.013.
[14] M. Ilcikova, M. Mrlik, Z. Spitalsky, M. Micusik, K. Csomorova, V. Sasinkova, A. Kleinova, J. Mosnacek, A tertiary amine in two competitive processes: reduction of graphene oxide vs. catalysis of atom transfer radical polymerization, RSC Adv. 5 (2015) 3370, https://doi.org/10.1039/c4ra12915f.
[15] C.M. Hui, J. Pietrasik, M. Schmitt, C. Mahoney, J. Choi, M.R. Bockstaller, K. Matyjaszewski, Surface-initiated polymerization as an enabling tool for multifunctional (nano-)engineered hybrid materials, Chem. Mater. 26 (2014) 745, https://doi.org/10.1021/cm4023634.
[16] S.T. Milner, Polymer brushes, Science 251 (1991) 905, https://doi.org/10.1126/science.251.4996.905.
[17] J. Osicka, M. Mrlik, M. Ilcikova, B. Hanulikova, P. Urbanek, M. Sedlacik, J. Mosnacek, Reversible actuation ability upon light stimulation of the smart systems with controllably grafted graphene oxide with poly (glycidyl methacrylate) and PDMS elastomer: effect of compatibility and graphene oxide reduction on the photo-actuation performance, Polymers 10 (2018) 14832, https://doi.org/10.3390/polym10080832.
[18] J. Osicka, M. Ilcikova, M. Mrlik, A. Minarik, V. Pavlinek, J. Mosnacek, The impact of polymer grafting from a graphene oxide surface on its compatibility with a PDMS matrix and the light-induced actuation of the composites, Polymers 9 (2017) 14264, https://doi.org/10.3390/polym9070264.
[19] Y.Y. Feng, M.M. Qin, H.Q. Guo, K. Yoshino, W. Feng, Infrared-actuated recovery of polyurethane filled by reduced graphene oxide/carbon nanotube hybrids with high energy density, ACS Appl. Mater. Interfaces 5 (2013) 10882, https://doi.org/10.1021/am403071k.
[20] J. Osicka, M. Mrlik, M. Ilcikova, B. Hanulikova, P. Urbanek, M. Sedlacik, J. Mosnacek, Reversible actuation ability upon light stimulation of the smart systems with controllably grafted graphene oxide with poly (glycidyl methacrylate) and PDMS elastomer: Effect of compatibility and graphene oxide reduction on the photo-actuation performance, Polymers 10 (2018) 832, https://doi.org/10.3390/polym10080832.
[21] W.S. Hummers, R.E. Offeman, Preparation of graphitic oxide, J. Am. Chem. Soc. 80 (1958) 1339, https://doi.org/10.1021/ja01539a017.
[22] http://www.ampolymer.com/Mark-Houwink.html
[23] T. Gruemdling, T. Junkers, M. Guilhaus, C. Barner-Kowollik, Mark-Houwink, Parameters fo the universal calibration of the acrylate and vinyl acetate polymers determined by online size-exclusion chromatrography-mass spectroscopy, Macromol. Chem. Phys. *211* (2010), https://doi.org/10.1002/macp.200900323.
[24] M. Ilcikova, M. Mrlik, T. Sedlacek, M. Slouf, A. Zhigunov, K. Koynov, J. Mosnacek, Synthesis of photoactuating acrylic thermoplastic elastomers containing diblock copolymer-grafted carbon nanotubes, ACS Macro Lett. 3 (2014) 999, https://doi.org/10.1021/mz500444m.
[25] M. Ilcikova, M. Mrlik, T. Sedlacek, M. Doroshenko, K. Koynov, M. Danko, J. Mosnacek, Tailoring of viscoelastic properties and light-induced actuation performance of triblock copolymer composites through surface modification of carbon nanotubes, Polymer 72 (2015) 368, https://doi.org/10.1016/j.polymer.2015.03.060.
[26] M. Cvek, M. Mrlik, M. Ilcikova, J. Mosnacek, L. Munster, V. Pavlinek, Synthesis of silicone elastomers containing silyl-based polymer grafted carbonyl iron particles: an efficient way to improve magnetorheological, damping, and sensing performances, Macromolecules *50* (2017) 2189, https://doi.org/10.1021/acs.macromol.6b02041.
[27] J. Loomis, B. King, T. Burkhead, P. Xu, N. Bessler, E. Terentjev, B. Panchapakesan, Graphene-nanoplatelet-based photomechanical actuators, Nanotechnology 23 (2012) 045501, , https://doi.org/10.1088/0957-4484/23/4/045501.

Utility model

ÚŘAD
PRŮMYSLOVÉHO
VLASTNICTVÍ

UŽITNÝ VZOR

(11) Číslo dokumentu:

31 633

(13) Druh dokumentu: **U1**

(51) Int. Cl.:

G01N 21/17 (2006.01)

(19) ČESKÁ REPUBLIKA

ÚŘAD PRŮMYSLOVÉHO VLASTNICTVÍ

(21) Číslo přihlášky: **2018-34578**

(22) Přihlášeno: **12.01.2018**

(47) Zapsáno: **20.03.2018**

(73) Majitel:
Univerzita Tomáše Bati ve Zlíně, Zlín, CZ

(72) Původce:
Ing. Miroslav Mrlík, Ph.D., Lípa, CZ
Ing. Josef Osička, Zlín, CZ

(74) Zástupce:
Ing. Jan Görig, Korábová 98, 763 16 Fryšták, Horní Ves

(54) Název užitného vzoru:

Zařízení ke sledování změn rozměrů materiálů vlivem světelné stimulace

CZ 31633 U1

Zařízení ke sledování změn rozměrů materiálů vlivem světelné stimulace

Oblast techniky

Technické řešení se týká zařízení ke sledování změn rozměrů materiálů vlivem světelné stimulace. Světelným stimulem může být jakékoliv světlo v rozmezí viditelného spektra (280 nm až 720 nm), nebo konkrétními vlnovými délkami s ohledem na jejich potenciální aplikaci. Zařízení tohoto typu lze využít pro výzkum, vývoj a testování materiálů, zejména polymerních a kompozitních systémů, kde je očekávaná aplikace takového materiálu, jenž by mohl vratně nebo nevratně měnit své rozměry.

Dosavadní stav techniky

Pro hodnocení změn rozměrů vlivem světelného stimulu v současné době není známo žádné jednoduše dostupné a dostatečně univerzální zařízení. Existují sice přípravky zhotovené pro určitý konkrétní účel přímo různými výzkumnými týmy, na kterých je takové hodnocení možné, ale jeho přesnost je v širší aplikační rovině velmi omezená. Z publikací jsou také známy metody testování a příslušná zařízení, které se omezují na hodnocení využitím dynamické mechanické analýzy. Není u nich ale spolehlivě vyřešena teplotní roztažnost čelistí, které mohou během ozařování měnit rozměry vlivem absorpce tepla a tím významně ovlivňovat výsledné hodnoty.

Podstata technického řešení

K odstranění výše uvedených nevýhod a nedostatků dosud známých systémů pro měření změny rozměrů pod vlivem světelného stimulu přispívá do značné míry zařízení ke sledování změn rozměrů materiálů vlivem světelné stimulace podle předloženého technického řešení, využívající termomechanickou analýzu a konstrukce s přesně nastavitelnou intenzitou a rozsahem světelné stimulace.

Podstata technického řešení spočívá v tom, že zařízení ke sledování změn rozměrů materiálů vlivem světelné stimulace obsahuje dvojici držáků k upnutí vzorku zkoušeného materiálu, konkrétně pevně vetknutý horní držák a dolní držák s vestavěným modulem k vyhodnocení vzdálenosti a generované síly odpovídající rozměrovým změnám materiálu vzorku. Proti ploše vzorku upnutého v držácích je na jedné straně na posuvném držáku stojanu umístěn světelný zdroj spolu s chladičem, se vzdáleností od vzorku nastavitelnou přesným mikrometrickým šroubem. Na druhé straně je proti ploše vzorku umístěno teplotní čidlo.

Držáky vzorku zkoušeného materiálu jsou s výhodou z křemičitého skla.

Světelným zdrojem může být s výhodou soustava LED diod, chladičem 6 pak mikroprocesorový chladič.

Vzdálenost teplotního čidla od povrchu vzorku zkoušeného materiálu s výhodou nepřesahuje 2 mm.

Vestavěný modul dolního držáku k vyhodnocení vzdálenosti a generované síly odpovídající rozměrovým změnám materiálu vzorku může být s výhodou propojen s platformou termomechanického analyzátoru pro krátkodobý, dlouhodobý a cyklický záznam hodnoty změny rozměrů vzorku a generované síly vlivem světelné stimulace.

Hlavní výhoda zařízení podle předloženého technického řešení spočívá v tom, že toto zařízení je unikátní z hlediska přesnosti hodnocení změn rozměrů materiálu vlivem světelného stimulu

a navíc také s výhodou umožňuje měření za konstantních teplotních podmínek a současných změn intenzity a rozsahu světelného stimulu. Samotná konstrukce zařízení podle technického řešení umožňuje snadnou manipulaci, jak při nastavení podmínek měření, tak i při uložení vzorku pro jeho samostatné hodnocení.

V důsledku těchto skutečností zařízení podle technického řešení poskytuje možnost realizovat nový typ měření - hodnocení změny rozměrů (kontrakce/expanze) vlivem světelné stimulace s velkou přesností (v řádu mikrometrů), Současně umožňuje měnit intenzitu a rozsah světelného stimulu a je schopno poskytovat záznam s využitím termomechanického analyzátoru.

Objasnění výkresů

K bližšímu objasnění podstaty technického řešení slouží přiložené výkresy, kde představuje:

- obr. 1 – schématický nárys zařízení ke sledování změn rozměrů materiálů vlivem světelné stimulace**;**

- obr. 2 – schématický bokorys zařízení ke sledování změn rozměrů materiálů vlivem světelné stimulace.

Příklad uskutečnění technického řešení

Zařízení ke sledování změn rozměrů materiálů vlivem světelné stimulace v příkladném provedení (viz obr. 1 a 2) obsahuje dvojici držáků 2, 3 k upnutí vzorku 1 zkoušeného materiálu. Konkrétně se jedná o pevně vetknutý horní držák 2 a dolní držák 3 s vestavěným modulem k vyhodnocení vzdálenosti a generované síly odpovídající rozměrovým změnám materiálu vzorku 1. Oba držáky 2, 3 jsou zhotoveny z křemičitého skla.

Proti ploše vzorku 1 upnutého v držácích 2, 3 je na jedné straně na posuvném držáku stojanu 5 umístěn světelný zdroj 7 tvořený soustavou LED diod. LED diody jsou z důvodu možného přehřívání a tedy lokálního vzrůstu teploty přilepeny teplovodivým lepidlem na mikroprocesorový chladič 6. Chladič 6 je upevněn na stojanu 5, který podpírá držák s otočným elementem 8 z důvodu možnosti změny LED diody s preferovanou vlnovou délkou. Přesný mikrometrový šroub 9 umožňující pohyb držáku s rotujícím elementem 8, umožňuje přesný pohyb chladiče 6, na kterém jsou LED diody 7 a tím přesné nastavení potřebné intenzity. Teplotní poměry v okolí vzorku jsou snímány teplotním čidlem 10, které není vzdáleno od hodnoceného materiálu víc než 2 mm. Platforma termomechanického analyzátoru 4, zajišťuje měření a zapisování změny rozměrů vzorku a definuje, nebo hodnotí použitou sílu, která byla vyvozena vlivem takovéto rozměrové změny.

Před samotným měřením se stojan 5 zafixuje k nosné konstrukci termomechanického analyzátoru (na výkrese není znázorněno). Následně se nastaví pomocí přesného mikrometrového šroubu 9 vzdálenost LED diod 7 od hodnoceného vzorku 1. Poté se nastaví držákem s otočným elementem 8 LED dioda a s preferovanou vlnovou délkou. Na upnutý hodnocený materiál 1 se aplikuje počáteční zatížení a pomocí platformy termomechanického analyzátoru 4 se hodnotí změny rozměrů a síly generované tímto pohybem v závislosti na zapnuté/vypnuté světelné stimulaci čímž je započato samotné měření.

Napájení a regulace zdroje LED diod 7 jsou zajišťovány externím zdrojem s regulátorem (na výkrese není znázorněno).

Průmyslová využitelnost

Na zařízení podle technického řešení lze, díky využití komponent z termomechanického analyzátoru a přesně nastavitelné intenzity a rozsahu světelné stimulace, měřit změny rozměrů různých typů materiálů, dlouhodobě, krátkodobě a cyklicky a tím postihnout možné problémy (nevratná deformace, zpožděná deformace, přetržení vzorku) pro použitý typ materiálu. Zařízení tohoto typu lze využít pro výzkum, vývoj a testování materiálů, zejména polymerních a kompozitních systémů, jenž by mohly vratně nebo nevratně měnit své rozměry vlivem světelné stimulace. Najde tedy uplatnění ve výzkumných ústavech, univerzitách a vývojových odděleních výrobních podniků zabývajících se chytrými senzory, dotykovými displeji a obecně u chytrých aplikací.

NÁROKY NA OCHRANU

1. Zařízení ke sledování změn rozměrů materiálů vlivem světelné stimulace, **vyznačující se tím**, že obsahuje dvojici držáků (2, 3) k upnutí vzorku (1) zkoušeného materiálu, konkrétně pevně vetknutý horní držák (2) a dolní držák (3) s vestavěným modulem k vyhodnocení vzdálenosti a generované síly odpovídající rozměrovým změnám materiálu vzorku (1), s tím, že proti ploše vzorku (1) upnutého v držácích (2, 3) je na jedné straně na posuvném držáku stojanu (5) umístěn světelný zdroj (7) spolu s chladičem (6), se vzdáleností od vzorku (1) nastavitelnou přesným mikrometrickým šroubem (9), zatím co na druhé straně je proti ploše vzorku (1) umístěno teplotní čidlo (10).

2. Zařízení podle nároku 1, **vyznačující se tím**, že držáky (2, 3) jsou z křemičitého skla.

3. Zařízení podle nároku 1, **vyznačující se tím**, že světelným zdrojem (7) je soustava LED diod s různou vlnovou délkou uložená na otočném elementu (8).

4. Zařízení podle nároku 1, **vyznačující se tím**, že chladičem (6) je mikroprocesorový chladič.

5. Zařízení podle nároku 1, **vyznačující se tím**, že vzdálenost teplotního čidla (10) od povrchu vzorku (1) zkoušeného materiálu je maximálně 2 mm.

6. Zařízení podle nároku 1, **vyznačující se tím**, že vestavěný modul dolního držáku (3) k vyhodnocení vzdálenosti a generované síly odpovídající rozměrovým změnám materiálu vzorku (1) je propojen s platformou termomechanického analyzátoru (4) pro krátkodobý, dlouhodobý a cyklický záznam hodnoty změny rozměrů vzorku (1) a generované síly vlivem světelné stimulace.

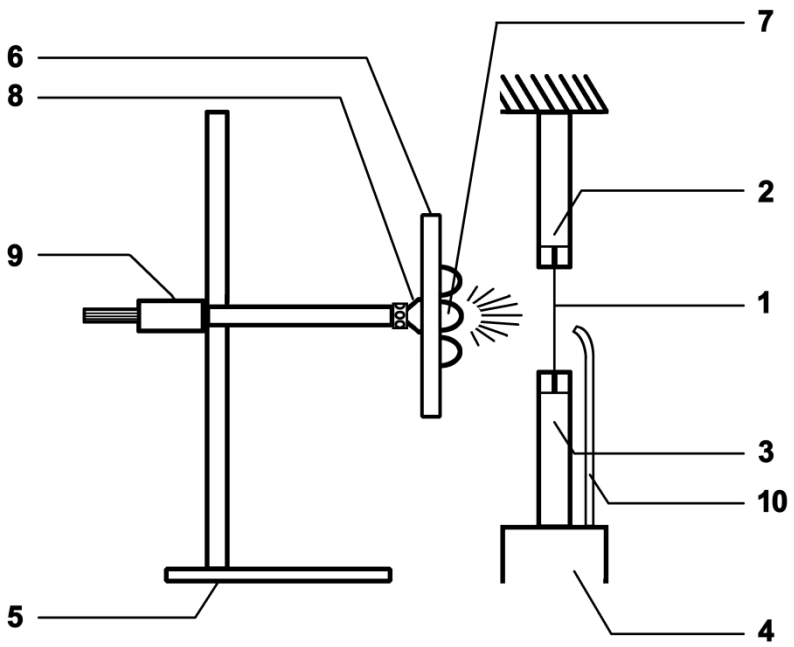

Obr. 1

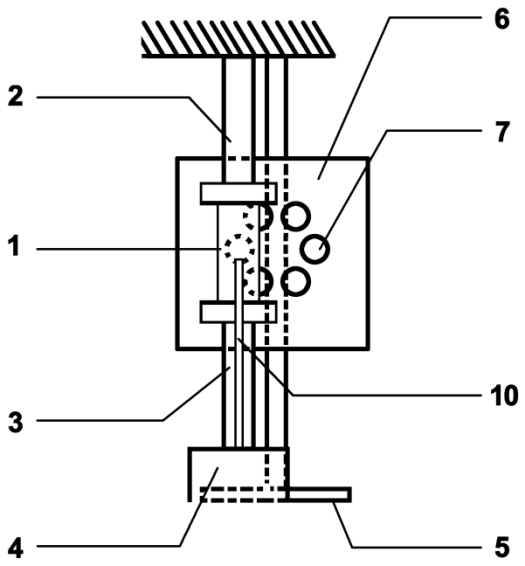

Obr. 2

Konec dokumentu

CURRICULUM VITAE

Personal Information	
Surname and name	Osička Josef
Address	Na Honech II / 4917, 76005 Zlín, Czech Rebublic
Telephone	+420 723 350 755
E-mail	osicka@utb.cz
Nationality	Czech
Date of Birth	14/9/1984
Work Experience	
Dates	09/2016 – present
Occupation or Position Held	Research assistant
Name of Employer	Tomas Bata University in Zlin, Centre of Polymer Systems
Dates	04/2018 – 12/2018
Occupation or Position Held	Manager for Logistic
Name of Employer	Czech Post Security
Dates	02/2014 – 06/2016
Occupation or Position Held	Research assistant
Name of Employer	Qatar University, Center for Advanced Materials
Dates	10/2007 – 06/2011
Occupation or Position Held	Supply and distribution department manager
Name of Employer	Studenta Media Ltd.
Education	
Dates	09/2016 – present
Title of Qualification Awarded	Doctoral Study – Expected defense in 08/2020
Principal Branch	Technology of Macromolecular Compounds
Organization Providing Education	Tomas Bata University in Zlin, Faculty of Technology
Dates	09/2009 – 06/2011
Title of Qualification Awarded	Ing. eq. M.Sc.
Principal Branch	Technology Risk Management
Organization Providing Education	Tomas Bata University in Zlin, Faculty of Technology
Dates	09/2006 – 06/2009
Title of Qualification Awarded	Bc.
Principal Branch	Logistics and Management
Organization Providing Education	Tomas Bata University in Zlin, Faculty of Technology

Training Abroad	
Dates	09/2020 – 11/2020
	Student traineeship at Lodz University of Technology, Institute of Polymers and Dye Technology (Poland)
Field of Study	Modification of surfaces by branched polymer chains using SI-ATRP technique
Dates	12/2018 (1 week)
	Research period at Slovak Academy of Sciences, Polymer Institute (Slovakia)
Field of Study	Modification of graphene oxide particles via Atom Transfer Radical Polymerization
Expertise	
Fields	Polymer processing, Mechanical properties of polymers, Polymer synthesis
Other Languages	**Level**
English	C1
German	A1
Awards	
	Best Poster Award (co-author) – 2017, Miskolc (Hungary), Conference paper *"Ferrous oxalate micro-rods as a promising material for electrorheology"*

LIST OF PUBLICATIONS

Publications in the Journals with Impact Factor:

[1] ZYGO, M.; MRLIK, M.; ILCIKOVA, M.; HRABALIKOVA, M.; OSICKA, J.; CVEK, M.; SEDLACIK, M.; HANULIKOVA, B.; MUNSTER, L.; SKODA, D.; URBANEK, P.; PIETRASIK, J.; MOSNACEK, J. Effect of Structure of Polymers Grafted from Graphene Oxide on the Compatibility of Particles with a Silicone-Based Environment and the Stimuli-Responsive Capabilities of Their Composites. *Nanomaterials*. **2020**, vol. 10, no. 3, pp.

[2] OSICKA, J.; MRLIK, M.; ILCIKOVA, M.; KRUPA, I.; SOBOLCIAK, P.; PLACHY, T.; MOSNACEK, J. Controllably coated graphene oxide particles with enhanced compatibility with poly(ethylene-co-propylene) thermoplastic elastomer for excellent photo-mechanical actuation capability. *Reactive & Functional Polymers*. **2020**, vol. 148, no., pp.

[3] SEDLACIK, M.; OSICKA, J.; PAVLINEK, V.; FOJTL, L. The influence of ultraviolet radiation on the optical properties of glass fibre reinforcements for polyurethane matrix composites. *Coloration Technology*. **2019**, vol. 135, no. 6, pp. 510-15.

[4] MRLIK, M.; ILCIKOVA, M.; OSICKA, J.; KUTALKOVA, E.; MINARIK, A.; VESEL, A.; MOSNACEK, J. Electrorheology of SI-ATRP-modified graphene oxide particles with poly(butyl methacrylate): effect of reduction and compatibility with silicone oil. *Rsc Advances*. **2019**, vol. 9, no. 3, pp. 1187-98.

[5] KUTALKOVA, E.; MRLIK, M.; ILCIKOVA, M.; OSICKA, J.; SEDLACIK, M.; MOSNACEK, J. Enhanced and Tunable Electrorheological Capability using Surface Initiated Atom Transfer Radical Polymerization Modification with Simultaneous Reduction of the Graphene Oxide by Silyl-Based Polymer Grafting. *Nanomaterials*. **2019**, vol. 9, no. 2, pp.

[6] DANKO, M.; KRONEKOVA, Z.; MRLIK, M.; OSICKA, J.; BIN YOUSAF, A.; MIHALOVA, A.; TKAC, J.; KASAK, P. Sulfobetaines Meet Carboxybetaines: Modulation of Thermo- and Ion-Responsivity, Water Structure, Mechanical Properties, and Cell Adhesion. *Langmuir*. **2019**, vol. 35, no. 5, pp. 1391-403.

[7] OSICKA, J.; MRLIK, M.; ILCIKOVA, M.; MUNSTER, L.; BAZANT, P.; SPITALSKY, Z.; MOSNACEK, J. Light-Induced Actuation of Poly(dimethylsiloxane) Filled with Graphene Oxide Grafted with Poly(2-(trimethylsilyloxy)ethyl Methacrylate). *Polymers*. **2018**, vol. 10, no. 10, pp.

[8] OSICKA, J.; MRLIK, M.; ILCIKOVA, M.; HANULIKOVA, B.; URBANEK, P.; SEDLACIK, M.; MOSNACEK, J. Reversible Actuation Ability upon Light Stimulation of the Smart Systems with Controllably Grafted Graphene Oxide with Poly (Glycidyl Methacrylate) and PDMS Elastomer: Effect of Compatibility and Graphene Oxide Reduction on the Photo-Actuation Performance. *Polymers*. **2018**, vol. 10, no. 8, pp.

[9] MRLIK, M.; CVEK, M.; OSICKA, J.; MOUCKA, R.; SEDLACIK, M.; PAVLINEK, V. Surface-initiated atom transfer radical polymerization from graphene oxide: A way towards fine tuning of electric conductivity and electro-responsive capabilities. *Materials Letters*. **2018**, vol. 211, no., pp. 138-41.

[10] MOSNACEK, J.; POPELKA, A.; OSICKA, J.; FILIP, J.; ILCIKOVA, M.; KOLLAR, J.; YOUSAF, A. B.; BERTOK, T.; TKAC, J.; KASAK, P. Modulation of wettability, gradient and adhesion on self-assembled monolayer by counterion exchange and pH. *Journal of Colloid and Interface Science*. **2018**, vol. 512, no., pp. 511-21.

[11] MOSNACEK, J.; OSICKA, J.; POPELKA, A.; ZAVAHIR, S.; BEN-HAMADOU, R.; KASAK, P. Photochemical grafting of polysulfobetaine onto polyethylene and polystyrene surfaces and investigation of long-term stability of the polysulfobetaine layer in seawater. *Polymers for Advanced Technologies*. **2018**, vol. 29, no. 7, pp. 1930-38.

[12] KUTALKOVA, E.; PLACHY, T.; OSICKA, J.; CVEK, M.; MRLIK, M.; SEDLACIK, M. Electrorheological behavior of iron(ii) oxalate micro-rods. *Rsc Advances*. **2018**, vol. 8, no. 44, pp. 24773-79.

[13] OSICKA, J.; ILCIKOVA, M.; MRLIK, M.; MINARIK, A.; PAVLINEK, V.; MOSNACEK, J. The Impact of Polymer Grafting from a Graphene Oxide Surface on Its Compatibility with a PDMS Matrix and the Light-Induced Actuation of the Composites. *Polymers*. **2017**, vol. 9, no. 7, pp.

[14] FILIP, J.; POPELKA, A.; BERTOK, T.; HOLAZOVA, A.; OSICKA, J.; KOLLAR, J.; ILCIKOVA, M.; TKAC, J.; KASAK, P. pH-Switchable Interaction of a Carboxybetaine Ester-Based SAM with DNA and Gold Nanoparticles. *Langmuir*. **2017**, vol. 33, no. 27, pp. 6657-66.

[15] OSICKA, J.; ILCIKOVA, M.; POPELKA, A.; FILIP, J.; BERTOK, T.; TKAC, J.; KASAK, P. Simple, Reversible, and Fast Modulation in Superwettability, Gradient, and Adsorption by Counterion Exchange on Self-Assembled Monolayer. *Langmuir*. **2016**, vol. 32, no. 22, pp. 5491-99.

[16] OSICKA, J.; ILCIKOVA, M.; MRLIK, M.; AL-MAADEED, M.; SLOUF, M.; TKAC, J.; KASAK, P. Anisotropy in CNT composite fabricated by combining directional freezing and gamma irradiation of acrylic acid. *Materials & Design*. **2016**, vol. 97, no., pp. 300-06.

Original Full Papers in Conference Proceedings (Indexed on Web of Science):

[1] OSICKA, J.; MRLIK, M.; ILCIKOVA, M.; MOSNACEK, J.; LTD, T. ELECTRORHEOLOGICAL PERFORMANCE OF GRAPHENE OXIDE PARTICLES GRAFTED WITH POLY(ALPHA-METHYLSTYRENE) USING SI-ATRP APPROACH. 9th International Conference on Nanomaterials - Research & Application; **2018**.

[2] MRLIK, M.; OSICKA, J.; SEDLACIK, M.; MOSNACEK, J.; LTD, T. MODIFICATION OF THE CARBONYL IRON PARTICLES USING SI-ATRP APPROACH WITH POLY(2-(1H-PYRROLE-1-YL)ETHYL METHACRYLATE. 9th International Conference on Nanomaterials - Research & Application; **2018**.

[3] OSICKA, J.; CVEK, M.; MRLIK, M.; ILCIKOVA, M.; PAVLINEK, V.; MOSNACEK, J. Light-Induced and Sensing Capabilities of SI-ATRP Modified Graphene Oxide Particles in Elastomeric Matrix. Active and Passive Smart Structures and Integrated Systems 2017; **2017**.

[4] MRLIK, M.; OSICKA, J.; ILCIKOVA, M.; PAVLINEK, V.; MOSNACEK, J. Smart composites based on controllably grafted graphene oxide particles and elastomeric matrix with sensing capability. Active and Passive Smart Structures and Integrated Systems 2017; **2017**.

Conference Contribution:

[1] OSICKA, J.; CVEK, M.; KUTALKOVA, E.; MOUCKA, R.; SEDLACIK, M. Magnetorheological elastomers as a lightweight, transparent piezoresistive sensor. In: *ERMR 2019 – International Conference on Electrorheological Fluids and Magnetorheorogical Suspensions*, (ed. Li, W.), **2019,** Wollongong, Australia.

[2] OSICKA, J.; MRLIK, M.; MUNSTER, L.; ILCIKOVA, M.; MOSNACEK, J.; SPITALSKY, Z. Photoactuative performance of graphene oxide attached by Poly [2-(trimethylsilyloxy)ethyl methacrylate] using SI-ATRP method in elastometric matrix. In: *ERMR 2018 - International Conference on Electrorheological Fluids and Magnetorheological Suspensions*, (ed. Wereley, N. M.), **2018,** College Park, Maryland, USA.

[3] MRLIK, M.; OSICKA, J.; ILCIKOVA, M.; J., K.; MOSNACEK, J. SI-ATRP modification of poly(2-isopropenyl oxazoline) from the graphene oxide and its electrorheological performance. In: *ERMR 2018 - International Conference on Electrorheological Fluids and Magnetorheological Suspensions*, (ed. Wereley, N. M.), **2018,** College Park, Maryland, USA.

[4] OSICKA, J.; MRLIK, M.; ILCIKOVA, M.; MOSNACEK, J. Electrorheological performance of graphene oxide particles grafted with poly(alpha-methylstyrene) using SI-ATRP approach In: *NANOCON 2017 - 9th International Conference on Nanomaterials - Research and Application*, (ed., **2017,** Brno, Czech Republic: TANGER LTD.

[5] OSICKA, J.; CVEK, M.; MRLIK, M.; ILCIKOVA, M.; PAVLINEK, V.; MOSNACEK, J. Light-induced and sensing capabilities of SI-ATRP modified graphene oxide particles in elastomeric matrix. In: *SPIE - Smart Structures and Materials & Nondestructive Evaluation*, (ed. Gyuhae, P.), **2017,** Portland, Oregon, USA.

[6] MRLIK, M.; OSICKA, J.; SEDLACIK, M.; MOSNACEK, J. Modification of the carbonyl iron particles using si-atrp approach with poly(2-(1H-pyrrole-1-YL)ethyl methacrylate. In: *NANOCON 2017 - 9th International Conference on Nanomaterials - Research and Application*, (ed., **2017,** Brno, Czech Republic: TANGER LTD.

[7] MRLIK, M.; OSICKA, J.; ILCIKOVA, M.; PAVLINEK, V.; MOSNACEK, J. Smart composites based on controllably grafted graphene oxide particles and elastomeric

matrix with sensing capability. In: *SPIE - Smart Structures and Materials & Nondestructive Evaluation*, (ed. Park, G.), **2017,** Portland, Oregon, USA.

[8] CVEK, M.; PLACHY, T.; OSICKA, J.; KUTALKOVA, E.; MRLIK, M.; SEDLACIK, M. Ferrous oxalate micro-rods as a promising material for electrorheology. In: *3rd International Conference on Rheology and Modelling of Materials*, (ed. Gömze, L. A.), **2017,** Miskolcs-Lillafüred, Hungary.

[9] OSICKA, J.; R., M.; KASAK, P. Nicotinamide based supergelator with self-healing and thixotropic properties. In: *ARF 2016 - Qatar Foundation Annual Research Forum*, (ed., **2016,** Doha, Qatar.

[10] KASAK, P.; OSICKA, J.; MRLIK, M.; ILCIKOVA, M. Anisotropic composite prepared by directional freezing and gamma irradiation. In: *Materials Science and Engineering Symposium*, (ed., **2015,** Doha, Qatar.

Utility models:

[1] MRLIK, M., OSICKA, J. Instrument for shape-change monitoring upon light stimulation, 2018-34578, 2018, Czech republic.

Work on projects:

Position	**Period**	**Project**
Member of research team	2019-2021	Czech Science Foundation (GACR), *Nanotechnologies in flow-through electrochemical sensors applied in environmental engineering,* GJ20-27735Y
Member of research team	2018-2020	Czech Science Foundation (GACR), *Manufacturing and analysis of flexible piezoelectric layers for smart engineering*, GA19-17457S
Member of research team	2020	Internal Grant Agency of TBU in Zlín, *Influence of Modifications Dispersion Particles on the Utility Properties of Magnetorheological Systems,* IGA/CPS/2020/006
Member of research team	2017-2019	Czech Science Foundation (GACR), *Novel Magnetorheological Elastomers Based on Modified Magnetic Fillers,* GA17-24730S
Principal investigator	2019	Internal Grant Agency of TBU in Zlín, *Influence of organic materials on the efficiency of intelligent systems*, IGA/CPS/2019/005
Principal investigator	2018	Internal Grant Agency of TBU in Zlín, *Preparation and characterization of electrorheological suspensions based on ferrous oxalates and clays*, IGA/CPS/2018/004
Member of research team	2016-2018	Czech Science Foundation (GACR), *Smart systems based on modified graphene oxide particles*. GJ16-20361Y
Member of research team	2017	Internal Grant Agency of TBU in Zlín, *Evaluation of Carbon-Based Nano-Additives' Influence on Magnetorheological*

		Performance and Preparation of Electrorheological Suspension with Enhanced Sedimentation Stability, IGA/CPS/2017/004
Principal investigator	2016	Internal Grant Agency of TBU in Zlín, *Optimization of viscoelastic properties of polyolefin blends intended for preparation of foams with controlled inner structure,* IGA/CPS/2016/009
Member of research team	2014-2016	National Priorities Research Program (NPRP), *Preparation, characterization and application of lectin biochips in cancer diagnosis and in discovery of cancer biomarkers*, NPRP 6-381-1-078

Josef Osička

Composite materials with photo-responsive capability

Kompozitní materiály s fotocitlivou odezvou

Doctoral thesis

Published by: Tomas Bata University in Zlin
nám. T. G. Masaryka 5555, 760 01 Zlín.

Typesetting by: Josef Osička
This publication has not undergone any proofreading or editorial review

Publication year: 2020

ISBN 978-80-……